PHYSICAL REVIEW
LETTERS

VOLUME 3 SEPTEMBER 1, 1959 NUMBER 5

SIGN OF THE GROUND-STATE CUBIC CRYSTAL FIELD SPLITTING PARAMETER IN Fe^{3+}

S. Geschwind
Bell Telephone Laboratories, Murray Hill, New Jersey
(Received June 10, 1959)

Recent interest has focused on the mechanism of the splitting of the nominally spherically symmetric $6S_{5/2}$ ground state of Fe^{3+} in cubic crystalline fields. Watanabe[1] has shown that a splitting arising from perturbations by excited states derived from the $3d^5$ configuration involve the cubic crystalline potential, $V=C(x^4+y^4+z^4-\frac{3}{5}r^4)$, to even powers only and will first appear as V^2. Consequently the sign of a in the cubic term of the ground-state spin Hamiltonian, $a(S_\xi^4+S_\eta^4+S_\zeta^4)$, should be independent of the sign of V. Thus, even though the cubic potentials have opposite signs at the center of a tetrahedron of point charges to that of an octahedron, the sign of a should be the same for both. We have verified that this is indeed the case for Fe^{3+} from the paramagnetic resonance spectrum of Fe^{3+} in octahedral and tetrahedral O^{2-} coordination in single crystals of yttrium gallium garnet, $3Y_2O_3\cdot 5Ga_2O_3$ (hereinafter called YGaG), a being positive in both sites. This result led us to re-examine the spectrum of Fe^{3+} in rubidium aluminum sulphate where a negative sign for a was reported earlier.[2] However, we find that a is positive in this case also.

YGaG is isostructural with yttrium iron garnet[3] (YIG). There are 16 octahedral sites and 24 tetrahedral sites per unit cell which are occupied by Ga^{3+}. A 0.1% Fe impurity enters as Fe^{3+} substitutionally for the Ga with a roughly 10:1 preference for the octahedral site. The octahedra are distorted by a stretching along the four different [111] directions (site symmetry C_{3i}), and the tetrahedra by a pulling along the three different cube edges (site symmetry S_4) giving rise to axial terms in the spin Hamiltonian for each site which are considerably larger than the cubic terms. The spin Hamiltonian for Fe^{3+} is given in reference 2. With the magnetic field in an arbitrary direction in the crystal, as many as seventy lines corresponding to $\Delta m=\pm 1$ transitions are possible (5 for each nonequivalent site as far as crystal field orientation is concerned). However, by confining the magnetic field to a (110) plane some of the sites will give identical spectra and an even further simplification results with H_{dc} along one of the principal axes. From the spectra with H_{dc} parallel to a [111] direction ($\theta=0$ spectrum), D and $(a-F)$ for the octahedral sites were determined with the signs found from the relative intensity of the lines at 4.2°K. Similarly, with H_{dc} parallel to the [100] direction, D and $(a+\frac{2}{3}F)$ were determined for the tetrahedral sites. To determine a separately, a detailed knowledge of the crystal structure is needed.

Among those tetrahedral sites having a common [100] axis of distortion, there are two types of sites. They differ from each other in that they are rotated about this [100] direction from a position in which the cubic axes of the tetrahedra are coincident with unit cell edges, through angles $+\alpha$ and $-\alpha$, respectively, for the two types of sites which we will call $d_{(1)}$ and $d_{(2)}$. These two sites will give rise to two distinct spectra corresponding to the term $a[S_+^4e^{i4(\varphi\pm\alpha)}+S_-^4e^{-i4(\varphi\pm\alpha)}]$ in the cubic part of the spin Hamiltonian for the tetrahedral site. Here φ is the angle between the projection of H_{dc} on the (100) plane and the [010] axis. As H_{dc} is rotated in the (100) plane, two perpendicular spectra ($\theta=90°$) will be observed as is shown in Fig. 1 for the $-1/2\rightarrow+1/2$

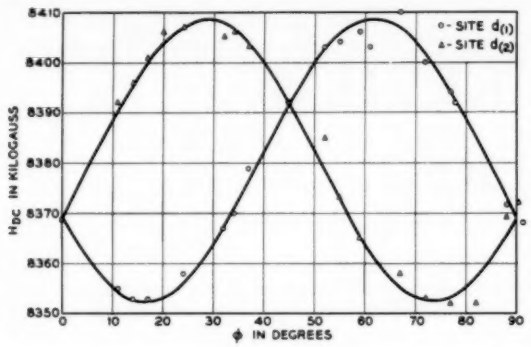

FIG. 1. Perpendicular spectrum of $-1/2 \rightarrow +1/2$ transition of Fe^{3+} in the tetrahedral site, with H_{dc} rotated in a (100) plane. The failure of some of the points to fall on the curve is due to extreme pulling of these lines by much stronger lines from the octahedral sites at certain angles of the field.

transition. The variation with φ will be of the form $C_T a \cos[4(\varphi \pm \alpha)]$, where C_T is a constant determined from first-order perturbation by diagonalization of the major portion of the spin Hamiltonian with parameters D and $(a + \frac{2}{3}F)$ determined from the parallel spectrum. As is seen from Fig. 1, α is either 16.5° or 28.5° and these two values give opposite signs for a. In the isostructural YIG, α was found to be 15.6° and we would expect it to be very much the same here, so that we can rule out with certainty 28.5° and therefore a is found to be positive.

Similarly, for those octahedral sites having the same [111] direction of distortion there are two types of sites rotated from each other about this [111] direction by an angle 2α. The site symmetry being C_{3i}, the cubic part of the spin Hamiltonian now has an $e^{+i3(\varphi \pm \alpha)}$ azimuthal dependence. Proceeding in the same manner as for the tetrahedral site and again using the crystal structure of YIG, one concludes that a is positive as Low[4] found for a similar O^{2-} coordination in MgO. The room-temperature parameters for both sites are listed in Table I.

Table I. Room-temperature parameters for both sites.

	Octahedral	Tetrahedral
D	−1384 ± 3 oersteds	−947 ± 5 oersteds
a	+ 198 ± 5 oersteds	+ 66 ± 3 oersteds
F	+ 28 ± 4 oersteds	− 42 ± 4 oersteds
g	2.003 ± 0.001	2.0047 ± 0.0005

The constant appearing in the cubic potential V is $-35q/9d^5$ and $+35q/4d^5$ for tetrahedral and octahedral sites, respectively, where d is the distance from the center of the site to the charges q located at the corners. If, in accordance with Watanabe,[1] $a \sim V^2$, then $a_{oct}/a_{tet} \equiv (9/4)^2(d_{tet}/d_{oct})^5$. Using the Fe-O distances given in reference 3, one predicts $a_{oct}/a_{tet} = 2.72 \pm 0.3$, the error arising from the error in d. This is in very good agreement with the experimental value 3.00 ± 0.1.

A study of the earlier work on Fe^{3+} in rubidium aluminum sulphate showed that under the conditions encountered, i.e., 20°K and 9000 Mc/sec, a difference of intensity of only 8.5% is to be expected between the $-3/2 \rightarrow -5/2$ and $+3/2 \rightarrow +5/2$ transitions. We re-examined the spectrum at 4.2°K and 1.6°K at 24 000 Mc/sec and it is shown in Fig. 2 for the external magnetic field parallel to a [100] direction in the crystal. The increase

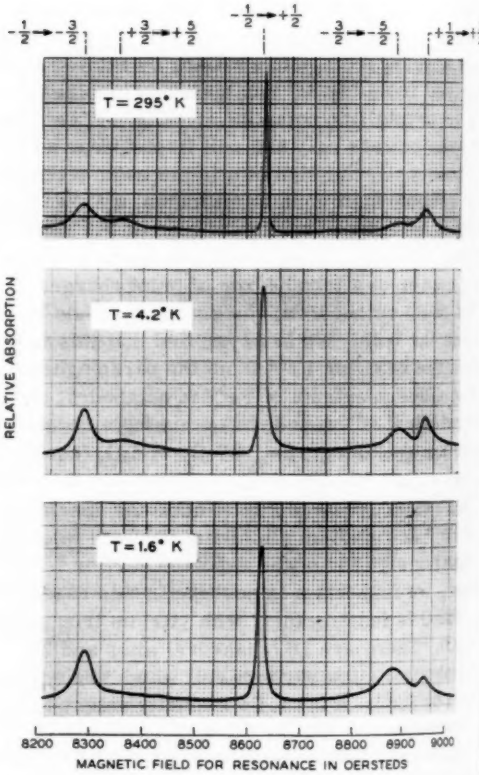

FIG. 2. Paramagnetic resonance spectrum at K-band of Fe^{3+} in rubidium aluminum sulphate with H_{dc} parallel to a [100] direction. The relative intensity at low temperature establishes the ground-state cubic field splitting parameter a as positive.

of the relative intensity of the inner high-field line and the outer low-field lines labels them as the $-3/2 \rightarrow -5/2$ and $-1/2 \rightarrow -3/2$ transitions, respectively, and establishes the positive sign of a for Fe^{3+} in octahedral water coordination.

Further details including the relation of the crystal field splitting parameters to ferrimagnetic anisotropy as well as a more detailed summary of splitting of S-state ions will appear in forthcoming publications.

The author should like to thank D. Linn for his experimental assistance; S. Geller for his extensive aid with the important crystallographic problems; J. W. Nielsen and J. P. Remeika for the difficult task of growing the garnet single crystals; K. D. Bowers, A. Clogston, A. Javan, M. Peter, E. Schulz-DuBois, and L. R. Walker for their many helpful discussions; and Miss B. Cetlin for her help with the computations on the IBM 704.

[1]H. Watanabe, Progr. Theoret. Phys. (Kyoto) 18, 405 (1957).
[2]B. Bleaney and R. S. Trenam, Proc. Roy. Soc. (London) A223, 1 (1954).
[3]S. Geller and M. A. Gilleo, J. Phys. Chem. Solids 3, 30 (1957).
[4]W. Low, Phys. Rev. 105, 792 (1957).

CANTED SPIN ARRANGEMENTS*

P.-G. de Gennes
Department of Physics, University of California, Berkeley, California
(Received August 3, 1959)

The aim of this Letter is to discuss two spin systems where canted spin arrangements are very likely to occur. These are (1) the ordered iron aluminum alloys[1]; (2) the tin-substituted yttrium iron garnets.[2]

(1) Iron aluminum alloys.—A very attractive model for exchange interactions in this system has been proposed by Arrott and Sato.[1] In the "ordered" alloys there are three sublattices. One of them, A, is only partially filled up with iron, and has the saturation magnetization $M_A = I\frac{1}{2}(1-2c)$ where I is the saturation magnetization of pure iron, and $c(<\frac{1}{2})$ the aluminum percentage. The other two sublattices B' and B'' are completely filled with iron and have magnetizations $M_{B'} = M_{B''} = \frac{1}{4}I$. The assumed spatial arrangement is made of planes $B'AB''AB'\ldots$ normal to a (100) direction of the bcc structure. The $B'B''$ coupling takes place through Al atoms and is antiferromagnetic. The AB' and AB'' couplings are taken as ferromagnetic. The resultant molecular fields may be written, in the notation of Yafet and Kittel,[3]

$$H_A = -n(M_{B'} + M_{B''}),$$
$$H_{B'} = -n(M_A - \gamma_2 M_{B''}),$$
$$H_{B''} = -n(M_A - \gamma_2 M_{B'}); \qquad (1)$$

n and γ_2 are negative here. $|\gamma_2| = 4c/\mu$ where μ is the absolute value of the ratio between ferromagnetic exchange integrals as defined in reference 1. A discussion similar to that of reference 3 then gives the following results:

	Ground state	Upper transition point
$0<c<c'$	Ferro	Ferro
$c'<c<c''$	Triangular	Ferro
$c''<c<\frac{1}{2}$	Triangular	Antiferro

c' and c'' are defined by the equations

$$\mu(1-2c') - 4c' = 0, \qquad (2)$$
$$\mu^2(1-2c'') - 8(c'')^2 = 0. \qquad (3)$$

Typical values are quoted below:

	$\mu = 2.00$	$\mu = 1.60$	Exp.[1]
c'	0.25	0.22	0.28
c''	0.36	0.33	0.33

The ground state is never antiferromagnetic (the different, incorrect result of reference 1 stems from the use of the Ising model). The spontaneous magnetization at $T=0$ is

$$M_0 = I(1-c), \qquad c<c'$$
$$M_0 = \tfrac{1}{2}I(1-2c)(1+\mu/4c), \quad c>c'. \qquad (4)$$

The M_0 vs c curve displays a typical change in slope which is indeed observed (Fig. 1). The low-temperature susceptibility, due to changes

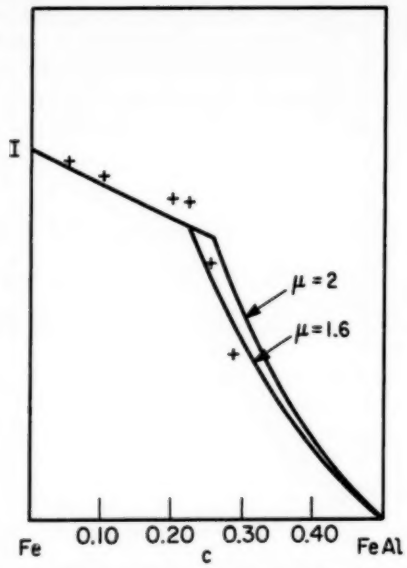

FIG. 1. Spontaneous moments in ordered iron aluminum alloys at $T=0$. Experimental points by Arrott and Sato.[1] Theoretical curves for two typical values of the exchange integral ratio μ.

of the angle between sublattice magnetizations, has the value $1/n\gamma_2$. (Detailed experimental data on this quantity are not yet available.)

(2) Sn-substituted garnets.—Pure YIG has two iron sublattices, A (octahedral) and B (tetrahedral), for which the molecular field equations may be written as[4]

$$H_A = -7000M_A - 15\,800M_B,$$
$$H_B = -15\,800M_A - 4200M_B. \qquad (5)$$

(In all equations M refers to magnetization per unit volume.) In the Sn-substituted garnets, we assume that (a) all Sn goes into the A lattice,[2] according to the symbolic formula

$$\{Y_{3-x}Ca_x\}[Sn_xFe_{2-x}](Fe_3)O_{12},$$

and (b) all exchange interactions have the values corresponding to YIG.

A natural way of further dividing A and B into sublattices is the following: The A sites form a bcc lattice and may be split into two simple cubic lattices $A'A''$. The B sites form a more complicated structure but may still be divided into two lattices $B'B''$ such that a B' site, for instance, has four nearest neighbors, all of them B''. The crystallographic positions of the B' sites in such an arrangement are the following: (3/8, 0, 1/4) (1/4, 3/8, 0)(0, 1/4, 3/8)(1/8, 0, 3/4)(3/4, 1/8,0) (0, 3/4, 1/8) plus six other positions deduced from the preceding ones by the translation (1/2, 1/2, 1/2). The molecular fields are taken to be

$$H_{A'} = n(\alpha_2 M_{A''} - M_{B'} - M_{B''}),$$
$$H_{A''} = n(\alpha_2 M_{A'} - M_{B'} - M_{B''}),$$
$$H_{B'} = n(-M_{A'} - M_{A''} + \gamma_2 M_{B''}),$$
$$H_{B''} = n(-M_{A'} - M_{A''} + \gamma_2 M_{B'}), \qquad (6)$$

where from Eq. (5) we may put $n\alpha_2 = -14\,000$, $n\gamma_2 = -8400$, $n = +15\,800$, $\alpha_2 = -0.88$, $\gamma_2 = -0.53$. The parameter $y = M_A/M_B$ of reference 3 takes the value $y = \frac{1}{3}(2-x)$. As $\alpha_2 < 1$ the A lattice never splits up in the ground state. The B lattice does split up, however, and the arrangement is then

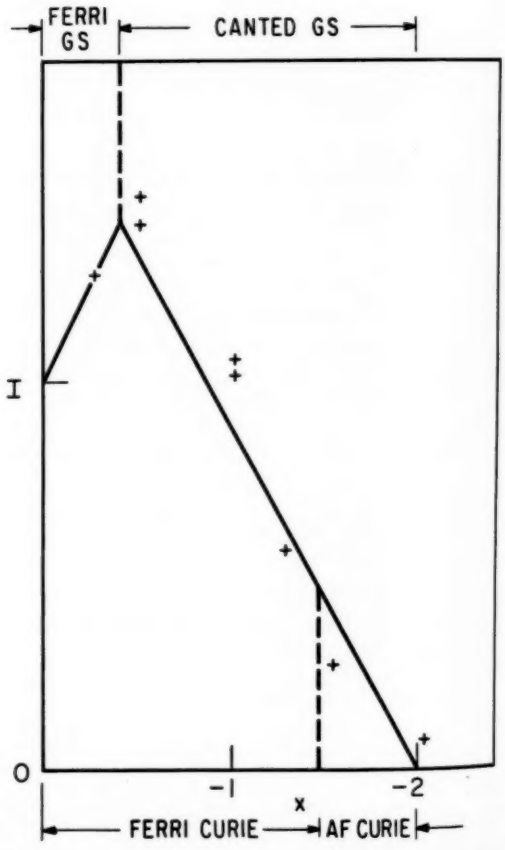

FIG. 2. Spontaneous moments in Sn-substituted YIG at $T=0$. Experimental points by Geller et al.[2]

triangular $AB'B''$, when $y < |\gamma_2|$, or $x > 0.41$. The spontaneous magnetization at $T = 0$ is

$$M_0 = I(1+x), \qquad y > |\gamma_2|$$
$$= I(2-x)(1/|\gamma_2| - 1), \quad y < |\gamma_2|, \qquad (7)$$

I being here the saturation magnetization of YIG. The resulting curve (in which there is no adjustable parameter) agrees rather well with experiment (Fig. 2). These considerations can be extended to higher temperatures. The upper Curie point corresponds to ferrimagnetic order when $y > \gamma_2^2/(2-\alpha_2\gamma_2)$, $(x < 1.45)$, and to antiferromagnetic order at higher x.

More information on these materials could be obtained from neutron diffraction, and from high-field susceptibilities (as in the manganite series).[5]

It is a pleasure to thank Professor C. Kittel for discussions on these and related matters.

---

*Supported in part by the National Science Foundation.

[1]A. Arrott and H. Sato (to be published).
[2]Geller, Bozorth, Gilleo, and Miller (to be published).
[3]Y. Yafet and C. Kittel, Phys. Rev. 87, 290 (1952).
[4]R. Pauthenet, Ann. phys. 3, 424 (1958).
[5]I. S. Jacobs, J. Phys. Chem. Solids (to be published).

ANTIPHASE ANTIFERROMAGNETIC STRUCTURE OF CHROMIUM*

L. M. Corliss and J. M. Hastings
Chemistry Department, Brookhaven National Laboratory, Upton, New York,

and

R. J. Weiss
Watertown Arsenal, Watertown, Massachusetts

(Received August 11, 1959)

In the course of a neutron diffraction study of single crystals of chromium grown by the strain-anneal method[1] it was observed that the antiferromagnetic superstructure reflections exhibited characteristic splittings. An analysis of these splittings has led to an interpretation in terms of an antiphase antiferromagnetic domain structure in analogy with antiphase domains in ordered alloys.[2]

The region around the (100) and (111) reciprocal lattice points was systematically explored by the traverses shown in Fig. 1. From the experimental observations, the intensity distribution in reciprocal space shown in Fig. 2 was deduced. This distribution can be characterized in the following manner: (a) The size of the individual

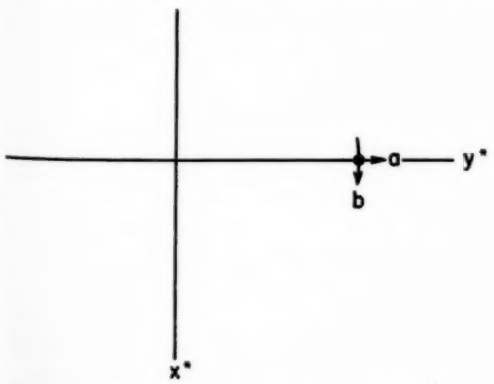

FIG. 1. Traverses of reciprocal lattice point. (a) Crystal and counter rotation in $\theta, 2\theta$ relationship, (b) Crystal rotated and counter fixed at $2\theta_{\text{Bragg}}$.

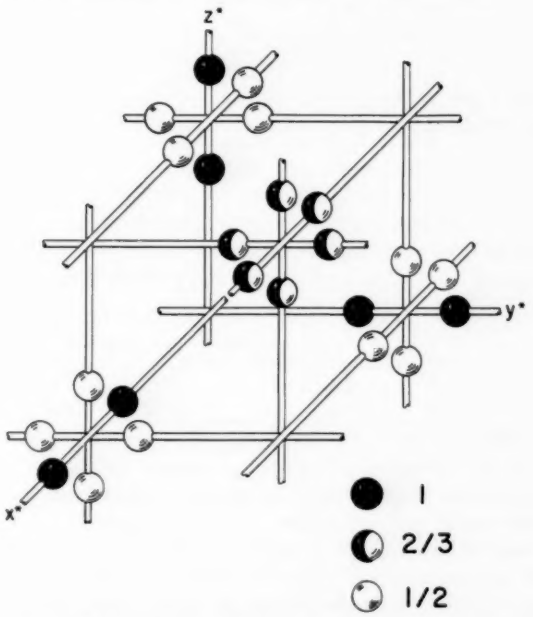

FIG. 2. Intensity distribution about the (100) and (111) reciprocal lattice points. The relative intensities are shown in the diagram.

spots is comparable to that observed for an ordinary nuclear reflection. (b) The spots in the neighborhood of each reciprocal lattice point exhibit octahedral spatial symmetry with relative intensities as shown in the figure. (c) The separation of the spots along the axes of each octahedron is $1/39\ A^{-1}$.

The following model accounts for the above observations. The antiferromagnetic structure of chromium (bcc) is one in which the body-centered spin is antiparallel to the corner spin. The splitting of the superstructure peaks is produced by platelike antiphase domains in which 180° spin reversals in the antiferromagnetic spin arrangement occur every 14 unit cells normal to the antiphase boundaries as follows:

$$+-+-+-+-+-+-\Big\}-+-+-+-+-+-+\Big\}+-+-\ \text{etc.}$$

These antiphase domain boundaries are parallel to the crystallographic cube faces, but the crystal as a whole consists of a random arrangement of regions in any one of which the domain boundary is parallel to a particular cube face. Within a domain the spins are parallel to the domain boundary. It is this restriction on spin direction which accounts for the observed relative intensities of the spots in the reciprocal lattice given in Fig. 2 since the magnetic intensity depends on the relative orientations of the spin and scattering vectors.

From the integrated intensities of the magnetic superstructure peaks (100), (111), and (210), the Bohr magneton number is found to be 0.4 ± 0.05 in agreement with Shull and Wilkinson.[3] It was also found that the magnetic form factor is in agreement with that of Mn^{+2}.[4] The magnetic intensity of the (100) peak as a function of temperature agreed with that derived from the Brillouin function for spin $\frac{1}{2}$ and gave a Néel temperature of $35°C \pm 2°$ which coincides with other physical anomalies such as resistivity, Young's modulus, and lattice expansion. This temperature, however, is not in agreement with powder neutron diffraction data previously reported by Shull and Wilkinson[3] ($T_N \cong 175°C$) and recently confirmed by us.

The origin of the antiphase domains is not known but a recent proposal of Kaplan[5] points out the possibility of lowering the energy by virtue of a nearest and next-nearest neighbor interaction, both of which are antiferromagnetic. In his proposed model the spins do not make an abrupt 180° reversal but rather spiral with a fixed period.

We wish to thank Professor C. G. Shull for his help in the initial experiments, Dr. T. Kaplan for discussions, and Dr. Earl Hays of the Bureau of Mines for supplying us with several samples of chromium.

---

* Research performed under the auspices of the U. S. Atomic Energy Commission.

[1] These crystals were supplied by Dr. H. Lipsitt at Wright Air Development Center.

[2] C. H. Johansson and J. O. Linde, Ann. Physik 25, 1 (1936).

[3] C. G. Shull and M. K. Wilkinson, Revs. Modern Phys. 25, 100 (1953).

[4] Corliss, Elliott, and Hastings, Phys. Rev. 104, 924 (1956).

[5] T. Kaplan (private communication).

HYPERFINE COUPLING IN CoFe AND CoNi ALLOYS AS DETERMINED BY HEAT CAPACITY MEASUREMENTS*

V. Arp,† D. Edmonds, and R. Petersen
Department of Physics, University of California, Berkeley, California
(Received August 5, 1959)

Each nucleus in a ferromagnet experiences an effective magnetic field (H_{eff}) caused by the hyperfine interaction with unpaired electrons. Marshall[1] has calculated the various contributions to this effective field and has shown how these contributions may be expected to depend on the electronic configuration surrounding the nucleus. The hyperfine interaction gives rise to a nuclear polarization at low temperatures and to a nuclear contribution to the specific heat given by

$$\frac{C_n}{Nk} = \tfrac{1}{3}\frac{I+1}{I}\left(\frac{\mu H_{\text{eff}}}{kT}\right)^2 + O\left(\frac{\mu H_{\text{eff}}}{kT}\right)^4,$$

where N is the number of nuclei, μ and I are the nuclear moment and spin, respectively, and k is Boltzmann's constant. Similar contributions to the specific heat in a ferromagnetic metal have previously been measured in cobalt[2-4] and

terbium.[4,5]

We have measured the specific heat of some CoFe and CoNi alloys in order to obtain further information about the electronic configuration in these iron group elements in connection with the suggestion of Weiss[6] that only about two $3d$ electrons are localized around each iron atom in metallic iron, whereas the conventional numbers of $3d$ electrons are 8.3 and 9.4 for metallic cobalt and nickel, respectively. The naturally occuring isotopes of iron and nickel have zero nuclear magnetic moment, whereas that of cobalt (Co^{59}) has a nuclear moment of 4.583 nuclear magnetons and a spin of 7/2. Thus the nuclear specific heat measured in the CoFe and CoNi alloys enables one to deduce the value of H_{eff} acting at a cobalt nucleus.

An annealed sample of alloy weighing about 12 grams was suspended inside a standard demagnetizing cryostat and linked through a lead superconducting thermal switch to a paramagnetic salt. By adiabatic demagnetization of the salt the sample was cooled to 0.35°K and then thermally isolated from the salt. The temperature of the sample was measured by means of a carbon resistance thermometer which was calibrated from 1°K to 0.35°K against the measured susceptibility of the paramagnetic salt during each experiment. Specific heat measurements were made in the range 0.35°K to 0.7°K. In this range only the nuclear ($\propto T^{-2}$) and electronic ($\propto T$) contributions to the specific heat are appreciable; the total specific heat has the form $C = aT^{-2} + bT$. By plotting CT^2 against T^3 a straight line was obtained from which the separate contributions were directly obtained. The experimental results are shown in Table I. The electronic specific heats of cobalt and iron are in reasonable agreement with the previously measured value of $5.0T$ millijoules/mole °K for both cobalt and iron.[7] In Fig. 1 the values of H_{eff} are plotted against cobalt concentration. The crystal structure of each specimen indicated in Fig. 1 was checked by x-ray diffraction of the specimen.

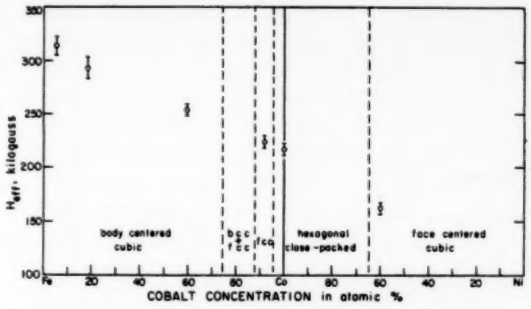

FIG. 1. Values of the effective (hyperfine) field as a function of cobalt concentration.

The approximately linear relation obtained in Fig. 1 gives no hint of any discontinuities in H_{eff} such as might be expected if the electronic configuration around each iron atom, and hence around each cobalt atom, were to change rapidly in a narrow concentration range. Such a rapid change, coming from an increase in the number of $3d$ electrons localized at each iron atom, has been postulated by Lomer and Marshall[8] to occur at about 35% Co in Fe, and by Mott and Stevens[9] at the bcc-fcc phase transition. Furthermore in the alloys of cubic structure the dipolar contribution to H_{eff} is zero, while in hexagonal cobalt the dipolar contribution has been estimated by Marshall to be some 81 kilogauss. There are however theoretical reasons to believe that this figure was considerably overestimated, as the band character was neglected entirely in making the estimate. Figure 1 shows that H_{eff} in hexag-

Table I. Experimental results.

Alloy [atomic %]	Specific heat [millijoules (mole °K)$^{-1}$]	H_{eff} [kilogauss]
60.0 Co, 40.0 Ni	$(1.55 \pm 0.07)(1/T^2) + (7.5 \pm 0.4)T$	161 ± 3
100 Co	$(4.78 \pm 0.12)(1/T^2) + (5.6 \pm 0.3)T$	219 ± 4
91.5 Co, 8.5 Fe	$(4.56 \pm 0.12)(1/T^2) + (4.7 \pm 0.7)T$	223 ± 4
58.7 Co, 41.3 Fe	$(3.87 \pm 0.07)(1/T^2) + (4.3 \pm 0.2)T$	256 ± 3
17.2 Co, 82.8 Fe	$(1.48 \pm 0.10)(1/T^2) + (3.8 \pm 0.3)T$	293 ±10
4.8 Co, 95.2 Fe	$(0.47 \pm 0.03)(1/T^2) + (4.7 \pm 0.2)T$	314 ± 9
100 Fe	$(0.1 \pm 0.2)(1/T^2) + (4.9 \pm 0.5)T$	...

onal cobalt has essentially the value one would deduce from the approximately linear variation found in the cubic alloys.

Our thanks are due to Dr. N. Kurti for his initial stimulus in this investigation, to Dr. C. Kittel for his continued interest, and to Dr. W. Marshall for many discussions.

---

*Supported by the National Science Foundation.

†Now at the National Bureau of Standards, Boulder, Colorado.

[1]W. Marshall, Phys. Rev. 110, 1280 (1958).

[2]C. V. Herr and R. A. Erickson, Phys. Rev. 108, 896 (1957).

[3]Arp, Kurti, and Petersen, Bull. Am. Phys. Soc. 2, 388 (1957).

[4]N. Kurti, Suppl. J. Appl. Phys. 30, 215 (1959).

[5]N. Kurti and R. S. Safrata, Phil. Mag. 3, 780 (1958).

[6]W. Marshall and R. J. Weiss, Suppl. J. Appl. Phys. 30, 220 (1959).

[7]P. H. Keesom and N. Pearlman, Handbuch der Physik, edited by S. Flügge (Springer-Verlag, Berlin, 1956), Vol. 14, p. 322.

[8]W. Lomer and W. Marshall, Phil. Mag. 3, 185 (1958).

[9]N. F. Mott and K. W. Stevens, Phil. Mag. 2, 1364 (1957).

ELECTROLUMINESCENCE AT POINT CONTACTS IN CUPROUS OXIDE AND THE MOBILITY OF Cu^+ IONS AT ROOM TEMPERATURE

R. Frerichs and I. Liberman
Department of Electrical Engineering, Northwestern University, Evanston, Illinois
(Received August 3, 1959)

The observation of electroluminescence in Cu_2O between -50 and +50°C[1] makes it possible to study the very small mobility of Cu^+ ions in this temperature range. Cu^+ vacancies, which are involved in the radiation emission in Cu_2O, are moved from the cathode, where the emission takes place, to the anode by the same field which produces the electroluminescence. In a one-dimensional arrangement this effect can be used to study the mobility of Cu^+ vacancies, which is of course identical with that of the Cu^+ ions.

A flattened copper wire ($d = 0.5$ mm) is oxidized at 1040°C, cooled in high vacuum, and mounted with four electrodes in a glass vacuum container (Fig. 1). A field of 800 volts/cm which moves the vacancies is applied between two platinum electrodes, Pt_1 and Pt_4, which are spaced 1.2 mm apart and are pressed by springs onto the Cu_2O. Platinum, due to its high work function, forms ohmic contacts with the p-type Cu_2O. The electroluminescence is observed at two zinc knife edges, Zn_2 and Zn_3, which are spaced 0.21 mm apart. Zinc with its low work function forms rectifying contacts with Cu_2O. A barrier layer at the cathode is the necessary condition for the generation of electroluminescence in this material. The radiation pulses ($\lambda = 0.8$ to 1.2 μ) are studied with an infrared-sensitive photomultiplier, a double-trace cathode-ray oscilloscope, and a Polaroid camera. Alternate periods of "driving" the vacancies by the dc field applied to Pt_1 and Pt_4 and of "reading out" the concentration of the vacancies at the electrodes Zn_2 and Zn_3 with ac (200 cycles/sec, 60 volts) are used (Fig. 2). If the distribution of the vacancies at the beginning of the experiment is uniform throughout the sample, a field in the direction Pt_4–Pt_1 will drive them towards Pt_4. The radiation pulses at Zn_2 and Zn_3 are observed at the scope. As the "read-out" voltage is simultaneously shown at the second trace of the scope, the radiation pulses which show up at the negative electrode can be coordinated to Zn_2 or Zn_3. The "read-out" period is short (2 sec) in order to prevent additional motion of the vacancies due to the ac field.

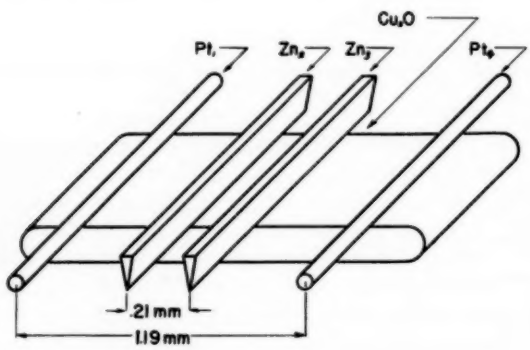

FIG. 1. Arrangement of electrodes on cuprous oxide.

Figure 2 gives the radiation pulses as function

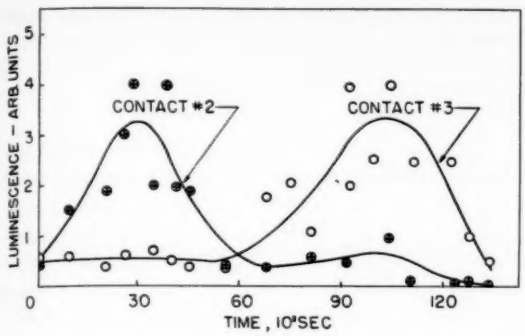

FIG. 2. Luminescence at contacts Zn_2 and Zn_3 as function of the "driving" time.

of the "driving" time. From the time necessary to shift the maximum of emission from Zn_2 to Zn_3 and from the field applied between Pt_1 and Pt_4 the mobility is determined to be $\lambda = 5\times10^{-10}$ cm²/volt sec. This determination is made under the assumption that the field between Pt_1 and Pt_4 is uniform and that the emission takes place close to the knife edges.

Mobilities of such small order have not been observed by other methods. From the conductivity and the transference number the mobility of Cu^+ ions in Cu_2O at 1000°C has been determined to be 5×10^{-4} cm²/volt sec.[2] Measurements of the diffusion coefficients of Cu^+ ions in Cu_2O, which are proportional to the mobility, have been made for 800, 900, and 1000°C.[3] An extrapolation of these values to room temperature does not seem to be justified. Experiments are in progress to study the mobility over the range -50 to +50°C. Furthermore, an analysis of the rearrangement of the vacancies after the driving field has been taken off should yield a test of the Nerst-Townsend-Einstein relation between diffusion coefficient and mobility. Finally it should be stated that such a determination of mobility and diffusion coefficient should be possible in other cases. For instance, in AlN the properties of the observed electroluminescence point to the same mechanism as it is assumed for Cu_2O.[4]

A detailed analysis of the electroluminescence at point contacts on Cu_2O, which forms the Master's thesis of I. Liberman, will be published in the near future.

[1]R. Frerichs and R. Handy, Phys. Rev. 113, 1191 (1959).

[2]C. Wagner and H. Hammen, Z. physik. Chem. (Leipzig) B40, 197 (1938).

[3]Bardeen, Brattain, and Shockley, J. Chem. Phys. 14, 714 (1946); G. W. Castellan and W. J. Moore, J. Chem. Phys. 17, 41 (1949).

[4]Wolff, Adams, and Mellichamp, Phys. Rev. Letters 3, 72 (1959).

PRESSURE EFFECTS AND CONFIGURATION COORDINATE MODELS OF KCl(Tl)*

L. Reiffel
Physics Division, Armour Research Foundation, Chicago, Illinois
(Received June 18, 1959; revised manuscript received July 24, 1959)

Extensive, albeit conflicting, theoretical calculations have been made in an attempt to account for the observed characteristics of the phosphor KCl(Tl). On the one hand, Williams and his coworkers have developed a theoretical configuration coordinate model for KCl(Tl) in a series of papers, the most recent of which[1] incorporates spin-orbit interaction and crystalline field effects for the $^3P^\circ$ and $^1P^\circ$ states of Tl^+ in KCl. These considerations lead to a configuration coordinate curve for the lowest excited state of substitutional Tl^+ exhibiting two minima which are suggested to account for the 3050 A and 4750 A emissions observed for KCl(Tl). The single coordinate in this model is taken to be the symmetrical radial displacement of the six nearest-neighbor Cl^- ions from the Tl^+ since earlier work had indicated that transition energies depend most strongly on this coordinate. The two minima in the lowest excited state of the Williams and Johnson model are separated in energy by 0.025 ev and are assumed to be in thermal equilibrium to account for observed temperature dependence of the ratio of 4750 A to 3050 A emission.[2]

On the other hand, Patterson and Klick[3] have presented evidence that the excitation spectra for the 3050 A emission and the 4750 A emission are different and propose, among other possibilities, that two entirely different thallium centers rather than two states (or one state with two potential minima) of the same center are involved. Thermal quenching in the 4750 A center, but not

in the 3050 A center, is then presumed to account for the dependence on temperature. Recently, Knox[4] has examined configuration interactions and electron transfer states and has suggested qualitative configuration coordinate curves for the states of interest which again do not involve the double minimum of the Williams and Johnson model.

It appears that a critical test of the validity of the Williams and Johnson model may be made using the methods already developed for general study of pressure effects and described elsewhere.[5] Consider the double-minimum configuration coordinate curve of their model as shown in Fig. 1, curve A, somewhat enlarged in energy scale from the original in reference 1. The abscissa is specifically the $Tl^+ - Cl^-$ separation. Application of hydrostatic stress in such a situation is equivalent[5] to adding a pressure-dependent contribution $E_p = \alpha p r$ to the original configuration coordinate curve. Here p is the applied pressure, α is the effective area of the system, and r is the $Tl^+ - Cl^-$ separation. If we take p as 40 000 psi and α as the projected area of the six nearest-neighbor Cl^- ions or 62 A^2 we obtain E_p (ev) $= 0.107 r$(A). The numerical value of α assumed is the same as that used by Johnson and Williams[6] to explain successfully their observations of a pressure shift in the absorption spectrum of KCl(Tl). Thus, since the two minima of Fig. 1 are normally separated by $\Delta r = 0.25$ A and by about 0.025 ev in E, radical changes are to be expected upon application of pressure as illustrated by curve B which is constructed to scale in energy. In general, a change in the emission

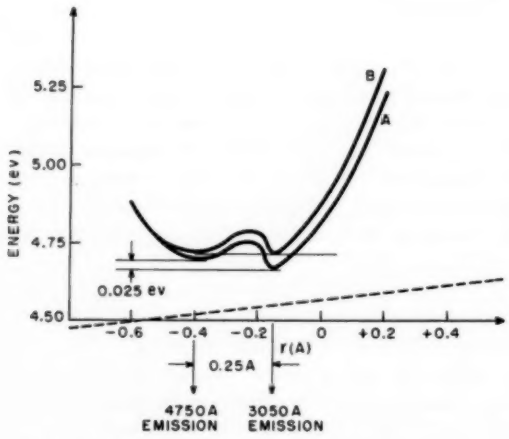

FIG. 1. Normal and pressurized configuration coordinate curves for KCl(Tl).

intensity of the 4750 A band relative to the 3050 A band by a factor R should be observed, where

$$R = \frac{\exp(\alpha p \Delta r - 0.025)/kT}{\exp(-0.025)/kT}.$$

Note that since thermal equilibrium between the two minima is assumed and is fundamental to the model, the excitation method should be immaterial. For 40 000 psi and 273°K, the model would require $R = 2.7$. Furthermore, for pressures above about 40 000 psi, the relative energy of the two minima changes sign, thus the temperature dependence of the intensity ratio for the two bands should go through zero and reverse.

We have studied R as a function of pressure in the vicinity of room temperature. The phosphor used was a single KCl crystal[7] grown from a melt containing 0.00018 Tl (mole fraction). Separation of the 3050 A and 4750 A emission was accomplished with Corning filters No. 9863 and No. 3389. In some cases, the shorter wavelength emission was isolated using an interference filter peaking at 3025 A with a bandwidth of about 150 A. At room temperature, the 3050 band shows a half-width of about 400 A and a long-wavelength tail[8] which extends to perhaps 4200 A but only about one percent of the emission lies beyond 3800 A. The 4750 A band typically exhibits about one-third the peak intensity of the 3050 A emission with a half-width of about 1200 A at room temperature.[9] For room temperature and below, the two emission bands can be adequately separated by the filters used and no appreciable reduction in the apparent value of R due to band overlap should occur.

The crystal, installed in a pressure vessel with quartz optics, was stimulated with an Ir^{192} gamma-ray source in a tungsten alloy collimator. Light emission was measured with a cooled type 5819 photomultiplier tube driving a standard electrometer circuit and equipped with a sodium salicylate wavelength shifter. Window luminescence and dark currents were investigated and shown to be negligible. Pressure changes in the optical coupling system amount to about five percent at 40 000 psi and are not strongly wavelength dependent.

Experimental results for R are shown in Table I. Clearly, practically no change in the ratio of 4750 A emission to 3050 A emission occurs under the conditions of this experiment. The small systematic change with temperature that may exist is felt to be the result of excitation of trapping states which feed the emitting states

Table I. Effect of pressure on band intensity ratio.

Temp °C	R for 40 000 psi
19	0.96
9.5	0.98
0	1.04
0	1.07
0	1.05

under observation. Since a straightforward extension of the Williams and Johnson configuration coordinate curves for the first excited state of KCl(Tl) coupled with their assumption of thermodynamic equilibrium requires very large changes in the emission ratio, these results do not lend support to their model. It appears that alternatives of the sort considered by Patterson and Klick and by Knox may be better able to describe the actual situation. These latter suggestions can be arranged to predict small changes in intensity ratio due to pressure.

The author wishes to acknowledge the assistance of R. M. Norton and J. F. Lemke in performing these experiments.

*This research was supported by the U. S. Air Force through the Air Force Office of Scientific Research of the Air Research and Development Command.

[1] F. E. Williams and P. D. Johnson, Phys. Rev. 113, 97 (1959).

[2] Very recently a possible alternative model for the Tl center dealing with the 3050 A emission and a new band at 2470 A has been proposed by these authors, but this work is still in a very preliminary stage since it does not deal with the 4750 A emission nor does it yet explain all previously available experimental data so it cannot be discussed further at this time. See P. D. Johnson and F. E. Williams, Bull. Am. Phys. Soc. 4, 147 (1959).

[3] D. A. Patterson and C. C. Klick, Phys. Rev. 105, 401 (1957).

[4] R. S. Knox, Phys. Rev. (to be published).

[5] L. Reiffel, Phys. Rev. (to be published).

[6] P. D. Johnson and F. E. Williams, Phys. Rev. 95, 69 (1954).

[7] Kindly supplied by Dr. C. J. Delbecq of Argonne National Laboratory.

[8] W. von Meyeren, Z. Physik 61, 321 (1930).

[9] W. Bunger and W. Flechsig, Z. Physik 67, 42 (1931); 69, 637 (1932).

g FACTOR OF ELECTRONS IN GERMANIUM*

Laura M. Roth and Benjamin Lax
Lincoln Laboratory, Massachusetts Institute of Technology, Lexington, Massachusetts
(Received August 12, 1959)

The failure, until recently, to detect spin resonance of electrons in germanium can be attributed to the anomalous character of the g factor. Two sets of experiments, one on the Zeeman effect of the indirect exciton[1] and a second on spin resonance of shallow donors in germanium,[2] have shed some light on this matter. In order to account for the g factor in the Zeeman experiments, Roth[3] has extended the perturbation calculation developed for spherical bands[4] and has applied these to the conduction band. The results of these calculations when only the nearest bands are considered and small terms due to more distant bands are neglected, show that the g factor of the electrons on a single ellipsoidal energy surface is anisotropic and is given by

$$g_{\parallel} - 2 \approx (-\delta/\Delta\mathcal{E}_{13}')[m/m_t - 1], \quad (1)$$

$$g_{\perp} - 2 \approx (-\delta/\Delta\mathcal{E}_{13}')[m/m_l - 1] + \Delta g_{\perp}', \quad (2)$$

where δ is the spin-orbit splitting of the L_3' valence band at the [111] edge of the Brillouin zone. We can estimate δ by using the wave functions at the center of the zone, giving $\delta \approx (2/3)\Delta$ where $\Delta = 0.3$ ev is the splitting of the valence band at $k = 0$. Hence $\delta \approx 0.2$ ev. $\Delta\mathcal{E}_{13}'$ is the energy separation of the L_3' and the L_1 band edges, the latter being the conduction band. The value of $\Delta\mathcal{E}_{13}'$ can be estimated from the experiments of Philipp and Taft[5] who find a strong absorption at ~2 ev which we believe corresponds to a vertical or direct transition of electrons from the L_3' band to the L_1 band.[6] The effective masses $m_t = 0.082m_0$ and $m_l = 1.68$ are those obtained from cyclotron resonance[7] and $g_{\parallel}$ and $g_{\perp}$ are the components of the g factor along and transverse to the principal axis of the ellipsoid, respectively. $\Delta g_{\perp}'$ is a small correction contributed by a term involving the L_3 band which is 5 ev above the L_1 band.[8] The sign of this term is uncertain

but the magnitude can be estimated. If we use the numbers above we find that

$$g_{\parallel} \approx 0.9, \qquad g_{\perp} \approx 2.04 \pm 0.04, \tag{3}$$

where the plus or minus sign reflects the ambiguity of sign of $\Delta g_{\parallel}'$. For a free electron which is moving in a single ellipsoidal surface, the effective g value is given by

$$g^2 = g_{\parallel}^2 \cos^2\phi + g_{\perp}^2 \sin^2\phi, \tag{4}$$

where ϕ is the angle which the magnetic field makes with the principal axis. If all the ellipsoids are taken into account then the g factor for the electrons would show an anisotropic character in the (110) plane as shown in Fig. 1.

This anisotropy should show up in the Zeeman experiments of the excitons. However, the present experiments[1] have as yet not explored this although the spin value of $1.6 \pm 15\%$ obtained from them in the [100] direction is consistent with the theoretical results. For the spin resonance experiments of Feher, Wilson, and Gere,[2] the results for bound donors of arsenic and phosphorus indicate that the electrons are in the singlet state in which the electron wave function is a symmetric linear combination of the four minima. The g factor in this case becomes isotropic and is given by

$$g = \tfrac{1}{3} g_{\parallel} + \tfrac{2}{3} g_{\perp}. \tag{5}$$

The g value obtained by the spin resonance for these two impurities is $g = 1.57$. Since $g_{\perp}$ is close to 2, using Eq. (5) we deduce that $g_{\parallel} = 0.63 \pm 0.08$. This is smaller than the value predicted from room-temperature data for the bands. Using Eq. (1) we find that $\Delta \mathcal{E}_{13}' \approx 1.6$ ev, which is somewhat smaller than the value obtained from the data of Philipp and Taft. The possibility exists that the bands L_1 and L_3' move closer to one another as the temperature is lowered, although this is in contrast to the change of the indirect gap with temperature. The alternative is that the estimate of δ may be too small.

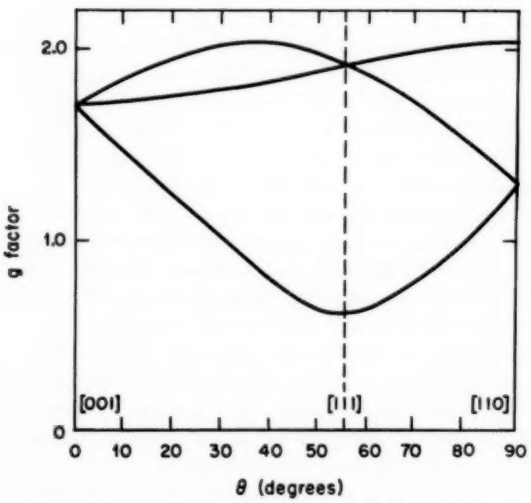

FIG. 1. Anisotropy of the g factor of free electrons in germanium with $\vec{H}$ in the $(1\bar{1}0)$ plane.

In antimony-doped germanium the g factor shows an anisotropy which varies from 1.6 with $H \parallel [100]$ to 1.9 with $H \parallel [\bar{1}10]$ direction.[2] Since this is a shallower impurity than arsenic or phosphorus, the degeneracy of the singlet and the triplet states is probably not split as much. The experimental[9] values of the binding energy are 14.0×10^{-3} ev, 12.8×10^{-3} ev, and 9.8×10^{-3} ev for As, P, and Sb, respectively, as compared to the theoretical value[10] of 9.2×10^{-3} ev. The estimated separations between the singlet and triplet are thus 5.8×10^{-3} ev, 3.6×10^{-3} ev, and 0.6×10^{-3} ev. Consequently the anisotropy may be due to the presence of the triplet state for antimony impurity. There are three g factors in this instance which must be obtained by solving a six-by-six secular equation. The results obtained to first order in the anisotropy, good to about 10%, are, for $\vec{H}$ in a $(1\bar{1}0)$ plane,

$$g_1 = \bar{g} + \tfrac{1}{3}(g_{\perp} - g_{\parallel}) \sin^2\theta,$$

$$g_{2,3} = \bar{g} - \tfrac{1}{6}(g_{\perp} - g_{\parallel})\{\sin^2\theta + \sin\theta\,(1 + 15\cos^2\theta)^{1/2}\}, \tag{6}$$

where $\bar{g}$ is given by Eq. (5), and θ is the angle of the magnetic field with the [001] axis. The anisotropy of the g factors associated with the triplet is shown in Fig. 2. Higher order terms in $(g_{\perp} - g_{\parallel})$ split the degeneracy as is indicated by the dashed lines in the figure. This structure has not yet been observed by the spin resonance experiments.

It is suggested that experiments at higher temperatures, i.e., 77°K, should permit the observation of the free-electron resonance corresponding to Fig. 1, whereas 4°K experiments with antimony or possibly lithium impurities should permit the anisotropy observations of the triplet. Such experiments in these and other semiconductors can apparently provide information about the bands, from the deviation of the g factor from 2 and from the anisotropy. This is particularly

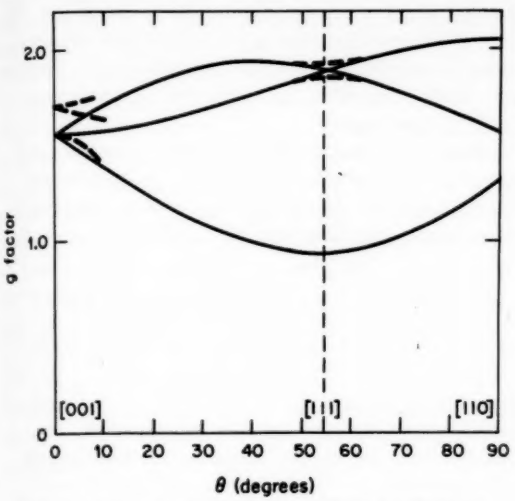

FIG. 2. Anisotropy of the g factor of bound electrons in the triplet state in germanium with $\vec{H}$ in the (110) plane. The solid lines are the first-order theory [Eq. (6)] and the splitting of the degeneracies are indicated by the dashed lines.

promising where the spin-orbit effect is large.

We would like to thank Dr. J. C. Phillips for his interest and helpful suggestions in connection with this problem.

*The work reported in this paper was performed by Lincoln Laboratory, a center for research operated by Massachusetts Institute of Technology with the joint support of the U. S. Army, Navy, and Air Force.

[1] Button, Roth, Kleiner, Zwerdling, and Lax, Phys. Rev. Letters 2, 161 (1959).

[2] Feher, Wilson, and Gere, Phys. Rev. Letters 3, 25 (1959).

[3] L. M. Roth, Lincoln Laboratory Research Quarterly Progress Report, January, 1959 (unpublished), p. 45.

[4] Roth, Lax, and Zwerdling, Phys. Rev. 114, 90 (1959).

[5] H. R. Philipp and E. A. Taft, Phys. Rev. 113, 1002 (1959).

[6] This has also been suggested by J. C. Phillips (private communications).

[7] Dexter, Zeiger, and Lax, Phys. Rev. 104, 637 (1956).

[8] J. C. Phillips, Phys. Rev. 112, 685 (1958).

[9] H. Y. Fan and P. Fisher, J. Phys. Chem. Solids 8, 270 (1959).

[10] W. Kohn, in Solid State Physics, edited by F. Seitz and D. Turnbull (Academic Press, Inc., New York, 1957), Vol. 5, p. 257.

INELASTIC ELECTRON SCATTERING FROM CARBON*

W. C. Barber and F. E. Gudden†
High-Energy Physics Laboratory, Stanford University, Stanford, California
(Received August 13, 1959)

We have measured the energy spectrum of electrons inelastically scattered from nuclei, with the aim of studying the giant-resonance region of nuclear excitation. Scattered electrons corresponding to excitation of the giant resonance have been observed at large angles for targets of Si and C. The scattering distribution from C has been investigated in some detail, and a scattering peak corresponding to a nuclear excitation of 15 Mev is also observed. The results indicate that the investigation of nuclear properties by inelastic electron scattering, which has already been successful in the study of many low-lying states,[1] can be extended to other types of nuclear excitation and can be carried out with lower-energy electron beams.

The Mark II linear accelerator[2] and an 18-in. double-focusing spectrometer[3] were used for the experiment. The double magnetic deflecting system of Mark II was set to $E_0 = 42.6$ Mev, with an energy spread of 1%.

For the measurement of the energy distribution of electrons scattered through 160°, we used a graphite target 0.327 g/cm² thick. The scattered and magnetically analyzed electrons were detected by means of two plastic scintillators, one mounted directly on the photocathode of an RCA-6810 photomultiplier, the other supported on an aluminum reflector, $1\frac{3}{4}$ in. in front of the second photomultiplier. The output pulses of the photomultipliers were fed directly into a coincidence circuit with a 6-mμsec resolution time. Use of coincidences significantly reduced the background, which was mainly due to neutrons. Beam monitoring initially was done with a secondary-emission monitor and later with a Faraday cup.

Figure 1 shows the results. The target-out background has been subtracted from each meas-

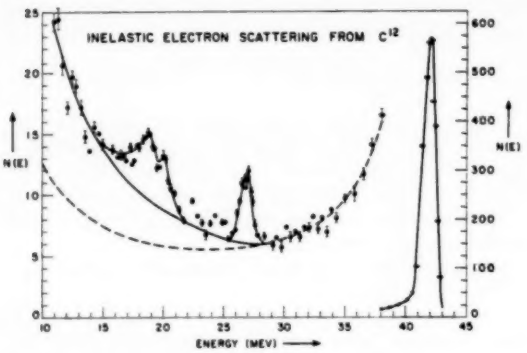

FIG. 1. Energy distribution of electrons scattered at 160° from carbon. The elastic peak is shown at the right with the ordinate scale indicated on the right margin. The dashed curve is the calculated tail of the elastic peak due to bremsstrahlung. The solid curves were drawn arbitrarily. The points without statistical errors indicated have errors comparable with those of neighboring points.

ured point, and the elastic peak has been corrected for counting losses. All points are corrected for the dispersion of the spectrometer to give the number of electrons at a certain energy per energy interval. Also shown is the calculated tail of the elastic peak due to bremsstrahlung accompanying the scattering event or produced in separate collisions preceding or following the scattering. While the agreement between the theoretical radiation tail and the measured spectrum is excellent for high energies, there is an increasing discrepancy toward lower final electron energies. Whether this is due to excitation of additional levels in the carbon nucleus, to contamination of the primary electron beam by low-energy electrons, or to some other cause, is not known. The sharp peak at 27 Mev undoubtedly belongs to the excitation of the well-known 15.1-Mev level with $J=1^+$, which is the first $T=1$ level in carbon. The giant resonance should be in the region of 19 Mev in Fig. 1. The data suggest two peaks, one at 20 Mev and the other at 19 Mev, corresponding to excitation energies of 22 and 23 Mev, respectively.

The expression

$$\frac{d\sigma_e}{d\Omega}(E_0, k_f, l) = \frac{dN_e}{d\Omega}(E_0, \theta, k_f, l)\frac{\sigma_\gamma(k_f)}{k_f} \qquad (1)$$

relates the inelastic-scattering cross section to the photon-absorption cross section $\sigma_\gamma(k_f)$, through the concept of virtual photons. In Eq. (1), $dN_e/d\Omega$ represents the virtual-photon intensity associated with a transition energy k_f and multipole order specified by l due to electrons scattering at an angle θ.

Dalitz and Yennie[4] have given expressions for virtual photon spectra which are in convenient form for determining $dN_e/d\Omega$. As an example we give the expression for $M1$ transitions:

$$\frac{dN_e^{M1}}{d\Omega} = \frac{\alpha}{4\pi^2}\left[\frac{p^2+p'^2+pp'(1-\cos\theta)}{p^2(1-\cos\theta)}\right]\frac{(1-\frac{1}{3}k^2\langle r^2\rangle)}{(1-\frac{1}{3}k_f^2\langle r^2\rangle)}, \qquad (2)$$

where p and p' are the magnitudes of the electron's momentum before and after scattering, respectively; k is the magnitude of the momentum transferred; and the units are such that $\hbar=c=1$. The terms containing $\langle r^2\rangle$ are an approximate small correction[5] for the finite nuclear radius r.

The relative areas of inelastic and elastic peaks can be expressed simply in terms of the integral of Eq. (1) and the Mott cross section for elastic scattering $d\sigma(E_0, Z)/d\Omega$. The result is

$$\frac{\text{Area}_{\text{inelastic}}}{\text{Area}_{\text{elastic}}} = \frac{\int (dN_e/d\Omega)\, k_f^{-1}\sigma_\gamma(k_f)\, dk_f}{[d\sigma(E_0, Z)/d\Omega]F^2(kr)}, \qquad (3)$$

where $F(kr)$ is the form factor for a momentum transfer $k = 2E_0\sin(\theta/2)$.

If the resonance is narrow, k_f and $dN_e/d\Omega$ can be considered constant and can be taken out of the integral in Eq. (3). The equation can then be solved for the integrated cross section for γ absorption.

For the peak at 27 Mev the measured ratio of the areas is 0.82×10^{-2}. The transition is magnetic dipole; therefore we use Eqs. (2) and (3), together with $F^2(kr)=0.7$ and $\langle r^2\rangle=(2.4\times10^{-13})^2$ taken from reference 1, to find an integrated cross section of 1.47 Mev-mb. Because of the uncertainties in the form factors involved in the theory, the result could be in error by approximately 20%. Fuller and Hayward[6] found (1.9 ± 0.27) Mev-mb, and Garwin[7] found (2.3 ± 0.19) Mev-mb for the integrated cross section by studying the elastic scattering of γ rays from this level.

A similar calculation for the giant resonance, assuming only $E1$ transitions and taking the area enclosed by the solid lines, which is 0.02 times the elastic peak, yields a value of 41 Mev-mb

for the integrated cross section. This is about three times smaller than the sum of the (γ, n) and (γ, p) integrated cross sections. Part of the discrepancy is because of the uncertainty in determining the background curve. The smooth curve we have drawn is certainly too high in that it does not allow for the long tail which is known to be present on the high-energy side of the (γ, n) cross section.[8] Until the difference between the calculated radiation tail and the measurements at low electron energies is understood, we have no unique way of determining the background curve. A quantitative interpretation of our results also requires a better understanding of the nuclear form factors in inelastic scattering for the process where the nucleus is excited as well as for the background process where bremsstrahlung occurs during the scattering.

*Supported by the Office of Naval Research, the U.S. Atomic Energy Commission, and the Air Force Office of Scientific Research.

†On leave from Technische Hochschule Darmstadt, under a grant from the German Ministry for Atoms.

[1] J. H. Fregeau and R. Hofstadter, Phys. Rev. 99, 1503 (1955).

[2] R. F. Post and N. S. Shiren, Rev. Sci. Instr. 26, 205 (1955).

[3] Constructed with the aid of a grant from the Research Corporation.

[4] R. H. Dalitz and D. R. Yennie, Phys. Rev. 105, 1598 (1957).

[5] W. C. Barber, Phys. Rev. 111, 1642 (1958).

[6] E. G. Fuller and E. Hayward, Phys. Rev. 106, 991 (1957).

[7] E. L. Garwin, Phys. Rev. 114, 143 (1959).

[8] Barber, George, and Reagan, Phys. Rev. 98, 73 (1955).

NUCLEAR RESONANCE ABSORPTION OF GAMMA RAYS IN Ir^{191}†

P. P. Craig, J. G. Dash, A. D. McGuire, D. Nagle, and R. R. Reiswig
Los Alamos Scientific Laboratory, University of California, Los Alamos, New Mexico
(Received August 3, 1959)

Conditions for resonant absorption of nuclear gamma rays are difficult to obtain, since the natural widths of nuclear excited states are typically small compared to the energy lost to nuclear recoil by the emitted gamma ray.[1] If E_0 is the energy of the nuclear excited state and the nucleus is free to recoil, the gamma-ray energy will be $E_0 - R$, where R is the recoil energy of the nucleus. Moreover, a gamma ray can be resonantly absorbed by a free nucleus at rest only if the gamma-ray energy equals $E_0 + R$, since the free absorbing nucleus must also recoil with energy R. Earlier systems for observation of resonance absorption all involved supplying the $2R$ energy deficit in one way or another; e.g., by Doppler-shifting the emitted gamma ray by ultracentrifuging the source.

Recently Mössbauer[2] has demonstrated a different technique for observing nuclear resonant absorption, based on the fact that in crystals at low temperature there can be an appreciable probability that gamma-ray absorption and/or emission take place with the recoil being absorbed by the crystal as a whole, i.e., with no phonon creation in the crystal and essentially no energy lost to recoil. If the recoil is shared by about 10^5 atoms in both the emission and absorption events, the energy deficit $2R$ is small compared to a typical nuclear energy level width, and the absorption cross section very large. Mössbauer demonstrated the existence of nuclear resonance absorption of the 129-kev gamma-ray of Ir^{191} in metallic Ir (38.5% Ir^{191}) with source and absorber at a temperature of 88°K. By mounting the source on a turntable, he measured the variation in transmission as a function of the Doppler shift of the emitted gamma rays, and thereby obtained the width of the first excited level of Ir^{191}.

This Letter reports our repetition of Mössbauer's measurements, the extension of the temperature range to 1.5°K, measurements on various foil thicknesses, and a demonstration of semiquantitative agreement of the results with theoretical calculations by Visscher[3] based upon a theory of Lamb.[4]

By neutron bombardment of metallic osmium we prepared 16-day Os^{191}, which decays to an excited state of Ir^{191}. The Os source and two absorber foils were mounted within a cryostat so that either foil could be moved into position between the source and a collimated detector beneath the cryostat. A triangular-wave drive could be applied to the source to provide linear mechanical motion relative to the absorber at

velocities of up to 13 cm/sec. Gamma-rays from the source pass through the absorber foil and the cryostat walls (0.025-in. stainless steel) to the NaI(Tl) scintillation detector, thence to a 10-channel pulse-height analyzer. The pulse-height spectrum obtained displayed a peak identified as the 129-kev gamma-ray in Ir^{191}. The area under this peak, corrected for background, was used as the measure of the intensity of the attenuated 129-kev gamma-rays.

The ratio $r(T)$ of the counting rate with a Pt absorber to that with a matched Ir absorber is obtained at temperatures T. A grand ratio, $G = r(T)/r(300)$, is dependent upon the nuclear cross section alone. Three types of observations are made: (a) measurement of transmission as a function of foil thickness; (b) determination of the variation of the resonance cross section as a function of (equal) source and absorber temperatures; and (c) Doppler shift of the incident gamma rays.

(a) Transmission versus foil thickness.—Transmission measurements at 4.0°K were carried out using four matched pairs of Pt and natural Ir foils. The transmission is not expected to follow the usual exponential variation with foil thickness n (atoms/cm^2) because of the selective absorption of the resonant portion of the radiation. If f denotes the fraction of the 129-kev radiation which is resonant, and f' denotes the probability of absorption with no phonon emission from an incident photon beam of constant energy spectrum, then the observable cross section for resonance absorption is $f'\sigma a$, where

$$\sigma = 2\pi\lambda^2 \frac{2I_e+1}{2I_g+1}\frac{1}{1+\alpha} = 63\,000 \text{ barns},$$

I_e = spin of excited state = 5/2,

I_g = spin of ground state = 3/2,

α = internal conversion coefficient = 2.47,

a = isotopic abundance of Ir^{191} = 0.385.

Introducing the variable $x = nf'\sigma a$,

$$G^{-1} = 1 - f[1 - I_0(\tfrac{1}{2}x)\exp(-\tfrac{1}{2}x)],$$

where $I_0(z) = J_0(iz)$.

In Fig. 1 we plot $G-1$ vs x for several values of f. By fitting the experimental points to the calculated curves, unique solutions for f and f' are obtained from which the Debye temperatures of Os and Ir may be found.[3] Our results are $f = 0.07 \pm 0.015$ and $f' = 0.047 \pm 0.015$, implying

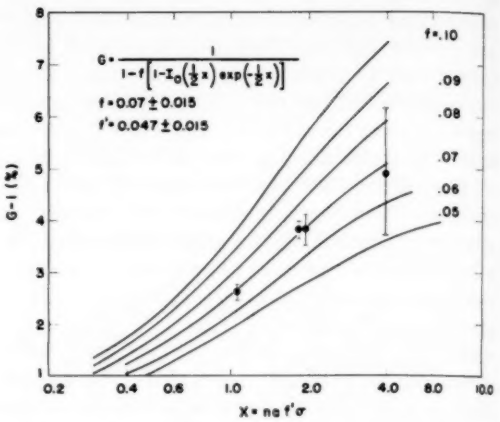

FIG. 1. Resonant absorption attenuation (%) of 129-kev gamma radiation in Ir^{191} at 4°K versus a parameter proportional to foil thickness.

Debye temperatures of 300 ± 25°K for Os and 262 ± 30°K for Ir.

(b) Temperature dependence.—Figure 2 presents $G-1$ as a function of temperature for an Ir foil of thickness 1.69×10^{21} atoms/cm^2. Above about 60°K this foil is thin to the resonance radiation. At lower temperatures, however, the foil is thick and corrections must be made. The temperature dependence of the corrected cross section is consistent with that predicted by Visscher using parameters chosen to fit Mössbauer's data at 88°K.

(c) Oscillating source measurements.—The third type of measurement was made with source

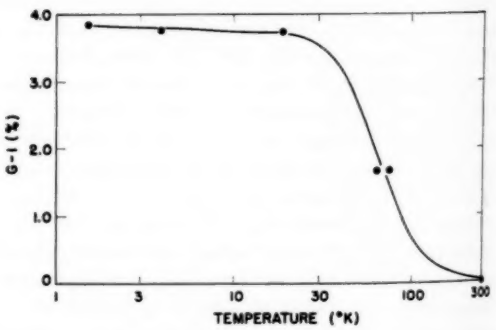

FIG. 2. Excess attenuation due to nuclear resonant absorption (%) versus (equal) source and absorber temperatures for an Ir absorber of thickness 1.69 $\times 10^{21}$ atoms/cm^2. After a foil thickness correction (not shown) the measurements agree with calculations by Visscher.

and absorber temperatures fixed at 4°K. The source was moved toward or away from the absorber at constant speeds of up to 13 cm/sec, thereby Doppler-shifting the emission spectrum. The counting rate with the Pt absorber was independent of source velocity while the rate with Ir varied with source speed. At high velocity the Pt/Ir counting ratio was equal within statistics to the 300°K ratio, suggesting that resonance absorption occurs neither at room temperature nor for high source speeds. The variation of cross section with velocity may be fitted by a single-level Breit-Wigner formula of half-width 2.15 ± 0.4 cm/sec. For the foil used ($n = 1.69 \times 10^{21}$ atoms/cm^2) this width must be corrected to 1.73 ± 0.34 cm/sec because of selective absorption of the resonant radiation, leading to a broadening of the resonance. We deduce that the width of the 129-kev level in Ir^{191} is $(3.72 \pm 0.74) \times 10^{-6}$ ev (the observed width is twice the state width because of overlapping of the emission and absorption spectra), and the corresponding lifetime of the state is $(1.1 \pm 0.2) \times 10^{-10}$ sec. [This value agrees with Mössbauer's result at 88°K of $(1.0^{+0.4}_{-0.2}) \times 10^{-10}$ sec.[2]]

We wish to thank R. L. Mössbauer for communicating to us results of his experiments in advance of publication; J. Marshall, Jr., for helpful discussions; and J. M. Dickinson for aid in preparation of the source and foils. We are especially indebted to W. Visscher for many discussions.

---

*Work performed under the auspices of the U. S. Atomic Energy Commission.

[1]This field is reviewed by K. G. Malmfors, in Beta- and Gamma-Ray Spectroscopy, edited by Kai Siegbahn (Interscience Press, New York, 1955), p. 521.

[2]R. L. Mössbauer, Z. Physik 151, 124 (1958); Naturwissenschaften 45, 538 (1958); Z. Naturforsch. 14a, 211 (1959).

[3]W. Visscher (to be published).

[4]W. E. Lamb, Phys. Rev. 55, 190 (1939).

NUCLEAR RESONANCE ABSORPTION OF GAMMA RAYS AT LOW TEMPERATURES*

L. L. Lee, Jr., L. Meyer-Schutzmeister, J. P. Schiffer, and D. Vincent
Argonne National Laboratory, Lemont, Illinois
(Received August 3, 1959)

Recent experiments by Mössbauer[1] have shown that nuclear resonance absorption of gamma rays can take place when both source and absorber are placed at liquid nitrogen temperature. This effect can be ascribed qualitatively to the fact that at low temperatures some of the emitting and absorbing atoms are not able to recoil in the crystal lattice and thus the recoil momentum is taken up by the entire crystal. This means that the emitting gamma ray loses virtually no energy to the recoiling system and that no energy is lost on recoil in absorption, so that nuclear resonance absorption can readily take place. In subsequent papers[2] Mössbauer reported that the resonance absorption could be destroyed by introducing a Doppler shift a few times as large as the width of the line. Moving the source at velocities of a few centimeters per second relative to the absorber accomplished this; in fact the shape of the line could be traced out as a function of velocity to obtain a resonance width which can be directly compared with the measurements of the lifetime of the state.

We have attempted to reproduce and extend Mössbauer's experimental results. The source used in his measurements was Os^{191} which decays to Ir^{191} with a 16-day half-life. This beta decay populates a 4.9-sec isomeric state which cascades through the 129-kev excited state of this nucleus. The experiment was designed to measure the lifetime of this excited state. A schematic diagram of our experimental arrangement is shown in Fig. 1. The sources and absorber were mounted on the bottom of liquid nitrogen containers in such a way that filling the containers did not change the amount of absorber the detected gamma rays had to pass through. A lead collimator was placed so that a source could be seen by the detectors only while its velocity along the line of sight differed from the mean by less than 5%. By the use of three sources, the arrangement was such that the detectors could see one of the sources at least 50% of the time. The sources consisted of powdered Os metal sealed between Al plates under pressure; the absorbers consisted of Ir metal foils. A single-channel pulse-height analyzer was gated on the 129-kev gamma-ray line. The counting rate was first measured with the sources stationary, and both absorber and sources at room temperature.

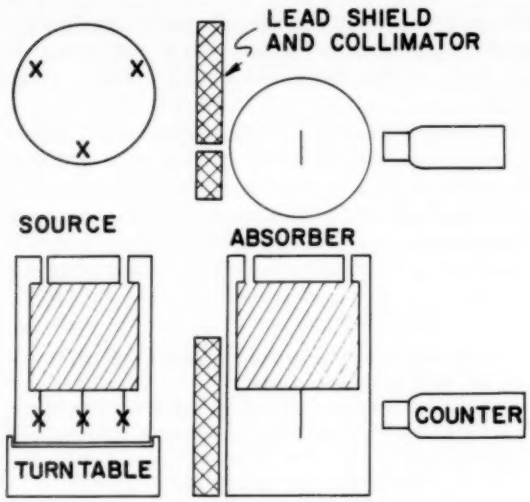

FIG. 1. Top and side views of the experimental arrangement used for the low-temperature resonance-absorption experiment. The shaded areas indicate the liquid nitrogen containers; the cross-hatched areas indicate lead shielding. The sources are represented by crosses.

Then the counting rate was measured with (a) only the sources cooled and (b) only the absorber cooled. On the basis of these measurements corrections could be made for effects of cooling, such as changes in alignment and the increase in density of source and absorber. Finally a measurement was made with both source and absorber cooled together. A similar sequence of measurements was repeated for each experiment performed with this equipment.

When the sources were stationary and the absorber was 880 mg/cm^2 of iridium metal foil, the net effect was a $1.14 \pm 0.05\%$ increase in absorption with both source and absorber cooled. The same experiment with a 285-mg/cm^2 iridium foil gave $0.83 \pm 0.04\%$. The fact that reducing the absorber thickness to 1/3 did not decrease the observed effect proportionally implies that partial saturation occurred in the absorption of the gamma rays that were emitted without loss of energy. This allows one to calculate the fraction of gamma rays that were emitted without energy loss and the fraction of the cross section in the absorber which was available for absorption without energy loss, by assuming Breit-Wigner line shapes and the usual exponential absorption formula. The above numbers then yield $2.0 \pm 0.5\%$ for the source and $11 \pm 3\%$ for the absorber. These measurements were made with both source and absorber at about 91°K as measured by thermocouples.

In an attempt to enhance the effect, we lowered the temperatures of both source and absorber to about 79°K. This was accomplished by evaporating the liquid nitrogen at reduced pressure until it solidified. At this temperature, with an absorber thickness of 880 mg/cm^2, the effect was $1.6 \pm 0.1\%$. An attempt was also made to measure the effect at liquid He temperatures (approximately 4°K). This required the construction of a cryostat in which both source and absorber could be surrounded by liquid He. Additional uncertainties were introduced by absorption in the liquid He and geometrical effects which could not be checked as thoroughly as for the measurements with liquid nitrogen. The effect obtained with 880 mg/cm^2 of iridium was $2.3 \pm 0.5\%$.

The results of the measurements with moving sources are shown in Fig. 2. The width obtained by a least-squares fit to the data was $(6.2 \pm 0.6) \times 10^{-6}$ ev. A correction has to be applied to this result because the absorber thickness used was so large that it would tend to widen the peak since saturation would occur in the absorption even when only the wings of the resonances in the emission and absorption spectra overlap. This

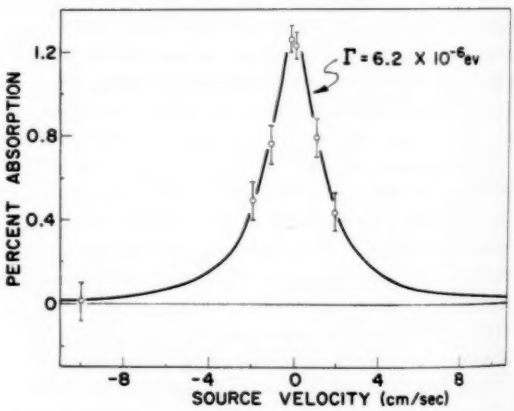

FIG. 2. Percentage of absorption plotted as a function of source velocity for the 129-kev Ir gamma ray following the decay of Os^{191}. The absorber was 0.88 g/cm^2 of iridium metal and both source and absorber were at the temperature of liquid nitrogen. The curve was calculated assuming Breit-Wigner shapes for both the emission and absorption with the width given in the figure. The errors shown for the points are those due to counting statistics alone.

correction can be calculated from the fraction of the cross section which is available for absorption without energy change. The resulting width of $(3.5 \pm 0.4) \times 10^{-6}$ ev corresponds to a half-life of $(1.3 \pm 0.3) \times 10^{-10}$ second. This number may be compared with the half-life 1.4×10^{-10} sec obtained by Mössbauer.

It is also of interest to compare our results on the absolute magnitude of the effect with Visscher's[3] calculations of the fraction of the absorption cross section which occurs without energy loss in an iridium crystal. Our value at liquid nitrogen temperature was 11% while Visscher's calculated value was ~1.2%. Visscher also predicts a factor of 2.8 increase in the number of atoms emitting or absorbing without energy loss as one goes from liquid nitrogen to liquid He temperatures. On the assumption that his results for Ir are also valid for Os, this would predict about a fourfold increase in the absorption whereas our measured increase is a factor of 2.5 ± 0.5. We have also investigated iridium chloride as an absorber instead of Ir metal. No resonance absorption was observed within 0.1%.

Resonance absorption has also been observed for the gamma ray from the decay of the 100-kev first excited state of W^{182} which results from the beta decay of Ta^{182}. This decay populates levels at excitations near 1.3 Mev and from these there is a gamma cascade through the 100-kev excited state. The background produced by the many high-energy gamma rays accounted for more than half the counting rate within the single-channel analyzer gate set for the 100-kev gamma ray. Thus it was not possible to make absolute measurements of the type that were obtained for the state in iridium. However the fact that the counting rate at liquid nitrogen temperatures showed a dip of 1.0% shows that the effect is probably somewhat stronger than in the case of Os-Ir. Because of the much stronger contribution of the higher-energy gamma rays it was not possible here to estimate the number of atoms emitting or absorbing without energy loss. The effect was studied, however, as a function of source velocity with two absorber thicknesses. The results give 0.73×10^{-6} ev for the width and a corresponding half-life of $(0.63 \pm 0.3) \times 10^{-9}$ sec for the 100-kev state of W^{182}. Sunyar[4] has measured the half-life of this state as $(1.3 \pm 0.1) \times 10^{-9}$ sec. The disagreement can probably be attributed to experimental difficulties, partly because of the high background but probably principally because it is hard to insure uniform velocities with the present turntable at the low speeds required for such a small width. It is hoped that an improvement in the equipment will clear up this difficulty.

It seems that this technique originated by Mössbauer will provide an effective tool in measuring lifetimes in a region overlapping with fast electronic techniques. It might also be possible to observe hyperfine structure effects splitting up the line into several components.[5] However, this would perhaps be more likely to be observable if the effect is found to persist for states whose lifetimes are at least an order of magnitude longer. Finally the comparison of the absolute magnitude of the effect with calculations such as Visscher's at various temperatures might be of interest in yielding further information on the structure of crystal lattices.

We would like to thank Dr. R. Thaler and others for having brought this problem to our attention at the time of a visit by one of us to the Los Alamos Scientific Laboratory. We would also kike to thank Dr. D. R. Inglis, Dr. H. Lipkin, and Dr. M. Hamermesh for many illuminating discussions, and acknowledge the help of Mr. Eiichi Fukushima for his help in the measurements on W.

---

*This work was performed under the auspices of the U. S. Atomic Energy Commission.

[1]R. L. Mössbauer, Z. Physik 151, 124 (1958).

[2]R. L. Mössbauer, Naturwissenschaften 45, 538 (1958); R. L. Mössbauer, Z. Naturforsch, 14a, 211 (1959).

[3]William M. Visscher (unpublished).

[4]A. W. Sunyar, Phys. Rev. 98, 653 (1955).

[5]This possibility was suggested to us by M. Hamermesh, and independently by R. Mössbauer (private communication).

LIFETIMES OF THE 118-kev AND 139-kev LEVELS OF Tm^{169} MEASURED BY A NEW METHOD

A. E. Blaugrund
Department of Physics, Weizmann Institute of Science, Rehovoth, Israel
(Received June 18, 1959)

The lifetimes of two rotational states in Tm^{169} have been measured by a new method which is a variation on ideas suggested by Devons[1] and Gerholm.[2] With this method it is possible to measure lifetimes in the region 10^{-11}-10^{-10} sec of levels situated between two low-energy highly converted γ transitions.

Description of the method.—A thin source is placed between two long lens β-spectrometers (see Fig. 1) which are tuned to the respective energies of the conversion electrons resulting from the cascade. Immediately after leaving the source the electrons are alternatingly accelerated and decelerated in high-frequency electric fields produced in re-entrant microwave cavities placed on both sides of the source. If this energy modulation is larger than the resolution of the spectrometer, the combination of microwave resonator plus spectrometer works a periodic shutter which transmits electrons to the detector only during short time intervals when the modulating field is zero. The two cavities are fed from the same oscillator—a CW magnetron of 80 w at 2450 Mc/sec—and the time delay between the opening of the two "shutters" can be changed by introducing a phase shift between the two modulating fields. This phase shift is measured on an interferometer. The coincidence rate is recorded as a function of the phase shift. In order to be able to determine the lifetime of the level from this curve it is necessary to know the response of the instrument to prompt radiation. The "prompt curve" is obtained by repeating the same measurement (coincidence rate as function of phase shift) with a modulating field of the same amplitude but of much lower frequency. As long as the modulating period T is very large compared with the mean life τ this response is independent of T. In the actual experiment a modulation frequency of 50 cps was used. Instead of modulating the energy of the conversion electrons the currents through the spectrometer coils were modulated.

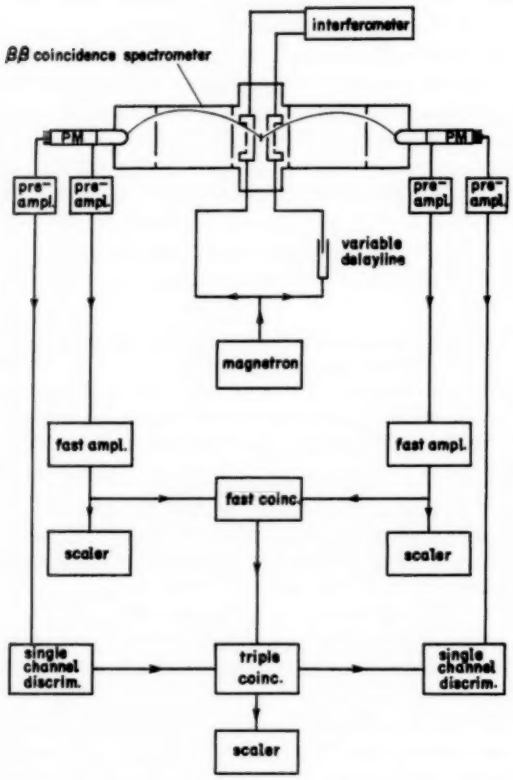

FIG. 1. Schematic diagram of the apparatus.

Measurements.—The excited levels in Tm^{169} were reached from Yb^{169}. The source was prepared by depositing Yb^{168} on an aluminium foil (150 $\mu g/cm^2$) in the mass separator of the Institute for Theoretical Physics in Copenhagen.[3] The sample was then irradiated for 3 weeks in a neutron flux of $1.5\times10^{13} n/cm^2$ sec. The sources were approximately 1 mm in diameter and 50μC strong. For measurements on the 118-kev level the spectrometers were tuned to the K-conversion lines of the 198-kev and 110-kev transitions. In the case of the 139-kev level coincidences between the 177-K and the 131-K electrons were registered. In all cases the amplitude of the modulation was about 4% of the electron energy. The ratio of true to random coincidences was better than 20:1. The spectrometers had a momentum resolution of 1% (full width at half height). The experimental points can be seen in Fig. 2. The "prompt curve" was obtained with a 50-cps modulation and the delayed curve with 2450-Mc/sec. The modulation depths were adjusted to be equal in the two measurements. By folding different lifetimes τ into the experimental prompt

curve, delayed curves can be calculated. In the case of rf modulation the absolute phase is not known and in Fig. 2 it has been chosen so as to give the best agreement between the experimental points and the calculated curves. No normalization of the ordinate is necessary because both the "prompt" and the delayed coincidences are measured for the same level and under the same experimental conditions. The values of lifetimes that give the best fit are $T_{1/2} = (6.2 \pm 1.0) \times 10^{-11}$ sec and $T_{1/2} = (2.9 \pm 0.7) \times 10^{-10}$ sec for the 118-kev and the 139-kev level, respectively. Using the branching ratios and conversion coefficients given by Hatch et al.,[4] one gets 1.2 and 1.8 for the relative reduced transition probabilities $B(E2)$ of the 118-kev and 131-kev transitions, respectively.

In earlier measurements the mean lifetime of the 97-kev level in Pt^{195} was determined to be about 2×10^{-10} sec. The experiment was made with a carrier-free sample of Au^{195} deposited by electrolysis.

The author would like to express his thanks to Dr. G. Goldring and Professor A. de-Shalit for their continued interest in this work.

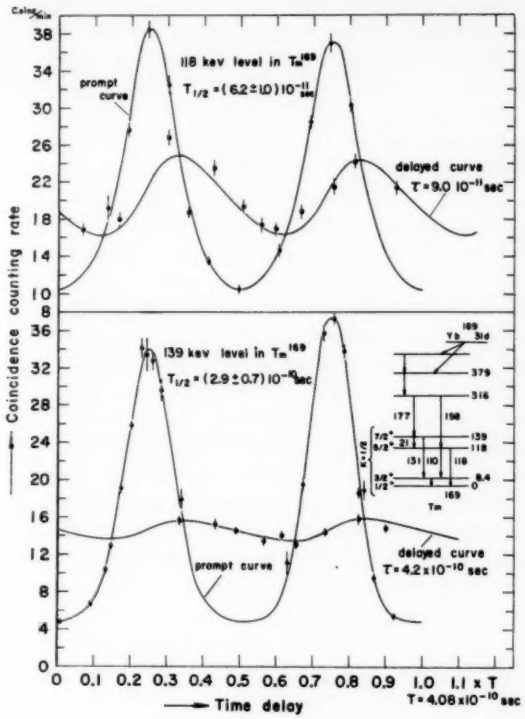
Coincidence counting rate
118 kev level in Tm^{169}
$T_{1/2} = (6.2 \pm 1.0) 10^{-11}$ sec
prompt curve
delayed curve
$T = 9.0\ 10^{-11}$ sec
139 kev level in Tm^{169}
$T_{1/2} = (2.9 \pm 0.7) 10^{-10}$ sec
prompt curve
delayed curve
$T = 4.2 \times 10^{-10}$ sec
Time delay
$T = 4.08 \times 10^{-10}$ sec

FIG. 2. Coincidence counting rate as a function of time delay (zero point arbitrary) for "prompt" and delayed coincidences.

[1] S. Devons (private communication).
[2] T. R. Gerholm, Arkiv Fysik 11, 55 (1956).
[3] We are greatly indebted to Dr. O. Skilbreit and Professor A. Bohr for their help and cooperation.
[4] E. N. Hatch et al., Phys. Rev. 104, 745 (1956).

BETA-SPECTROMETRIC STUDY OF THE ANGULAR DISTRIBUTION OF THE K-, L-, AND $M+N+\ldots$-SHELL PHOTOELECTRONS FROM URANIUM

Sölve Hultberg and Ziemowid Sujkowski*
Nobel Institute of Physics, Stockholm, Sweden
(Received July 6, 1959)

As an extension of previous work[1] we have investigated the longitudinal angular dependence (or Θ dependence) of the K, L, and $M+N+\ldots$ shells by a beta-spectrometric study of the photoelectrons ejected from a thin uranium converter (2.19 ± 0.02 mg U/cm^2) by the action of unpolarized gamma radiation ($h\nu = 412$, 662, and 1332 kev). The experimental arrangement is similar to that used earlier by Hultberg and Novakov[1] and a detailed description is given by Hultberg.[2] Full definitions of all symbols used here are given in reference 2.

The uranium foil of 14.6-mm diameter was placed at the ordinary source position in the double focusing β-ray spectrometer. A special construction permitted the cylindrical gamma-ray source (2×2 mm) to be rotated around the foil center, in the plane of the central electron orbit in the spectrometer. The source-converter distance was $a = 30$ mm. The angle between the direction of incidence of the gamma-rays and the direction of emission of the photoelectrons is described by the symbol Θ (see Fig. 2 in reference 2). For a specific value of the relative angle Θ, the photoline spectrum of the K, L, and $M+N+\ldots$ lines was recorded in the ordinary way. An illustration is given in Fig. 1, where K, L, and $M+N+\ldots$ photolines are shown at the energy

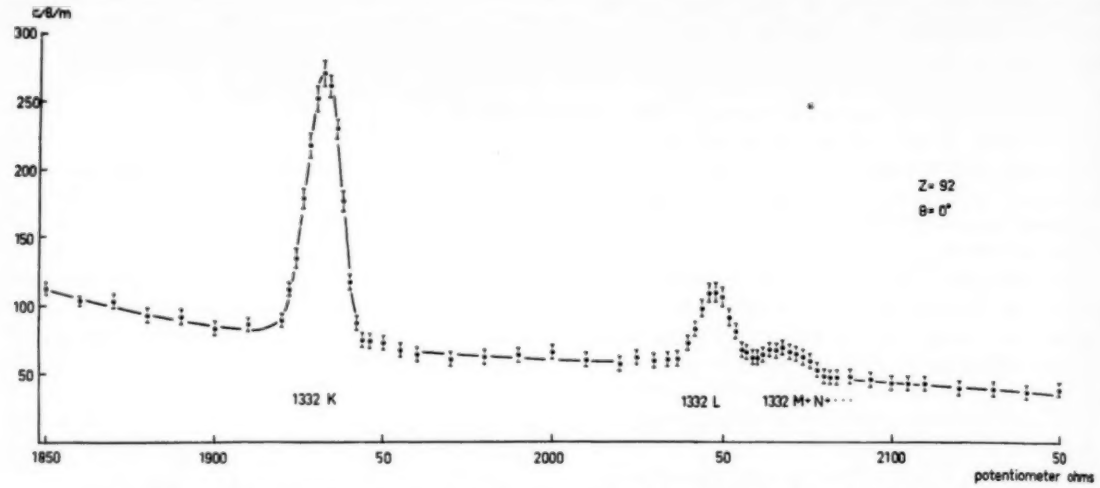

FIG. 1. Photoelectron spectrum for specific values of the energy and the relative angle ($h\nu = 1332$ kev, $\Theta = 0°$). The errors are statistical and the numbers at the ordinate axis represent 1/8 of the counting rate per 1 minute.

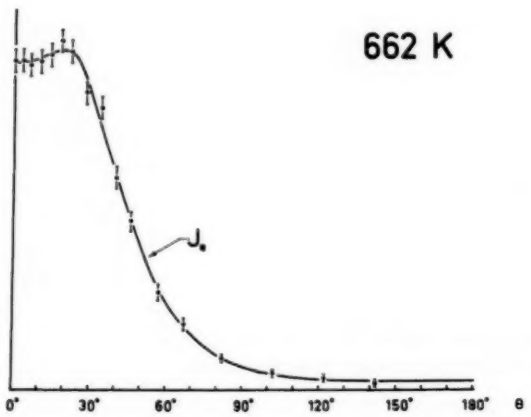

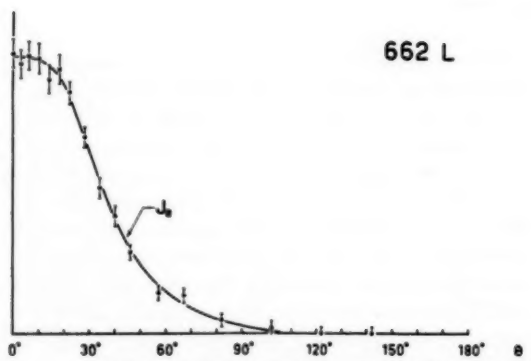

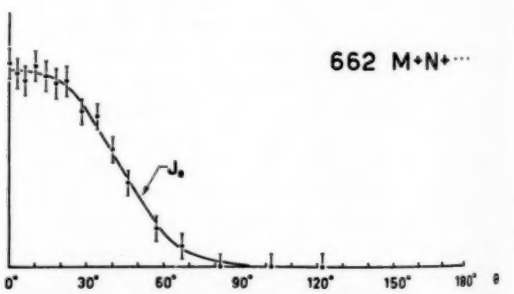

FIG. 2. Uncorrected experimental representations J_e of the Θ dependence of the photoeffect in uranium, at $h\nu = 662$ kev. A 2.2-mg/cm^2 U converter was used and the photoelectrons were studied in a double-focusing beta spectrometer (see reference 2).

$h\nu = 1332$ kev and the angle $\Theta = 0°$. Such measurements were repeated at each of the above-mentioned energies for a large number of Θ values between 0 and π. By plotting the line areas versus Θ, experimental representations of the K-, L-, and $M+N+\ldots$-shell angular dependence of the photoeffect for uranium were obtained at each of the three energies. An illustration is given in Fig. 2.

The uncertainties indicated in Fig. 2 represent the estimated errors in the evaluation of the photoline areas and generally vary between 5 and 50%, depending upon the angle Θ.

Since the converter subtends a certain solid angle at the gamma-ray source, the angular resolution is finite and depends strongly on Θ. This means that Θ cannot be sharply defined and

the influence on the measurements that results can be described as the "geometric distortion." Further contributions to the latter arise from the finite extensions of the source and the spectrometer aperture but these effects were negligible in the present experiments (see reference 2). The multiple scattering of the photoelectrons inside the converter material also influences the angular resolution by confusing the emission directions of the photoelectrons to an extent depending on the converter thickness (the "scattering distortion"). By performing special experiments it was, however, possible to infer the "true" angular distributions from the experimental ones.[2] It then turned out that the above-mentioned distortions generally were, in our experiments, significant only at very small angles. The "true" distributions thus obtained can be directly compared with available theories. The latter are, however, not yet in a state that permits a reliable comparison, at least not when the photoelectrons are ejected from heavy elements.

It should perhaps be pointed out that the angular dependence of the photoeffect has never before been carefully studied for gamma-ray energies above 100 kev. Thus there is an obvious academic interest for a better knowledge of the mechanism of the photoeffect. For instance, the curves of Fig. 2 might be used to calculate the photoelectric absorption ratios for the K, L, and $M+N+\ldots$ shells of the uranium atom, at 662 kev. In particular $\tau_K/\tau_{\text{atom}}$ ratios can be obtained and used to compare the results from absorption measurements (giving τ_{atom}) with theoretical calculations of the K-shell cross section τ_K.[2]

From the practical point of view, a detailed knowledge of the differential photoelectric cross sections is very important in the analysis of beta-spectrometrically recorded photolines. Since not all of the ejected photoelectrons can be accepted by the spectrometer aperture, the integrated photoelectric cross section of a certain atomic shell must be corrected for this effect. Here the complications are due to the photoelectric anisotropy (Fig. 2) which, moreover, is energy dependent. For the deduction of gamma-ray intensities from recorded photolines the photoelectric cross section to be used can conveniently be written τf. Here τ represents the tabulated (theoretical) cross section of a specific shell ($\tau = \tau_K$ in most practical cases), and f is a correction factor which is obtained as the ratio between simple integrals over the angular distribution functions. The limits of the integrals are determined by the geometry of the experimental setup. In reference 2 such functions are given numerically for the K, L, and $M+N+\ldots$ shells at $h\nu = 412$, 662, and 1332 kev, together with full details about the calculation of f for arbitrary dimensions of the source and the converter if they are circular or rectangular in shape. Here the gamma-ray source can even be allowed to be larger than the converter if required for the sake of intensity. From the presented curves it is also possible to calculate the expected ratio between the experimentally observed intensities of photolines belonging to different atomic shells. This often permits much more information to be obtained from a photoline spectrum than the instrumental resolution would seem to allow.[3]

The correct analysis of photolines, as briefly outlined above, leads in a natural way to the application of a new method for the determination of absolute values of internal conversion coefficients and photoelectric cross sections.[4,5] The technique is a convenient one in that it allows very easy manipulation and since only a very small fraction of the total instrumental $H\rho$ region is used. The method has been applied to a number of cases[3-5] and has been found to work very satisfactorily.

In order to facilitate the universal use of our photoelectric angular functions as presented in reference 2, one of the authors (S. H.) is now preparing for the Swedish fast electronic computer BESK a routine which will calculate the factor f on the basis of a specification of the $J(\Theta)$ function and the parameters c, c_Q, h, h_Q, a, m (see reference 2 for definitions), for the flat type spectrometer. Such calculations can also be undertaken on request.

One of us (Z. S.) would like to thank Professor Manne Siegbahn for his kind hospitality at the Nobel Institute of Physics. He also gratefully acknowledges the scholarship from the Swedish Institute.

---

*On leave of absence from the Institute of Nuclear Research, Warsaw, Poland.

[1]S. Hultberg and T. Novakov, Nuclear Phys. 4, 120 (1957).

[2]S. Hultberg, Arkiv Fysik 15, 307 (1959).

[3]R. Stockendal and S. Hultberg, Arkiv Fysik 15, 33 (1959).

[4]S. Hultberg and R. Stockendal, Arkiv Fysik 14, 565 (1959).

[5]S. Hultberg and R. Stockendal, Arkiv Fysik 15, 355 (1959).

INTERPRETATION OF "ANOMALOUS INELASTIC SCATTERING"

C. D. Goodman
Oak Ridge National Laboratory, Oak Ridge, Tennessee
(Received March 16, 1959; revised manuscript received July 31, 1959)

Studies of (p,d) reactions currently in progress at Oak Ridge National Laboratory[1] show that (1) the reaction mechanism is direct; only a few levels in the residual nucleus are excited; (2) the shell model provides a good description of the states which are excited; and (3) the reaction may be pictured as an interaction of the proton with only a single nucleon (i.e., the neutron which it picks up), while the other nucleons remain undisturbed in their shell states. This picture qualitatively explains the similarity of the deuteron spectra from neighboring isotopes in the region of shell closures as shown, for example, in Fig. 1. The peaks were assumed to be due to removal of neutrons from single-particle bound states, and angular distributions were used to confirm shell assignments. Details will be published.

The initial system is identical to that for "anomalous" proton inelastic scattering observed by Cohen and coworkers[2-4] who find also that (p,p') is a direct interaction and that a selection of states occurs. They reject single-particle excitation as the selection mechanism and assume instead that (p,p'), in contrast to (p,d), excites collective states preferentially.

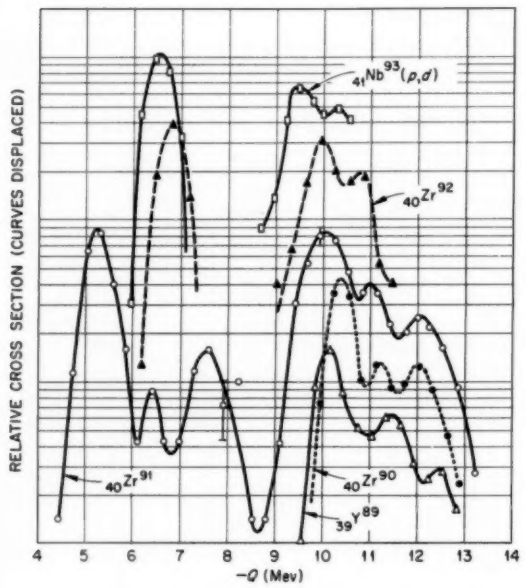

FIG. 1. Preliminary (p,d) spectra from the targets indicated. The separated isotope targets are oxides on Mylar backings. The energy scales are uncertain by as much as 0.5 Mev, due to uncertainties in the target thicknesses. The peak near $Q=-8$ Mev is probably due to nitrogen on the target.

It is the purpose of this Letter to re-examine Cohen's arguments in the light of our (p,d) data and to suggest that the shell model may also be a good description of the states involved in (p,p') reactions. No attempt is made here to calculate the relative intensities of the peaks. It is merely assumed that states due to the excitation of single particles appear in the (p,p') spectra, and states due to the excitation of two or more particles are sufficiently inhibited to be unimportant in describing the gross features of the spectra.

The arguments presented by Cohen and Rubin[4] against single-particle states are that in poor resolution the "anomalous" peak appears at the same energy for neighboring even and odd nuclei and for nuclei above and below shell closures. Also certain states which are strongly excited by Coulomb excitation are also strongly excited in proton inelastic scattering, and certain states which are strongly excited in inelastic scattering do not appear in (p,d) reactions. Three of these arguments are consistent with shell-model selection rules. The addition of an unpaired nucleon does not change the transition energies for the other particles. New peaks due to transitions involving the odd particle should and do appear, however, in the fine resolution data. Certain transitions become unavailable as a shell is filled. All other transitions are unaffected by a shell closure, however. Energy levels due to a proton excitation and due to neutron excitation resulting in a hole plus an excited neutron would not be strongly excited in (p,d) reactions. Single-hole states would be seen strongly in (p,d) and in proton inelastic scattering. The meaning of the correlation with Coulomb excitation of the cross section for certain levels is not clear.

Cohen's hypothesized dichotomy between inelastic scattering on the one hand and pickup and stripping on the other[4,5] is subject to experimental verification. The (p,d) and (d,He^3) or (t,α) reactions could be used to locate the single-particle levels. From this information the loca-

tions of peaks in (p, p') spectra due to single-particle transitions could be inferred. The peaks would be expected to appear only weakly, while other peaks due to states better described by collective parameters should appear strongly.

Definitive information on this matter is not yet available. Tamura and Choudhury[6] have shown, however, that single-particle transitions between the known shell-model states account well for the observed (p, p') spectra in lead and copper.

A (p, d) spectrum from iron is shown in Fig. 2. A (p, p') spectrum from iron is also available.[4] In the (p, d) case, angular distributions identify the peak at $Q = -8.9$ Mev as due to the removal of a $p_{3/2}$ neutron, and the peak at $Q = -10.1$ as due to the removal of an $f_{7/2}$ neutron. If one assumes that the peak at 0.85 Mev in the (p, p') spectrum is due to the breaking of the $2p_{3/2}$ pairing bond, and is thus a measure of the $2p_{3/2}$ pairing energy, one can find the energies of the expected (p, p') peaks due to single-neutron excitation from the various states to a vacancy in the $2p_{3/2}$ state by adding 0.85 Mev to the energy differences between the $2p_{3/2}$ peak and the other peaks in the (p, d) spectrum. This accounts for the peaks at 0.85, 2.0, 3.1, and 4.0 Mev in the (p, p') spectrum within the accuracy of the data, and leaves unaccounted for the peaks at 1.3, 2.7, and 3.4 Mev. If the levels unaccounted for are due to proton excitation, then the shell model gives an adequate description of proton inelastic scattering in this case, too. It is hoped that more data of this type can be obtained.

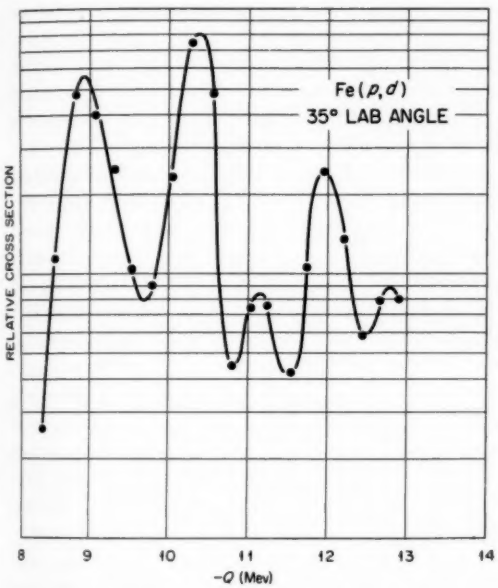

FIG. 2. Preliminary (p,d) spectra from natural iron.

That the shell model can account for a grouping of (p, p') peaks in the region of 2-3 Mev over a large range of atomic numbers can be seen from calculated positions of the single-particle levels as given, for example, by Green.[7]

---

*Operated for the U. S. Atomic Energy Commission by Union Carbide Corporation.

[1]C. D. Goodman and J. B. Ball, Bull. Am. Phys. Soc. 4, 9 (1959); 4, 287 (1959); and Proceedings of the International Conference on the Optical Model, Florida State University, Tallahassee, 1959 (unpublished), p. 257.

[2]B. L. Cohen, Phys. Rev. 105, 1549 (1957).

[3]B. L. Cohen and S. W. Mosko, Phys. Rev. 106, 995 (1957).

[4]B. L. Cohen and A. G. Rubin, Phys. Rev. 111, 1568 (1958).

[5]B. L. Cohen and A. G. Rubin, Phys. Rev. 114, 1143 (1959).

[6]T. Tamura and D. C. Choudhury, Phys. Rev. 113, 552 (1959).

[7]A. E. S. Green, Phys. Rev. 104, 1620 (1956).

COMPLEX NUCLEON TRANSFER REACTIONS OF HEAVY IONS*

Richard Kaufmann† and Richard Wolfgang
Department of Chemistry, Yale University, New Haven, Connecticut
(Received August 12, 1959)

The transfer of a single nucleon in heavy ion reactions involving N^{14} has been studied quite intensively.[1-5] The results are consistent with a mechanism involving tunneling through the Coulomb barrier of nucleons Coulomb-excited to virtual levels.[6] This Letter concerns some studies of high-energy reactions in which several nucleons are transferred. Such reactions were found to be quite prominent and imply the existence of an important new mechanism for transfer reactions.

In initial experiments, stacks of target foils backed with gold catcher foils were irradiated with 160-Mev O^{16} and 140-Mev N^{14}. The thickness of these stacks was adjusted so that when the beam reached the gold its energy had been degraded below the energy necessary to give reaction. Thus, after irradiation, the only radioactivity in the gold was due to products which had recoiled into it from the target. This method provides a simple criterion for transfer reaction, since only those products which are formed by pickup and stripping from the projectile (and therefore have sufficient range to reach the catcher) are observed. The distribution of activities in the catcher in a typical experiment (160-Mev O^{16} on tin) is given in Fig. 1. The average ranges of the F^{18}, O^{15}, N^{13}, and C^{11} products correspond to a velocity at the time of their formation which approximates that of the incident O^{16}. However, the range straggling increases with the number of nucleons transferred, reflecting a wider range of momentum exchange in the more complex transfer interactions.

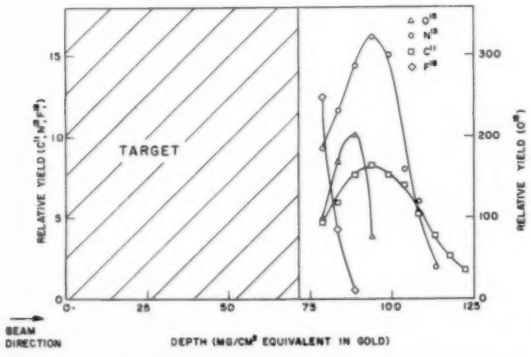

FIG. 1. Distribution of products with depth from the O^{16} bombardment of a tin target.

The average cross sections for these reactions are given in Table I. Two generalizations emerge: (1) The cross section for $(p2n)$ and $(2p3n)$ transfers are appreciable compared to single nucleon transfers. [This holds also for (pn) transfers.] This result is somewhat surprising in view of the result of Alkhazov et al.[7] who find that two-neutron transfer to give N^{16} from N^{14} is reduced by several orders of magnitude compared to single-neutron transfer. (2) The ratio of cross sections for $(p2n)$ to (n) transfers appears constant at about 0.2 and that for $(2p3n)$ to (n) at 0.1 over a wide range of interacting systems.

The high cross sections for the $(p2n)$ and $(2p3n)$ transfers are not consistent with tunneling through the Coulomb barrier. Further, the relatively minor dependence on both the binding energy of the transferred group of nucleons and the Q value of the reaction would not be predicted by barrier penetration considerations. These conclusions hold regardless of the entities that are actually transferred. [It seems plausible that the $(p2n)$ stripping actually involves double exchange of a proton and alpha particle, while the $(2p3n)$ events

Table I. Thick target cross sections (mb).

Target \ Reaction[a]	$(-n)$		$(-p2n)$		$(-2p3n)$
Error	±30%		±50%		±50%
Beam	N^{14}	O^{16}	N^{14}	O^{16}	O^{16}
Al		20		4.0	2.3
Cu	28	29	≤8	4.7	2.9
Sn	(20)	7.9	(4.2)	1.4	0.78

Ratios of thick target cross sections.

Target \ Reaction[a]	$\frac{(-p2n)}{(-n)}$		$\frac{(-2p3n)}{(-n)}$
Error	±20%		±20%
Beam	N^{14}	O^{16}	O^{16}
Al		0.20	0.12
Cu	≤0.29	0.16	0.10
Sn	0.21	0.18	0.10

[a]To remove indicated number of nucleons from projectile.

represent transfer of an alpha and a neutron.]

It is postulated that in most of the complex stripping reactions, the projectile approaches with an impact parameter comparable to its radius and breaks through the Coulomb barrier to form a dumbbell-shaped system. Normally this might lead to formation of a compound nucleus. However, it can easily be shown that if the incident energy and the impact parameter exceed certain values, the combined centripetal and Coulomb forces are sufficient to break the nuclear bond before the system has made half a rotation. Yet the time of such contact is certainly sufficient to permit the transfer of particles. We have calculated that the threshold for such "contact transfer" reactions is about 40 Mev for the system O^{16} + Cu and rises rapidly to approximately one barn at 120 Mev. (This estimate includes events in which there is no net transfer.) However, such calculations are quite sensitively dependent on the somewhat arbitrary assumptions that must be made regarding the nuclear binding in the neck of the dumbbell.

It appears likely that such "contact transfer" is the mechanism of the buckshot effect invoked by Chackett et al.[8] to account for product distributions observed in heavy-ion bombardment of aluminum.

Since contact stripping involves penetration of the attractive core, the angular distribution of products from it will be more forward than that from nucleon transfer across the Coulomb barrier. This forward displacement should increase with increasing energy and decreasing impact parameter until finally the deflection becomes attractive rather than repulsive. So many assumptions are involved in our calculation of such deflections that we confine ourselves to the qualitative prediction that the distribution should be peaked near or at zero degrees.

The results of a typical experiment on the angular distribution of radioactive products from bombardment of rhodium with 160-Mev O^{16} is shown in Fig. 2. Evidently the results on C^{11}, N^{13}, and F^{18} are qualitatively in accordance with the contact transfer model. The distribution of the single-nucleon transfer product O^{15} was somewhat unexpected. A distinct peak, similar to that observed for $N^{14}(Ag^{107,109}, Ag^{108,110})N^{13}$ reactions,[5] should appear at about 24° according to the tunneling mechanism. However, only a small peak or flat spot is found there. We interpret this fact to mean that the tunneling mechanism is no longer dominant for O^{16} because of the higher binding

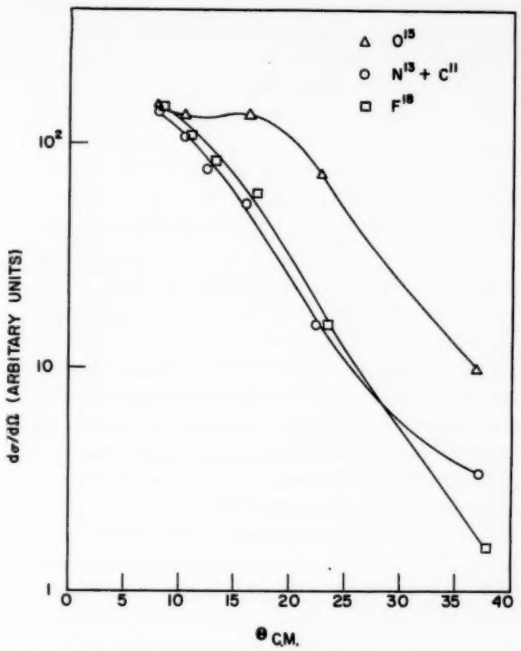

FIG. 2. Angular distribution of several products from the O^{16} bombardment of a 7-mg/cm² rhodium foil.

energy of the last neutron. Instead, the contact transfer mechanism in which this binding energy is not critical becomes important for the single-nucleon transfer also. Preliminary work on angular distributions of single-neutron stripping products from C^{12}, N^{14}, and F^{19} bombardments appears to support this view.

This work was performed under the auspices of the U. S. Atomic Energy Commission. The help of the staff of the Yale Heavy Ion Accelerator is greatly acknowledged, as is the courtesy of Professor G. Breit in reviewing this manuscript.

---

*Contribution No. 1571 of Sterling Chemistry Laboratory.

†In partial fulfillment of requirements for the Ph.D. degree at Yale University.

[1]K. F. Chackett and J. H. Fremlin, Phil. Mag. 45, 735 (1954).

[2]H. L. Reynolds and A. Zucker, Phys. Rev. 101, 166 (1956).

[3]Halbert, Handley, Pinajian, Webb, and Zucker, Phys. Rev. 106, 251 (1957).

[4]M. L. Halbert and A. Zucker, Phys. Rev. 108, 336 (1957).

[5]Volkov, Pasiuk, and Flerov, J. Exptl. Theoret. Phys. (U.S.S.R.) 33, 595 (1957)[translation: Soviet Phys. JETP 6, 459 (1958)].
[6]G. Breit and M. E. Ebel, Phys. Rev. 104, 1030 (1956).
[7]Alkhazov, Gangrskii, and Lemberg, J. Exptl. Theoret. Phys. (U.S.S.R.) 33, 1160 (1957) [translation: Soviet Phys. JETP 6, 892 (1958)].
[8]Chackett, Fremlin, and Walker, Phil. Mag. 45, 173 (1954).

FISSION OF U^{238} INDUCED BY μ^- CAPTURE*

Justo Diaz, Selig N. Kaplan, Burns MacDonald, and Robert V. Pyle
Lawrence Radiation Laboratory, University of California, Berkeley, California
(Received July 23, 1959)

It has been pointed out by Wheeler[1] that there are two ways in which a μ^- meson stopped in uranium may induce nuclear fission. The energy released in the nonradiative transition of the mesonic atom to its 1s state as well as that liberated in the nuclear-capture process, $\mu^- + U^{238} \rightarrow Pa^{238} + \nu$, should be sufficient sometimes to induce fission. These two possible fission-inducing mechanisms can be distinguished experimentally, since the fissions induced by atomic transition would be observed to occur promptly ($\tau \ll 10^{-9}$ sec), whereas those due to nuclear capture would occur with the characteristic mean lifetime of a μ^- meson stopped in uranium.[2]

Galbraith and Whitehouse failed to observe fission by cosmic-ray mesons in an ionization chamber and set an upper limit of 0.25 on the fission-to-stopping ratio.[3] John and Fry, using uranium-loaded nuclear emulsions, observed 7 μ^- fissions, from which they estimated that fission occurs about 15% of the time when a meson stops in uranium.[4] Considering only the nonradiative atomic transitions, Zaretsky[5] has recently calculated a fission probability that is consistent with the results of John and Fry.

The preliminary results of an experiment performed to obtain the relative probabilities of the two meson-induced fission mechanisms are presented in this Letter. A gas scintillation counter containing nine stainless steel disks $3\frac{1}{4}$ in. in diam by 0.015 in. thick, coated on both sides with 0.85 mg/cm^2 UF_4 (natural isotopic mixture), was filled to 45 psi above atmospheric pressure with a mixture of 80% A and 20% N_2. The μ^- beam, obtained at the 184-inch cyclotron for studies of the neutron multiplicities from μ^- capture in various elements,[6] was estimated to contain not more than one π^- per 1000 μ^- mesons.

An oscilloscope was triggered by a threefold coincidence between the two photomultiplier tubes looking at the gas scintillator, and a 3.7×10^{-7}-second gate triggered by the coincidence-anticoincidence pulse. This pulse was formed by simultaneous pulses in the plastic scintillators S_2, S_3, and S_4, together with the absence of a pulse in the water Čerenkov counter C (Fig. 1). The absence of a prompt pulse in the last plastic scintillator, A, was not required for triggering the oscilloscope because of our concern about accidental pulses in A induced by mesonic x-rays or products of a prompt fission. Pulses from S_3, S_4, and A, as well as a sum pulse from the two gas-scintillator phototubes were displayed on the oscilloscope and photographed. A precision, 50-Mc/sec oscillator was used to calibrate the sweep speed of the oscilloscope, and a weak Cf^{252} spontaneous-fission source was included in the chamber to permit frequent calibrations of the fission-fragment detection efficiency.

The zero-time calibration was obtained by photographing the pulses when a piece of plastic scintillator was placed in the fission chamber and also by photographing π^--induced fissions. In both cases the uncertainty in the zero time was about 3×10^{-9} sec. The background counting rate when

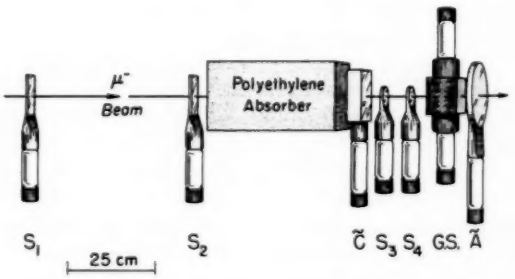

FIG. 1. Counter-telescope arrangement. Here S_1, S_2, S_3, S_4, and A are plastic phosphors, C is a water Čerenkov counter in anticoincidence to eliminate the small electron contamination in the beam, and $G.S.$ is the gas scintillator containing the uranium-covered plates.

plates that were not uranium-coated were bombarded was completely negligible. The random fission background with uranium in the chamber was $2.4 \pm 0.8\%$ fissions per coincidence-anticoincidence trigger, presumably caused by the neutron flux from the accelerator. Pulses from A (usually quite small) were observed about 10% of the time. In nearly all of these cases they were in coincidence with the fission pulse and not with the other counter-telescope pulses. The few observed cases of an S_2S_3A coincidence were not associated with prompt fissions. They are included in the data.

The number of fissions per 1×10^{-8}-sec interval is shown in Fig. 2 as a function of the time elapsed after the stopping of the meson. The background has not been subtracted in the figure. It was considered possible that a $\tau = 20\times10^{-8}$-sec component[2,7] might be created by fissions produced by neutrons from the nuclear capture of mesons in the stainless steel plates. In this case, Be plates might be necessary, but the counting rate for delays greater than a few mean lifetimes is consistent with that expected from the random background. Accordingly, the data, excluding the first time interval, were analyzed by the method of Peierls,[8] and a total mean life of $(7.54 \pm 0.55) \times10^{-8}$ sec was obtained. This value is slightly smaller than, but consistent with, the $(8.8 \pm 0.4) \times10^{-8}$-sec mean life of μ^- mesons in U as measured by Sens.[2] It is also in agreement with the theoretical value of 7.4×10^{-8} sec calculated by Primakoff.[9]

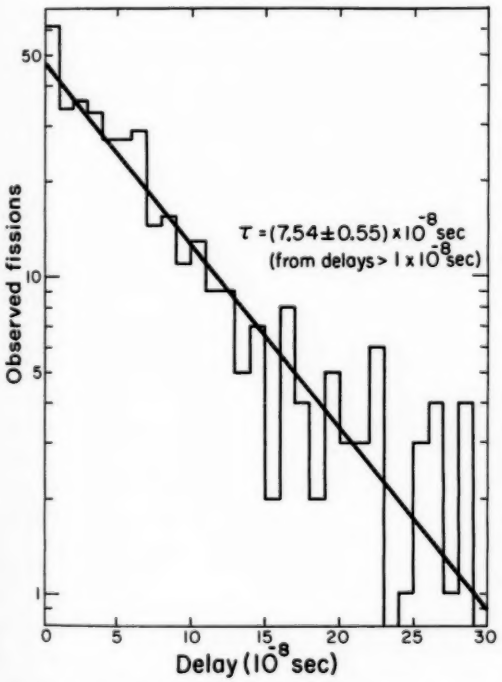

FIG. 2. Histogram of μ^--induced fission events before subtraction of 2.4% background.

The fissions associated with this lifetime must be due to nuclear capture. By extrapolating these results to the first time interval, we may say that 44.7 ± 3.0 fissions were to be expected. The number actually observed was 62. We therefore conclude that the fraction of the fissions that occurred promptly, due to the nonradiative transition of μ^- mesons to the lowest mesonic Bohr orbit, was $5.6 \pm 2.7\%$ (at most only a small fraction of the total). An absolute fission probability cannot be given at this time, because of the uncertainty of the relative stopping power of the U at the end of the μ^- range.

We wish to thank B. J. Moyer and C. M. Van Atta for supporting this experiment, H. Bowman for advice on the filling of the gas scintillation counter, and S. Thompson and T. Sikkeland for providing the Cf^{252} source.

---

*Work done under the auspices of the U. S. Atomic Energy Commission.

[1]J. A. Wheeler, Revs. Modern Phys. 21, 133 (1949).
[2]J. C. Sens, Phys. Rev. 113, 679 (1959).
[3]W. Galbraith and W. J. Whitehouse, Phil. Mag. 44, 77 (1953).
[4]W. John and W. F. Fry, Phys. Rev. 91, 1234 (1953).
[5]D. F. Zaretsky, Proceedings of the Second United Nations International Conference on the Peaceful Uses of Atomic Energy, Geneva, 1958 (United Nations, New York, 1958), Vol. 15, p. 175
[6]Kaplan, MacDonald, Moyer, Pyle, and Diaz, University of California Radiation Laboratory Report UCRL-8795 Abstract, June, 1959 (unpublished).
[7]Barrett, Holstrom, and Keuffel, Phys. Rev. 113, 661 (1959).
[8]R. Peierls, Proc. Roy. Soc. (London) A149, 467 (1935).
[9]H. Primakoff, Proceedings of the Fifth Annual Rochester Conference on High-Energy Physics (Interscience Publishers, Inc., New York, 1955); quoted in Sens, Swanson, Telegdi, and Yovanovitch, Phys. Rev. 107, 1464 (1957).

PARITY CONSERVATION IN HYPERON PRODUCTION BY 1.15-Bev/c K^- MESONS ON PROPANE

Richard L. Lander, Wilson M. Powell, and Howard S. White
Lawrence Radiation Laboratory, University of California, Berkeley, California
(Received August 5, 1959)

Several experiments have indicated a possible forward-backward asymmetry in the decay of Λ^0 hyperon.[1] The effect was such that, in the Λ^0 rest frame, the decay pion preferred forward emission with respect to the Λ^0 line of flight. In view of the known decay asymmetry of the Λ^0 with respect to its direction of polarization,[2] the above asymmetry would imply a nonzero longitudinal component of polarization of the Λ^0, which immediately suggests nonconservation of parity in the production interaction, assuming that parity doublets of the Λ^0 do not exist.[3]

A recent exposure of the Lawrence Radiation Laboratory 30-inch propane bubble chamber[4] to a 1.15-Bev/c separated K^- beam[5] offers the opportunity to explore the question further. Several thousand K^- interactions were photographed. This paper reports the initial results from a sample of 141 V^0 decays.

No separation is made here between production from hydrogen and from carbon. The sample includes both direct Λ^0 production and production that may result from secondary interactions such as $\Sigma^+ + N \rightarrow \Lambda^0 + N$ conversion in carbon or from $\Sigma \rightarrow \Lambda^0 + \gamma$ decay. The hyperons are subject to possible scattering within carbon nuclei; therefore lack of an observed polarization does not guarantee lack of polarization from the initial production. (These conditions are found in most of the experiments referred to above.)

The beam consisted of ~25% K particles and ~75% muons, with ~0.15 π^- per K^-, and was collimated so as to traverse only the thin window before entering the propane. This π^- flux should have produced in the sample used for this experiment only one or two hyperons of all kinds. Thus the Λ^0-producing interactions in the chamber were predominantly those of beam K^- mesons. Each K^- star could be readily observed in scanning and an exhaustive search could be made for a V^0 decay.

No selection criterion was applied except that a few V^0's originating in the window were rejected. The number of neutral-induced background stars was completely negligible. The possible bias that might result from failure to observe V^0's with one very short track has been considered. The fraction of Λ^0 decays yielding a proton ≤ 3 mm in length, assuming the decay to be isotropic in the Λ^0 rest frame, is zero for Λ^0 momenta ≥ 350 Mev/c and increases rapidly for lower momenta. However, since so much of the Λ^0 momentum spectrum lies beyond 350 Mev/c, the bias is only ~6% in favor of forward protons. Similarly the fraction of Λ^0 decays with pions less than 3 mm in length is a maximum of ~5% at 600 Mev/c and over the observed spectrum yields a 2% bias against forward protons. Thus a net bias of only a few percent might exist if ranges less than 3 mm were unobservable. No corrections were made.

One-hundred-forty-one V^0's were observed and identified as follows: 110 Λ^0; 19 θ^0; 10 Λ^0 or θ^0, consistent with either; 2 of poor quality, unidentifiable. Thus the distortion of the sample resulting from uncertain identifications is small. The identification was aided by the relatively low momenta of the Λ^0's (Fig. 1), yielding, in general, decay protons with ionization considerably above minimum. Observation of the parent star in each case fixed the V^0 line of flight, resulting in an overdetermination of the V^0 decay kinematics.

The decay of the Λ^0's results in a distribution of decay products in the Λ^0 rest frame of the form $(1 + \alpha \bar{P}_3 \cos\theta)$, where θ is the angle between the decay pion and the Λ^0 direction of motion, $\bar{P}_3$ is the average component of polarization of the Λ^0 in this same direction, and α is the decay-asymmetry parameter for complete polarization of the Λ^0. Figure 2 shows the observed distribution in $\cos\theta$ for 110 Λ^0 decays. Also shown (shaded) are the 10 events that were consistent

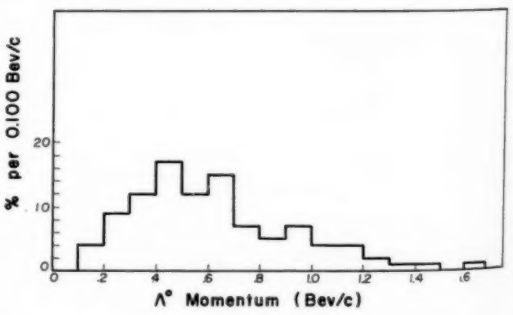

FIG. 1. Λ^0 momentum distribution.

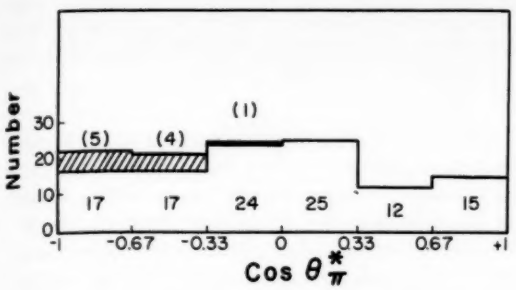

FIG. 2. Angular distribution of decay pions from 110 Λ^0 decays. $\theta_\pi{}^*$ is the angle in the Λ^0 rest frame between π direction and direction of motion of Λ^0. Ten events consistent with Λ^0 or $\theta_1{}^0$ are shown shaded. The numbers of events within each interval are shown. The numbers of $\Lambda^0/\theta_1{}^0$ events are in parentheses.

with either Λ^0 or θ^0. A χ^2 test of the assumption $\alpha\bar{P}_3 = 0$ yields $\chi^2 = 7.1$ (five degrees of freedom). Probability of $\chi^2 > 7.1 = 0.25$. That is, the data are quite consistent with zero longitudinal polarization of the Λ^0.

A measure of $\alpha\bar{P}_3$ obtained from

$$\alpha\bar{P}_3 = \frac{3}{N}\sum_{i=1}^{N}\cos\theta_i \pm \left[\frac{3-(\alpha\bar{P}_3)^2}{N}\right]^{1/2}$$

yields $\alpha\bar{P}_3 = -0.090 \pm 0.17$ for the 110 Λ^0 events, and -0.24 ± 0.16 with the inclusion of the 10 Λ^0 or θ^0 events. A subset consisting of 65 events satisfying 300 Mev/$c \leq p_{\Lambda^0} \leq$ 700 Mev/c yields $\alpha\bar{P}_3 = -0.06 \pm 0.21$. For these 65 events, the ionization of the decay proton is always greater than twice minimum, and the range of the proton is $\gtrsim$3 mm.

The likelihood ratio, $\mathfrak{R}$, for comparing the relative likelihood of any choice of $\alpha\bar{P}_3$ to the choice $\alpha\bar{P}_3 = 0$ is given by

$$\mathfrak{R} = \prod_{i=1}^{N}(1+\alpha\bar{P}_3\cos\theta_i).$$

This function is plotted in Fig. 3 for the 110 Λ^0's. These data, although consistent with $\alpha\bar{P}_3 = 0$, are clearly not sufficient to rule out small values of $|\alpha\bar{P}_3|$. To obtain a value of $\mathfrak{R}$ equal to 0.01 for the choice $\alpha\bar{P}_3 = \pm 0.2$, for example, assuming the true value were zero, would require on the average ~350 events. Similarly, to rule out $\alpha\bar{P}_3 = \pm 0.1$ at the same level would require ~1000 events. These numbers of events are available for future analysis.

This exposure was performed in collaboration with the Lawrence Radiation Laboratory hydrogen bubble chamber group, who established and maintained the separated K^- beam. We wish to thank Dr. Edward J. Lofgren and the Bevatron staff for their excellent cooperation and Larry O. Oswald and the bubble chamber crew for operation of the chamber.

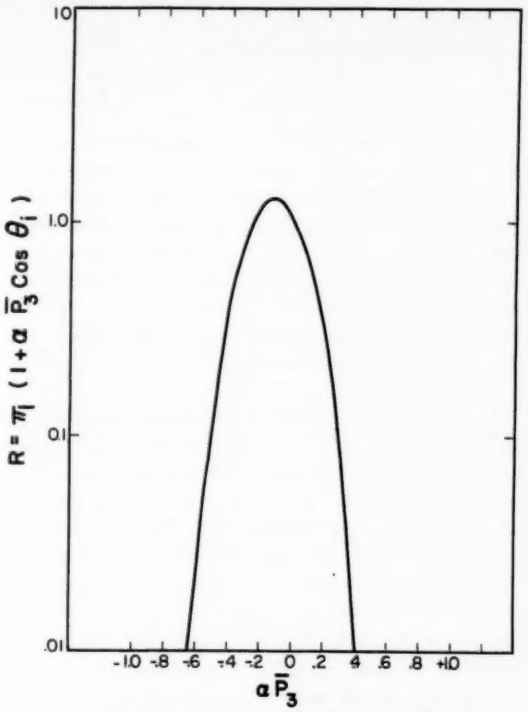

FIG. 3. Plot of likelihood ratio, $\mathfrak{R}$, vs $\alpha\bar{P}_3$. $\mathfrak{R}$ is a measure of the relative likelihood for any value of $\alpha\bar{P}_3$ vs the choice $\alpha\bar{P}_3 = 0$.

[1]Blumenfeld, Chinowsky, and Lederman, Nuovo cimento 8, 296 (1958), and references therein; Cooper, Filthuth, Montanet, Newth, Petrucci, Salmeron, and Zichichi, Nuovo cimento 8, 471 (1958); Baxter Armstrong, thesis, University of California Radiation Laboratory Report UCRL-3470, July, 1956 (unpublished); $\pi^- - p$ collisions near the Λ^0 threshold in hydrogen show no forward-backward asymmetry: Crawford, Cresti, Good, Solmitz, and Stevenson, Phys. Rev. Letters 1, 209 (1958); 2, 11 (1959).

[2]Crawford, Cresti, Good, Gottstein, Lyman, Solmitz, Stevenson, and Ticho, Phys. Rev. 108, 1102 (1957).

[3]T. D. Lee and C. N. Yang, Phys. Rev. 104, 254 (1956); Lee, Steinberger, Feinberg, Kabir, and Yang, Phys. Rev. 106, 1367 (1957).

[4]Powell, Fowler, and Oswald, Rev. Sci. Instr. 29, 874 (1958).

[5]Alvarez, Eberhard, Good, Graziano, Ticho, and Wojcicki, Phys. Rev. Letters 2, 215 (1959).

SIGMA SPIN AND PARITY CONSERVATION IN $K^- + p \to \Sigma^+ + \pi^-$ *

Jack Leitner,† Paul Nordin, Jr., Arthur H. Rosenfeld, Frank T. Solmitz, and Robert D. Tripp
Lawrence Radiation Laboratory, University of California, Berkeley, California
(Received August 10, 1959)

Day, Snow, and Sucher have recently shown that when K^- mesons come to rest in liquid hydrogen, they are captured from s orbits.[1] Such s-state capture leads to Σ-decay angular distributions that are unique functions of the Σ spin. On the basis of an analysis of 145 Σ^+ hyperons produced in K^- absorption,[2] we find very strong evidence for a spin-$\frac{1}{2}$ sigma. We also report a check on the hypothesis of parity conservation in the reaction $K^- + p \to \Sigma^+ + \pi^-$.

The sample considered here consisted of 82 "Σ_0^+" events (i.e., $\Sigma^+ \to \pi^0 + p$) and 63 "Σ_+^+" events (i.e., $\Sigma^+ \to \pi^+ + n$), 95% of which came from K^- absorption at rest. In order to eliminate biases and avoid confusing various possible reactions, only Σ^+ events longer than 0.9 mm were accepted in the analyzed sample. Possible confusion of the event types Σ_0^+ and Σ_+^+, where the decay secondary is too short to provide a reliable ionization estimate, is eliminated by submitting the event to a full kinematic analysis. Events in which the Σ^+ and primary π^- were clearly noncollinear were discarded, since in these cases the K definitely interacted in flight.

The observed center-of-mass angular distribution, folded through 90°, for all Σ^+-decay pions is shown in Fig. 1. In order to determine the Σ spin from this distribution, certain assumptions must be made, since the most general form of the Σ-decay angular distribution contains undetermined parameters.[3] If we assume that the K meson has zero spin[4] and is captured from an s state, the maximum component of angular momentum that the Σ can have along its direction of flight is 1/2. Further, if the Σ has spin greater than 1/2, this leads to an alignment of its spin, J, perpendicular to its direction of motion. The decay angular distribution, $f_J(\theta)$, is thus unique for a given value of J.[5]

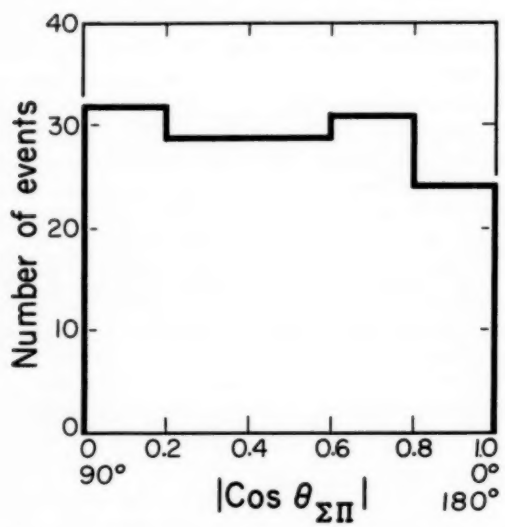

FIG. 1. Folded angular distribution of all Σ^+ decays (145 events).

The crucial assumption of s-state capture has recently been investigated by Day, Snow, and Sucher.[1] They consider hydrogen atoms in an excited state with large quantum number, n, colliding with protons in liquid hydrogen. They point out that the Stark effect serves to oscillate the K-particle wave function between ns and nl states. Since the capture probability from ns states is large compared to the radiative transition probability from all l states of the n level, K particles presumably do not cascade to the $2p$ level, but rather are captured directly from s states. Quantitatively, Day et al. estimate that about 99% of all K-p absorptions occur from s states. We, therefore, feel that the assumption of s-state capture is well grounded.[6]

With these assumptions,[7] the folded distributions $f_J(|\cos\theta|)$ become $f_{1/2} = 1$, $f_{3/2} = \frac{1}{2}(1 + 3\cos^2\theta)$. The forms for higher spin values are given by Adair.[3] For practical purposes, since the observed distribution is quite isotropic, we have analyzed the data in terms of the normalized function, F:

$$F(|\cos\theta|) = \tfrac{1}{2}(1 + A\cos^2\theta)(1 + A/3)^{-1}. \quad (1)$$

An approximate maximum-likelihood solution of Eq. (1) for the best-fit value of A gives $A = +0.12 \pm 0.14$. This is clearly consistent with $J = 1/2$, and moreover is over 20 standard deviations from the expected value of 3 for spin 3/2. This constitutes the strongest evidence to date that the sigma spin is 1/2.[8]

Next, we describe a search for evidence of parity nonconservation in the reaction

$$K^- + p \to \Sigma^+ + \pi^-,$$

using the Σ_0^+ decay mode as an analyzer. Parity

conservation in strong, strange-particle-producing reactions has been carefully checked only for the reaction $\pi^- + p \to \Lambda + K^0$, observed in the associated-production experiments of Crawford et al.[9] The question of parity conservation in other strong, strange-particle-producing interactions is still unsettled and is a subject of much theoretical interest.[10]

To detect parity violation, we look for a nonzero average value of a pseudoscalar variable—namely, the component of the Σ spin in the direction of its momentum. Because the Σ spin is 1/2, the angular distribution of the Σ decay products in the Σ rest frame can be written in the form

$$1 + \alpha P_\Sigma \cos\theta,$$

where α is the decay-asymmetry parameter and P_Σ is the component of polarization along the axis from which θ is measured.

The analyzing properties of the Σ_0^+ mode have been demonstrated by Cool et al.[11] They find $\alpha_{\pi^0} \geq 0.7 \pm 0.3$. It follows, then, that for Σ^+ of polarization P_Σ, we should observe an asymmetry $\geq (0.7 \pm 0.3) P_\Sigma$ in the π^0 angular distribution. This in turn would indicate some degree of parity nonconservation in the reaction $K^- + p \to \Sigma^+ + \pi^-$.

The experimental angular distribution is shown in Fig. 2. There is no statistically significant asymmetry. Using the expression

$$\langle \alpha_{\pi^0} P_\Sigma \rangle = \frac{3}{N} \sum_{i=1}^{N} \cos\theta_i \pm \left(\frac{3}{N}\right)^{\frac{1}{2}},$$

we obtain $\langle \alpha_{\pi^0} P_\Sigma \rangle = 0.02 \pm 0.19$. Hence we find no evidence for parity nonconservation in Σ^+ production.

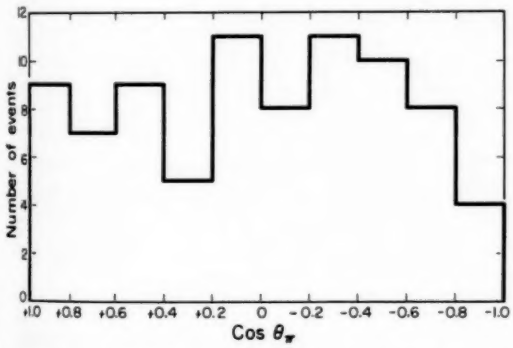

FIG. 2. Angular distribution of pions from $\Sigma^+ \to p + \pi^0$ (83 events).

We check our procedure by noting that Cool et al. find no asymmetry for the Σ_+^+ decay mode. Thus by analyzing our Σ_+^+ events in the same way as we have treated the Σ_0^+, we should find $\langle \alpha_{\pi^+} P_\Sigma \rangle$ close to zero. We have done this and find $\langle \alpha_{\pi^+} P_\Sigma \rangle = -0.03 \pm 0.22$, which is indeed isotropic and constitutes indirect evidence against hidden biases.

*Supported in part by the U. S. Atomic Energy Commission and Office of Scientific Research, U. S. Air Force.

†On leave from Syracuse University, New York.

[1]Day, Snow, and Sucher, Phys. Rev. Letters 3, 61 (1959).

[2]Alvarez, Bradner, Rosenfeld, Solmitz, and Tripp, Nuovo cimento 5, 1026 (1956).

[3]R. K. Adair, Phys. Rev. 100, 1540 (1955).

[4]The evidence that the K^- spin is indeed 0, although indirect, is quite strong. For a rather complete evaluation of this evidence see F. Eisler et al. (reference 8).

[5]S. Trieman, Phys. Rev. 101, 1216 (1956).

[6]Before the work of Day et al., analysis of our data could only give much weaker evidence for a sigma spin of 1/2. This is reported in Leitner, Nordin, Rosenfeld, Solmitz, and Tripp, University of California Radiation Laboratory Report UCRL-8737, May, 1959 (unpublished).

[7]Parity nonconservation in the Σ decay does not complicate the distribution if it is folded about 90 deg, because then all odd powers of $\cos\theta$ vanish. For details of this argument, see N. Samios, thesis, Nevis Cyclotron Laboratory Report No. 32, January, 1957 (unpublished).

[8]F. Eisler et al., Nuovo cimento 7, 222 (1958).

[9]Crawford, Cresti, Good, Solmitz, and Stevenson, Phys. Rev. Letters 1, 418 (1958).

[10]G. Feinberg, Phys. Rev. 108, 898 (1957); V. Soleviev, Nuclear Phys. 6, 618 (1958); A. Pais, Phys. Rev. Letters 1, 418 (1958).

[11]Cool, Cork, Cronin, and Wenzel, Phys. Rev. 114, 912 (1959).

PHOTOPRODUCTION OF NEUTRAL MESONS FROM HYDROGEN NEAR THRESHOLD*

P. D. Luckey, L. S. Osborne, and J. J. Russell
Physics Department and Laboratory for Nuclear Science, Massachusetts Institute of Technology, Cambridge, Massachusetts
(Received August 11, 1959)

The differential cross section for the reaction $\gamma + p \rightarrow p + \pi^0$ has been measured for mean incident γ-ray energies of 170 and 190 Mev by measuring single π^0-decay γ-ray yields from a liquid hydrogen target at laboratory angles 48°, 81°, and 141°, and bremsstrahlung peak energies 160, 180, and 200 Mev. The π^0 γ rays are detected by a total absorption spectrometer consisting of a 1/2-in. plastic anticoincidence counter, a 4-in. diameter by 2-in.-thick NaI crystal in which the incident γ ray is required to convert, and a $7\frac{3}{4}$-in.-thick, $9\frac{1}{2}$-in. diameter NaI crystal which absorbs most of the shower initiated in the thin NaI crystal. The outputs of the two NaI crystals are added and pulse-height analyzed; the gains of the two counters are adjusted to give the same voltage output per Mev of energy lost. The energy resolution of the spectrometer has been measured for monoenergetic electrons of various energies and found to have a 23% full width at half-maximum. The relative efficiency as a function of energy was determined by observing a bremsstrahlung spectrum first in the large crystal alone and then with the two-crystal combination; from the NaI γ-ray absorption cross section at high energies where the efficiency is constant, this value was calculated to be 64%.

The spectrum of π^0-decay γ rays in the center of mass of the reaction $\gamma + p \rightarrow p + \pi^0$ is given by an effective γ-ray production cross section[1]

$$\frac{d^2\sigma^\gamma}{d\Omega dE}_\gamma = \frac{2}{q}\sum_n a_n P_n(\theta_\gamma) P_n(\varphi),$$

if the original π^0 cross section is written as

$$d\sigma^\pi/d\Omega = \sum_n a_n P_n(\theta_\pi),$$

where $\varphi = \cos^{-1}(1/\beta - \mu^2/2qE_\gamma)$ is the angle between the observed γ ray and its parent π^0; μ, β, and q are the π^0 mass, velocity, and momentum in the center-of-mass system, respectively; and P_n is the Legendre polynomial of order n. Only the portion of the spectrum above $\cos\varphi = 0$ was used for analysis, since for negative values of $\cos\varphi$ the corresponding γ-ray energies E_γ are sufficiently small that the spectrometer efficiency is low and not accurately known. The data were divided into bins of $\Delta(\cos\varphi) = 0.2$ wide and for each bin the coefficients $a_0P_0(\varphi)$, $a_1P_1(\varphi)$, and $a_2P_2(\varphi)$ were determined. These values are plotted in Fig. 1. A fit to the various $P_n(\varphi)$ was then made to determine the coefficients a_0, a_1, and a_2. The values thus obtained are shown in Table I, together with theoretical values to be

Table I. Angular distribution coefficients. All values are in μb/sterad. k' is the mean incident laboratory γ-ray energy.

k'		a_0	a_1	a_2
170	Exp.	0.37 ± 0.03	−0.05 ± 0.05	−0.11 ± 0.13
	Chew	0.42	−0.22	+0.03
190	Exp.	1.02 ± 0.05	−0.29 ± 0.11	−0.07 ± 0.09
	Chew	1.15	−0.47	−0.09

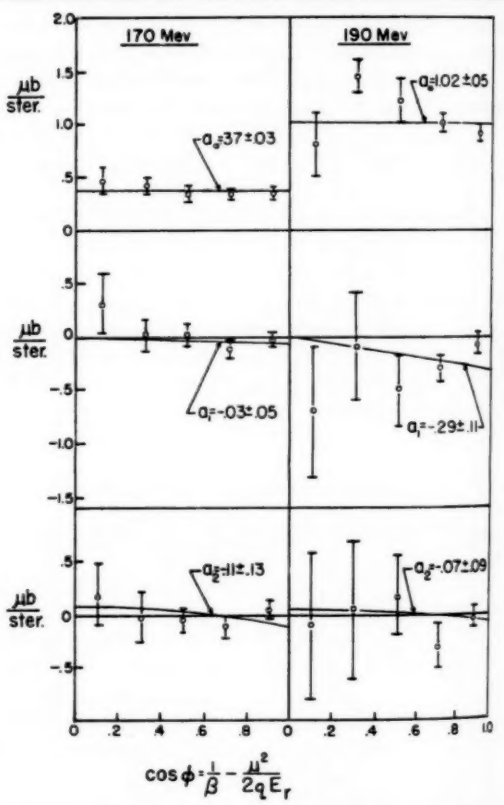

FIG. 1. Angular distribution coefficients as a function of decay γ-ray energy. See text for explanation.

discussed below. The spectra appear consistent with this analysis.

The errors associated with the values in Table I include three sources: (1) statistics; (2) uncertainty in the counter efficiency at low energies due to variation of the biasing level in the large NaI crystal; for low-energy γ rays, an insufficient portion of the shower may penetrate the large crystal to trigger the discriminator associated with it; (3) uncertainty in the location of the energy E_γ corresponding to a particular value of $\cos\varphi$, due to uncertainty in the absolute calibration of the energy scale and to the variation of E_γ with β, i.e., the variation over the band of incident γ rays accepted. This effect is most important for the large $\cos\varphi$ values.

A correction was necessary for distortion of the spectrum by the finite energy resolution of the counter. By constructing a theoretical spectrum and then combining it with a series of Gaussian resolution functions having a full width at half-maximum of 23% (chosen to fit the monoenergetic electron response), a correction factor for distortion due to resolution was calculated. This correction is important only at large values also; its maximum value is 40%.

From the relativistic dispersion relation approach of Chew, Low, Goldberger, and Nambu,[2] the π^0 angular distribution may be written as

$$\frac{1}{e^2f^2}\frac{k}{q}\frac{d\sigma}{d\Omega}=[|S|^2+\tfrac{1}{3}q^2k^2(|P_1|^2+|P_2|^2+|P_3|^2)]P_0(\theta)$$
$$+2qk\mathrm{Re}(S^*P_1)P_1(\theta)$$
$$+\tfrac{1}{3}q^2k^2(2|P_1|^2-|P_2|^2-|P_3|^2)P_2(\theta),$$

where S is the $E1$, S-wave amplitude; P_1, P_2, and P_3 are combinations of the $P_{1/2}$, $M1$ amplitude and the $P_{3/2}$, $M1$ and $E2$ amplitudes; k is the incident photon momentum. A small recoil correction to the $M1$ amplitudes and a term describing the interaction between the photon and the recoil-proton current have both been neglected in the equation above; they have been evaluated numerically and found to be negligible. Following reference 1, the real part of the amplitude S is given by

$$\mathrm{Re}S=\omega N^+-\omega[(g_p+g_n)/2M],$$

where g_p, g_n, and M are the proton and neutron anomalous moments and M the nucleon mass; $\omega=(q^2+1)^{1/2}+q^2/2M$; and N^+ is an integral over the S and the small P scattering phase shifts. Lack of experimental data makes it difficult to evaluate.

Setting $N^+=0$, the amplitudes above have been evaluated to give the values shown in Table I. From the cross section given above it is possible to calculate separately $\mathrm{Re}S$, $|P_1|$, and $P_2^2+P_3^2$; on the assumption that $P_1=-P_2$, as predicted by the Chew calculation, we can calculate separately P_3. In Table II are given the values of the amplitudes calculated from the experimental values in Table I.

The experimental values of the P's are substantially lower than the predictions of Chew et al. Agreement with the experimental values of S could be obtained with a value of $N^+=+0.04$; Chew et al. have estimated that $|N^+|<0.2$.

In addition to the data mentioned above, γ-ray yields were also measured at a peak bremsstrahlung energy of 140 Mev. The excitation function at 81° of γ rays above $\cos\varphi=0$ (the energy E_γ corresponding to $\cos\varphi=0$ is almost independent of β, the π^0 velocity) was analyzed in terms of an excitation function having q, q^3, and q^5 momentum dependences. The coefficient of the q (S-wave) term corresponds to an S-wave contribution to the total cross section of 0.03 ± 0.03

Table II. Production amplitudes determined from the data in Table I. k' is the mean incident laboratory γ-ray energy.

k'		S	$P_1=-P_2$	P_3	$(\lvert P_2\rvert^2+\lvert P_3\rvert^2)^{1/2}$
170	Exp.	-0.01 ± 0.01	0.26 ± 0.07	0.40 ± 0.09	0.48 ± 0.04
	Chew et al.[a]	$-0.07+N^+$	0.41	0.45	0.62
190	Exp.	-0.05 ± 0.02	0.34 ± 0.02	0.38 ± 0.03	0.50 ± 0.02
	Chew et al.[a]	$-0.08+N^+$	0.42	0.52	0.66

[a]See reference 2.

μb at 150 Mev; this value is consistent with the S-wave total cross section predicted by the value of S determined from the angular distribution. The theory of Drell, Friedman, and Zachariasen,[3] taking into account the internal rescattering of a photoproduced π^+ in an S state, predicts a total cross section of 1 μb at 150 Mev.

The authors wish to express their appreciation to Gilbert Davidson and Zvi Westreich for their help in taking data.

*This work is supported in part through funds provided by the U. S. Atomic Energy Commission, the Office of Naval Research, and the Air Force Office of Scientific Research.

[1]H. L. Anderson and M. Glicksman, Phys. Rev. 100, 268 (1955).

[2]Chew, Low, Goldberger, and Nambu, Phys. Rev. 106, 1345 (1957).

[3]Drell, Friedman, and Zachariasen, Phys. Rev. 104, 236 (1956).

NOTES ON ANTIBARYON INTERACTIONS*

A. Pais†

Lawrence Radiation Laboratory, University of California, Berkeley, California

(Received August 3, 1959)

This note presents some simple consequences of (or checks for) invariance considerations as applied to interactions of antibaryons.

A. P conservation in strong interactions.—Consider the reactions $\bar{p}+p\to n$ particles. If the reaction occurs at rest for $n\geq 4$ or in flight for $n\geq 3$, there are enough independent momentum vectors to form, in any coordinate system, a nonvanishing quantity $\vec{p}_1\cdot(\vec{p}_2\times\vec{p}_3)$. The condition of symmetry in the up-down distribution of $\vec{p}_1$ relative to the (p_2, p_3) plane is then a consequence of P conservation, unless other inherent symmetries require this distribution to be symmetrical anyway. Thus, consider the reaction in flight

$$\bar{p}+p\to 1+2+R, \tag{1}$$

where 1 and 2 are some specific particles and where the "rest" R may be any assembly of particles. We always work in the $(\bar{p}, p)$-c.m. system and consider exclusively unpolarized beams and targets. The initial state is in general not an eigenstate of P. But it is an eigenstate of PR, where R is a 180° rotation around any axis perpendicular to $(\bar{p}, p)$ and which we may take perpendicular to $(\bar{p}, 1)$. Let $W(1, E_1, \theta_1;\ 2, E_2, \theta_2, \phi)$ denote the probability of finding particle 1 (2) with an energy E_1 (E_2) at an angle θ_1 (θ_2) relative to the direction of $\bar{p}$, where ϕ is the azimuth of 2 relative to the $(\bar{p}, 1)$ plane. Then PR implies

$$W(1, E_1, \theta_1;\ 2, E_2, \theta_2, \phi) = W(1, E_1, \theta_1;\ 2, E_2, \theta_2, -\phi). \tag{2}$$

As an example of other symmetries which would imply Eq. (2), we note that if 1 and 2 are both π^+, Eq. (2) is valid as a consequence of Bose statistics. If one considers the triple $(\bar{p}, \pi^+, \pi^-)$, however, there seems to be no other known symmetry than PR which leads to Eq. (2).

B. C invariance of strong interactions.—Consider again Reaction (1) and also

$$\bar{p}+p\to\bar{1}+\bar{2}+\bar{R} \tag{3}$$

[The products in Reaction (3) may or may not be identical with those of Reaction (1).] The initial state ψ_S ($S=0, 1$ is the total spin) is in general not an eigenstate of C. However, we have

$$CR\psi_S=(-1)^{S+S_z}\psi_S, \tag{4}$$

which makes CR useful for an unpolarized beam and target, as here the cross section for any reaction does not involve interference between initial spin states so that CR invariance may be applied to the final states. Let the probabilities referring to Eq. (2) be denoted by $\bar{W}$. Then CR implies

$$W(1, E_1, \theta_1;\ 2, E_2, \theta_2, \phi) = \bar{W}(\bar{1}, E_1, \pi-\theta_1;\ \bar{2}, E_2, \pi-\theta_2, \pi-\phi). \tag{5}$$

In the case of pure pion annihilation the symbols $\bar{W}$ and W refer to the same reaction. In other instances, such as $\bar{p}+p\to\bar{p}+\Lambda+K^+$, $\bar{p}+p\to p+\bar{\Lambda}+K^-$, they refer to different reactions.

We may also apply CP to the final states, as

$$CP\psi_S=(-1)^{S+1}\psi_S, \tag{6}$$

and obtain

$$W(1, E_1, \theta_1;\ 2, E_2, \theta_2, \phi) = \bar{W}(\bar{1}, E_1, \pi-\theta_1;\ \bar{2}, E_2, \pi-\theta_2, \pi+\phi). \tag{7}$$

Equations (2), (5), and (7) are derived channel by

channel. They may therefore also be applied to sums over channels so that there are no complications because of incomplete knowledge of the neutral particles produced.

Whenever P conservation is established, one may check C by using a relation that, in itself, follows either from CR or from CP, such as

$$W(1, E, \theta) = \overline{W}(\overline{1}, E, \pi - \theta). \tag{8}$$

From this relation it follows that the π^0 distribution in any pure pion annihilation channel is symmetric around 90°.

Because antinucleons play a virtual role in low-energy nuclear phenomena, the high degree to which P conservation is known to hold in the latter domain has implications also for these antiparticles. In this sense, relations like Eqs. (2), (5), and (7) may be considered as a useful complement to the low-energy information. Their applicability to very-high-energy phenomena (regardless of the complexity of the events) makes it possible to verify the validity of these conservation laws at frequencies that are perhaps not as sensitively explored in the low-energy nuclear effects.

For two-body reactions like

$$\bar{p} + p \rightarrow \overline{\Lambda} + \Lambda, \tag{9}$$

Eqs. (5) and (7) are trivial. However, here CP also has a useful application. If we denote by $\vec{q}(\Lambda, \theta)$ and $\vec{q}(\overline{\Lambda}, \theta)$, respectively, the polarizations of Λ and $\overline{\Lambda}$, if any, where θ is the angle between the particle in question and the $\bar{p}$ direction, then CP implies

$$\vec{q}(\Lambda, \theta) = \vec{q}(\overline{\Lambda}, \pi - \theta). \tag{10}$$

(Of course P implies more stringently that the $\vec{q}$ vectors are perpendicular to the production plane.) Equation (6) is here also valid in the final state, so that the differential cross section of Eq. (9) is the sum of a triplet–triplet and a singlet–singlet differential cross section. Furthermore, it is readily shown that Eq. (10) also applies generally if $\vec{q}(\Lambda, \theta)$ refers to Reaction (1) and $\vec{q}(\overline{\Lambda}, \theta)$ to (3), again as a consequence of CP. Thus Eq. (10) holds for $(\overline{\Lambda}, \Sigma^0)$ as compared to $(\Lambda, \overline{\Sigma}^0)$ production; the partial cross sections of these reactions should be each other's mirror around 90°.

C. Charge symmetry (CS) and charge independence (CI).—Antihyperon annihilations via strong interactions provide in principle various means to verify CS and CI. In practice, large numbers of antihyperon events are needed for this.[1]

For $(\overline{\Lambda}, p)$ annihilation, we have[2] from CI

$$(\overline{\Lambda}, p \rightarrow K^0, \pi^+) = 2(\overline{\Lambda}, p \rightarrow K^+, \pi^0). \tag{11}$$

This is the only relation that CI imposes.[3] A much more interesting situation obtains if the $\overline{\Lambda}$'s are annihilated in deuterium. The reason is that the $(\overline{\Lambda}, d)$ system is self-charge symmetric. [It shares this property with (Λ, d), but it has considerable phase-space advantage.] Thus let $W(K^+)$ and $W(K^0)$ be the probabilities, respectively, of producing a K^+ (K^0) in $(\overline{\Lambda}, d)$ annihilation. Then CS tells us[2]

$$W(K^+) = W(K^0), \tag{12}$$

regardless of the complexity of the various annihilation modes possible.[4] Thus $(\overline{\Lambda}, d)$ interactions may be of particular interest at very high energies. In addition, we have[5] from CI

$$(\overline{\Lambda}, d \rightarrow n, K^+, \pi^0) = \tfrac{1}{4}(\overline{\Lambda}, d \rightarrow n, K^0, \pi^+). \tag{13}$$

The annihilation in flight of $\overline{\Sigma}^{\pm}$ in d also tests CS. Call $W_{\pm}(K)$ the probability of producing a K in $\overline{\Sigma}^{\pm}$ - d reactions. Then we have

$$W_{\pm}(K^+) = W_{\mp}(K^0). \tag{14}$$

Finally, production reactions in d yield a few CI relations, namely:

$$(\bar{p}, d \rightarrow \overline{\Lambda}, \Lambda, p, \pi^-) = 2(\bar{p}, d \rightarrow \overline{\Lambda}, \Lambda, n, \pi^0), \tag{15}$$

$$(\bar{p}, d \rightarrow \overline{\Sigma}^+, \Lambda, p) = 2(\bar{p}, d \rightarrow \overline{\Sigma}^0, \Lambda, n), \tag{16}$$

$$(\bar{p}, d \rightarrow \overline{\Lambda}, \Sigma^-, p) = 2(\bar{p}, d \rightarrow \overline{\Lambda}, \Sigma^0, n). \tag{17}$$

D. $\overline{\Lambda}$ decay and T invariance.—It has been noted by Okubo[6] that CPT invariance by itself does not imply the equality of the partial lifetimes of hyperon decay into a given channel and of antihyperon decay into the corresponding charge-conjugate channel. In general there are three independent sufficient grounds for two such quantities to be equal, namely (a) absence of final-state interactions, (b) C invariance, and (c) T invariance. In the case of the $\overline{\Lambda}$, there is a fourth independent sufficient ground, namely the $\Delta I = \frac{1}{2}$ rule.[7] Thus the validity of the latter rule would obviate the possibility of testing T invariance by means of a partial lifetime comparison. This is in principle not the case when one compares the up-down asymmetries α_{ch} and $\bar{\alpha}_{ch}$ of the decays $\Lambda \rightarrow p + \pi^-$ and $\overline{\Lambda} \rightarrow \bar{p} + \pi^+$. In fact, if one assumes the $\Delta I = \frac{1}{2}$ rule to be valid, one has

$$\rho \equiv \frac{\alpha_{ch}}{\bar{\alpha}_{ch}} = \frac{\sin(\delta_{11} - \delta_1 - \Delta)}{\sin(\delta_{11} - \delta_1 + \Delta)}, \tag{18}$$

where δ_{11} and δ_1 are the $P_{1/2}$ and $S_{1/2}$ π-nucleon phase shifts in the $I=\frac{1}{2}$ state. Here Δ has the following properties: If C invariance holds, we have $\Delta=0$, so $\rho=1$; if T invariance holds, we have $\Delta=\pi/2$, so $\rho=-1$. From the magnitude of α_{ch} we know already[8] that $|\Delta| \gtrsim \pi/4$. We also see that $\rho=-1$ if $\delta_{11}-\delta_1$ is neglected relative to Δ. As this neglect is justified to a good approximation, it follows that a 20% deviation from $\rho=-1$ is the most that can be anticipated.[9]

I am indebted to many physicists at the Lawrence Radiation Laboratory for stimulating discussions.

*This work done under the auspices of the U. S. Atomic Energy Commission.

†Permanent address: Institute for Advanced Study, Princeton, New Jersey.

[1]Thus for $\bar{\Lambda}$ production in hydrogen by 1-Bev antiprotons, one would need to have an annihilation cross section as large as ~50 mb to have an effect ~1%.

[2]The relations (11) to (17) refer to relative rates and are valid for all energies and all angles.

[3]In this note, we do not consider inequalities following from CI.

[4]Of course Eq. (12) may also be applied to an individual channel and its charge-symmetric one, such as (n,K^0,π^+) versus (p,K^+,π^-), etc.

[5]Here the pure $I=1$ state of the K-nucleon system is involved. In $(\bar{\Lambda},d\to p,K^0)=(\bar{\Lambda},d\to n,K^+)$ we deal with the corresponding pure $I=0$ state.

[6]S. Okubo, Phys. Rev. 109, 984 (1958).

[7]Electromagnetic effects are ignored here.

[8]R. Gatto, Phys. Rev. 108, 1103 (1957); see also S. Weinberg, Phys. Rev 110, 782 (1958).

[9]Putting $\Delta=\pi/2-\epsilon$, $\rho\simeq-(1+0,2\tan\epsilon)$.

ERRATA

VALLEY-ORBIT SPLITTING OF ARSENIC DONOR GROUND STATE IN GERMANIUM. G. Weinreich, W. S. Boyle, H. G. White, and K. F. Rodgers [Phys. Rev. Letters 2, 96 (1959)].

In the previous Letter we reported measurements which indicated that in the arsenic donor ground state in germanium the triplet component has a lower energy than the singlet. Since very strong evidence to the contrary[1,2] has now appeared, we were led to re-examine our experimental procedure in order to attempt to locate the origin of the discrepancy.

We have modified our equipment so as to improve greatly both the homogeneity of the applied strain and the certainty of its orientation. Data taken with the new arrangement indeed reveal a line splitting opposite to the one we previously reported, establishing that the singlet is the lower state in agreement with the other evidence quoted. Apparently we had been dealing with a rather peculiar pattern of inhomogeneity which, instead of simply broadening the absorption, produced the deceptive line shape shown in our first report.

These new experiments were performed on samples with about ten times less arsenic content than the original ones, since at this concentration the line is much better defined. We do not believe, however, that the different results are connected with the different concentration, since the new samples under the old strain conditions show the same spurious behavior as the more strongly doped ones.

A full report of the experiment will be submitted to the Physical Review.

[1]H. Fritzsche, Bull. Am. Phys. Soc. 4, 185 (1959).

[2]G. Feher, D. K. Wilson, and E. A. Gere, Phys. Rev. Letters 3, 25 (1959).

ELECTROMAGNETIC TRANSITIONS BETWEEN μ MESON AND ELECTRON. S. Weinberg and G. Feinberg [Phys. Rev. Letters 3, 111 (1959)].

In comparing the rate $\omega_{N\to N'}$ for $\mu^-+N\to e^-+N'$ via virtual photon absorption with the rate ω_{abs} for ordinary muon absorption, an important numerical factor was omitted from ω_{abs}. Equation (11) should read[1]

$$\omega_{abs}\simeq(1/2\pi^2)Z_{eff}{}^4\alpha^3\xi_\beta{}^2 m_\mu C, \qquad (11)'$$

$$C = (\langle \nu_N \rangle / m_\mu)^2 (1 - \frac{A - Z}{2A} \delta).$$

Here $\langle \nu_N \rangle \approx 0.75 m_\mu$ is the mean neutrino momentum for all final states, and $\{1 - [(A - Z)/2A]\delta\}$ represents the inhibition of muon absorption due to the Pauli principle; δ is about 3. The factor C is essential in bringing (11)′ into agreement with experiment.[2] Equation (13) should be corrected to read

$$\omega_{N \to N'} / \omega_{\text{abs}} \approx 32\pi^2 \alpha^2 Z |F_{N'N}|^2 \xi_0^{\,2} / C \xi_\beta^{\,2}. \quad (13)'$$

C varies from 0.14 in the lightest elements to 0.05 for Pb^{208}. For all nuclei heavier than about $A \sim 60$ we now expect the ratio of the total rates to be approximately constant, and given by

$$R = \sum_{N'} \omega_{N \to N'} / \omega_{\text{abs}} \approx 1.0 \xi_0^{\,2} / \xi_\beta^{\,2}.$$

Thus because of the possibility of coherent absorption ($\mu^- + N \to e^- + N$), experiments on possible fast electrons from muon capture are far more sensitive as tests of a possible $\mu - e - \gamma$ interaction than one might otherwise suppose. The experimental upper limit already set[3] on R now gives

$$\xi_0^{\,2} / \xi_\beta^{\,2} \leq 5 \times 10^{-4} \quad (19)'$$

for the ratio of the $\mu - e - \gamma$ monopole transition strength to the β-decay coupling constants. This upper limit is already not very much greater (a factor of perhaps 100) than what one would expect in an intermediate boson theory.

Similar remarks also apply to the original purpose of the Steinberger-Wolfe experiment, which was to set an upper limit on the coupling constant $G_{\mu e}^{\,2}$ of an equal μepp and μenn interaction. We expect from this interaction a branching ratio

$$R \approx G_{\mu e}^{\,2} A^2 \textstyle\sum_{N'} |F_{N'N}|^2 / C Z \xi_\beta^{\,2},$$

so that their experiment is about 65 times more sensitive than they estimated.

We should like to take this opportunity to also correct a minor typographical error. Our metric is given by

$$q^2 = q_\lambda q^\lambda = \vec{q}^{\,2} - (q^0)^2,$$

and not as stated in the Letter.

---

[1] H. Primakoff, Revs. Modern Phys. 31, 802 (1959).

[2] Sens, Swanson, Telegdi, and Yovanovitch, Phys. Rev. 107, 1464 (1957).

[3] J. Steinberger and H. Wolfe, Phys. Rev. 100, 1490 (1955).

ABSTRACTS

In this section are printed the abstracts of Articles that have been forwarded to The American Institute of Physics for publication in THE PHYSICAL REVIEW. In quoting information obtained from this section before the appearance of the corresponding Article, reference should be made to "Physical Review (to be published)" rather than to this Journal.

SELF-CONSISTENT FIELD APPROACH TO THE MANY-ELECTRON PROBLEM. H. Ehrenreich, General Electric Research Laboratory, Schenectady, New York, and M. H. Cohen, Institute for the Study of Metals, University of Chicago, Chicago, Illinois (Received March 30, 1959).

The self-consistent field method in which a many-electron system is described by a time-dependent interaction of a single electron with a self-consistent electromagnetic field is shown to be equivalent for many purposes to the treatment given by Sawada and Brout. Starting with the correct many-electron Hamiltonian, it is found, when the approximations characteristic of the Sawada-Brout scheme are made, that the equation of motion for the pair creation operators is the same as that for the one-particle density matrix in the self-consistent field framework. These approximations are seen to correspond to (1) factorization of the two-particle density matrix and (2) linearization with respect to off-diagonal components of the one-particle density matrix. The complex, frequency-dependent dielectric constant is obtained straightforwardly from the self-consistent field approach both for a free electron gas and a real solid. It is found to be the same as that obtained by Nozières and Pines in the random phase approximation. The resulting plasma dispersion relation for the solid in the limit of long wavelengths is discussed.

ENERGY LEVELS OF A BOSE-EINSTEIN SYSTEM OF PARTICLES WITH ATTRACTIVE INTERACTIONS. Kerson Huang, Department of Physics and Laboratory for Nuclear Science, Massachusetts Institute of Technology, Cambridge, Massachusetts (Received March 17, 1959).

An N-body Bose-Einstein system of particles with long-range attraction and hard-sphere repulsion between particles is considered. It is shown that if the constants of the interaction have values within a certain range it is possible to calculate the ground-state energy of the system as a function of Ω/N, where Ω is the volume of the box containing the system, in the limit $N\to\infty$, $\Omega\to\infty$, with $N/\Omega=\rho$ fixed. The results show that the system can possess an N-body bound state, which has an equilibrium density and negative energy, and that the interactions can be saturating. Excited states are also considered. It is shown that low-lying excitations consist purely of phonons, whose velocity agrees with that computed from the macroscopic compressibility, furnished by the ground-state energy. The formula for the general excited energy levels suggests that thermodynamically the system may have a "gas" phase and two "liquid" phases, the transition between the two "liquid" phases being the analog of the Bose-Einstein condensation of the ideal gas. Thermodynamic considerations are however not contained in this paper.

THEORY OF MANY-PARTICLE SYSTEMS. I. Paul C. Martin and Julian Schwinger, Lyman Laboratory of Physics, Harvard University, Cambridge, Massachusetts (Received March 20, 1959).

This is the first of a series of papers dealing with many-particle systems from a unified, nonperturbative point of view. It contains derivations and discussions of various field-theoretical techniques which will be applied in subsequent papers. In a short introduction the general method of approach is summarized, and its relationship to other field-theoretic problems indicated. In the second section the macroscopic properties of the spectra of many-particle systems are described. Asymptotic evaluations are performed which characterize these macroscopic features in terms of intensive parameters, and the relationship of these parameters to thermodynamics is discussed. The special characteristics of the ground state are shown to follow as a limiting case of the asymptotic evaluations. The third section is devoted to the time-dependent field correlation functions, or Green's functions, which describe the microscopic behavior of a multiparticle system. These functions are defined, and related to intensive macroscopic variables when the energy and number of particles are large. Spectral representations and other properties of various one-particle Green's

functions are derived. In the fourth section the treatment of nonequilibrium processes is considered. As a particular example, the electromagnetic properties of a system are expressed in terms of the special two-particle Green's function which describes current correlation. The discussion yields specifically a fluctuation-dissipation theorem, a sum rule for conductivity, and certain dispersion relations. The fifth section deals with the differential equations which determine the Green's functions. The boundary conditions that characterize the equations for the Green's functions are exhibited without reference to adiabatic decoupling. A method for solving the equation approximately, by treating the correlations among successively larger numbers of particles, is considered. The approximation in this sequence is shown to yield a generalized Hartree-like equation. A related, but rigorous identity for the single-particle Green's function is then derived. A second approximation, which takes certain two-particle correlations into account, is shown to produce various additional effects: the interaction between particles is altered in a manner characterized by the intensive macroscopic parameters, and the modification and spread of the energy-momentum relation come into play. In the final section compact formal expressions for the Green's functions and other physical quantities are derived. Alternative equations and systematic approximations for the Green's functions are obtained.

ADIABATIC INVARIANTS OF PERIODIC CLASSICAL SYSTEMS. C. S. Gardner, Poulter Laboratories, Stanford Research Institute, Menlo Park, California (Received March 23, 1959).

Recently there has been renewed interest in adiabatic invariants of simply periodic classical systems subject to perturbation by slow variation of parameters. In several interesting cases it has been shown that if the system varies slowly from one steady state to a different steady state, the appropriate adiabatic invariant is constant to an arbitrarily high order in a slowness parameter. It is shown here how these and similar results may be derived by systematic use of a technique of perturbation theory for classical Hamiltonian systems. The method is essentially iteration of the transformation to action and angle variables.

PROPOSED DIRECT TEST OF THE UNCERTAINTY PRINCIPLE. P. R. Ryason, California Research Corporation, Richmond, California (Received May 15, 1957; revised manuscript received April 28, 1959).

The behavior of single particles is a central issue in the interpretation of the quantum theory. Yet, the observation of single particles under well-controlled conditions has been difficult. Field-ion and field-emission microscopy permit the ready observation of single particles. It is proposed to test the relation $\Delta E\,\Delta t \approx \hbar$ by the pulsed-field desorption of single particles from the tip of a field-emission microscope. The conditions for such an experiment are briefly discussed.

INFLUENCE OF COLLECTIVE EFFECTS ON THE MAGNETORESISTANCE OF METALS. Rosemary A. Coldwell-Horsfall and D. ter Haar, Clarendon Laboratory, Oxford, England (Received March 30, 1959).

We have investigated the influence of the correlations between carriers on the magnetoresistance, β, of metals. Using the expressions derived by Fletcher and Larson, the change in β is evaluated for a one-band model. We have also used Landau's theory of a Fermi liquid as modified by Silin to apply to the conduction electrons in a metal. The change in β both in a one-band and in a two-band model is considered. It is found that for a semiconductor like InSb the change would be negligible, but that for a metal such as Al there would be a change of about 10%.

CONFIGURATION INTERACTION IN ALKALI HALIDE PHOSPHORS. Robert S. Knox, Department of Physics, University of Illinois, Urbana, Illinois (Received March 23, 1959).

It is shown that excited-state wave functions of free activator ions do not provide a completely adequate basis for a quantitative theory of the luminescence of alkali halides activated by heavy metals. It is proposed that better zero-order wave functions may be obtained by allowing interaction between different types of states of excitation, and as a practical example of an electronic configuration which can interact with excited activator configurations, the electron transfer states of the Seitz model are discussed

in detail. These states have generally been ruled out because of the absence of a halogen-like doublet in the phosphor absorption spectra, but a closer analysis shows that the doublet character of the activator atom is of equal importance. Neither of the doublets is expected to appear explicitly in the spectra. A numerical estimate of the coupling between an excited activator $6s6p$ state and a typical electron transfer state indicates the possibility of strong interaction between these configurations. It is concluded that the Seitz model is capable of explaining recent experiments on excitation bands, polarization effects, and lattice structure dependence of absorption spectra, provided that more emphasis is placed on electron-transfer states or other excited states of the host crystal which can interact with excited activator configurations.

ELECTRODYNAMICS OF CHARGE CARRIERS OF NEGATIVE EFFECTIVE MASS IN CRYSTALS. Sergio Rodriguez, Department of Physics, University of Washington, Seattle, Washington (Received March 23, 1959).

The transport properties of negative-effective-mass carriers in crystals are studied. The electrical conductivity of a sample in which the electron distribution function is weakly perturbed from its thermal equilibrium value is always positive, even in the presence of a magnetic field. Therefore, cyclotron resonance experiments in equilibrium should display energy absorption, although the negative-mass carriers will circulate in the sense opposite to that of positive-mass carriers of the same charge.

GAIN-BANDWIDTH PRODUCT OF PHOTOCONDUCTORS. R. W. Redington, General Electric Research Laboratory, Schenectady, New York (Received March 27, 1959).

The relaxation time of a photoconductor with space-charge limited dark current is shown to be less than or equal to the transit time under space-charge limited current conditions for an arbitrary distribution of impurity levels. Thus the gain-bandwidth product of a photoconductor with space-charge limited dark current is always less than or equal to the reciprocal of the relaxation time. This inclusion of arbitrary impurity levels in the derivation gives a firm upper limit for the gain-bandwidth product in the space-charge limited dark current region. Rose and Lampert concluded that under some conditions this performance in the space-charge limited current region could be exceeded. The difference between these two conclusions results entirely from a different choice of measure of the relaxation time. The arguments presented suggest that most photoconductors with space-charge limited dark current closely approach this maximum performance.

In addition, a relation between the variation with light level of the photoconductor's gamma, relaxation time, and response time is noted and its usefulness in predicting the performance of photoconductors is suggested.

SIMPLIFIED LCAO METHOD FOR ZINC BLENDE, WURTZITE, AND MIXED CRYSTAL STRUCTURES. Joseph L. Birman, Research Laboratories, Sylvania Electric Products Incorporated, Bayside, New York (Received January 22, 1959).

The tight-binding (LCAO) method is a convenient, if qualitative, way of comparing energy bands in the zinc blende and wurtzite structures. By using this method it is shown that wurtzite states along Γ-Γ' ("c" direction in the zone) can be obtained by perturbing corresponding zinc blende states along Γ-Λ ([111] zone direction). The perturbation is the difference of crystal potential, $V' = V(\mathrm{ZB}) - V(\mathrm{Wur})$, which takes the zinc blende structure into the wurtzite and results in a splitting and shifting of these corresponding states. For $\vec{k}$ perpendicular to these directions the correspondence of $\vec{k}$ vectors and of states is not so clear, although some comparison can still be made.

The discussion of corresponding zinc blende and wurtzite states is helpful in understanding the nature of the energy states in mixed crystals (wurtzite structure [111] twinned on zinc blende), and in faulted crystals ([111] stacking faults). We can show that barriers (discontinuities in energy surfaces) exist for electron propagation (current) parallel to the "c" axis of a twinned or faulted crystal due to two effects: a symmetry effect and a polar effect. The second effect is simply illustrated for rotation-twinned zinc blende. For randomly faulted crystals, band gaps depend on α, the probability of faulting. Quantitative theories of these effects remain to be developed.

ANALYTIC PROPERTIES OF BLOCH WAVES AND WANNIER FUNCTIONS. W. Kohn, Department of Physics, Carnegie Institute of Technology, Pittsburgh, Pennsylvania (Received March 16, 1959).

The one-dimensional Schrödinger equation with a periodic and symmetric potential is considered, under the assumption that the energy bands do not intersect. The Bloch waves, ϕ_{nk}, and energy bands, E_{nk}, are studied as functions of the complex variable, k. In the complex plane, they are branches of multivalued analytic and periodic functions, ϕ_k and E_k, with branch points, k', off the real axis. A simple procedure is described for locating the branch points. Application is made to the power-series and Fourier-series developments of these functions. The analyticity and periodicity of ϕ_{nk} has some consequences for the form of the Wannier functions. In particular, it is shown that for each band there exists one and only one Wannier function which is real, symmetric or antisymmetric under an appropriate reflection, and falling off exponentially with distance. The rate of falloff is determined by the distance of the branch points k' from the real axis.

FLUORESCENT RESPONSE OF CESIUM IODIDE CRYSTALS TO HEAVY IONS. A. R. Quinton, C. E. Anderson, and W. J. Knox, Heavy Ion Accelerator Laboratory, Yale University, New Haven, Connecticut (Received March 23, 1959).

The light output from thallium-activated cesium iodide crystals has been determined using C^{12}, N^{14}, and O^{16} as incident particles, with energies up to 10 Mev per nucleon. A photocathode with S-11 response viewed the scintillator light and the photomultiplier pulses were compared with those produced by alpha particles and protons of known energies. There is evidence that low-energy heavy ions are inefficient producers of light in this spectral region.

ORIGIN OF THE CHARACTERISTIC ELECTRON ENERGY LOSSES IN ALUMINUM. C. J. Powell and J. B. Swan, Department of Physics, University of Western Australia, Nedlands, Western Australia (Received March 30, 1959).

The characteristic electron energy loss spectrum of aluminum has been measured by analyzing the energy distribution of 760-, 1,000-, 1520-, and 2020-ev electrons scattered by an evaporated specimen through 90°. Twelve loss peaks were observed, made up of combinations of elementary 10.3- and 15.3-ev losses. The former, the low-lying loss, is identified with the lowered plasma loss proposed by Ritchie, and the latter with the plasma loss proposed by Bohm and Pines and previously observed by many other workers. In measurements made with very thin evaporated targets, it was found that the low-lying loss changed considerably in position, as well as in intensity relative to the 15.3-ev loss. These changes, which are interpreted in terms of Ritchie's theory, definitely indicate that the low-lying loss is influenced by the surface layers of the specimen. As targets of high surface and volume purity could be prepared, it is concluded that results obtained by the present reflection technique, when examining loss behavior affected by surface phenomena, are superior to measurements of the characteristic loss spectrum of electrons transmitted through thin films.

EFFECTS OF MnO AND CoO ON THE 0.24-ev NiO ABSORPTION LINE. R. Newman* and R. M. Chrenko, General Electric Research Laboratory, Schenectady, New York (Received March 19, 1959).

Measurements are reported of the change in the 0.24-ev NiO absorption band due to additions of MnO and CoO to NiO crystals. The results support the interpretation that the band has its origin in an antiferromagnetic effect.

*Present address: Materials Research Laboratory, Hughes Products, Newport Beach, California.

THERMAL CONDUCTIVITY OF INDIUM ANTIMONIDE AT LOW TEMPERATURES. Eugenie V. Mielczarek* and H. P. R. Frederikse, National Bureau of Standards, Washington, D. C. (Received March 27, 1959).

Thermal conductivity measurements were made on a monocrystalline sample of indium antimonide from 10 to 50°K. Umklapp, isotope, and boundary scattering contributions to the thermal resistivity were calculated from theoretical expressions and then subtracted from the measured value of thermal resistivity. The subsequent deduction of impurity scattering

gives a value for the number of point impurities which is compatible with that given by electrical measurements.

*Present address: Physics Department, Catholic University of America, Washington, D. C.

NITROGEN, A MAJOR IMPURITY IN COMMON TYPE I DIAMOND. W. Kaiser and W. L. Bond, Bell Telephone Laboratories, Murray Hill, New Jersey (Received March 27, 1959).

Common Type I diamonds (as classified by Robertson et al.) have additional absorption in the infrared and ultraviolet. It is shown that the strongest absorption band in the infrared at 7.8 μ and the ultraviolet absorption at 3065 A are proportional to the nitrogen concentration of the crystal. A corresponding increase in lattice constant is found to be as high as 0.01% for a nitrogen content of 0.2%. Concentration, x-ray, and density data suggest that nitrogen occupies a substitutional position in the diamond lattice. The infrared absorption bands at 7.8, 8.3, 9.1, and 20.8 μ are considered to be C-N molecular vibrations. Several optical, electrical, and thermal properties of diamond are discussed in view of our findings.

METAL TO SEMICONDUCTOR CONTACTS: INJECTION OR EXTRACTION FOR EITHER DIRECTION OF CURRENT FLOW. N. J. Harrick, Philips Laboratories, Irvington-on-Hudson, New York (Received March 17, 1959).

A study of metal to semiconductor contacts has been carried out using infrared radiation to measure the current versus added carrier density (J-Δp) characteristics. It is found that the nature of the semiconductor surface rather than the metal is a major factor in controlling the characteristics of the metal to semiconductor contact. Two unusual classes of results are described; viz., where injection into the semiconductor bulk is observed regardless of the direction of current flow and where extraction is observed regardless of the direction of current flow. The model proposed to explain these unusual results utilizes an insulating film between the metal and the semiconductor. Two competing effects are discussed, voltage-controlled injection and extraction, which can explain these results. Extraction for either direction of current flow is explained by the occurrence of the field effect at the metal to semiconductor contact. Injection for either direction of current flow is tentatively explained by a change, due to the applied voltage, in the communication of the current carriers in the metal with the valence and conduction bands of the semiconductor, resulting in a change in the current composition entering the semiconductor. Relaxation effects, which are attributed to the action of slow surface states, have also been observed in the J-Δp characteristics. The relaxation is always in a direction of increasing the injection level or decreasing the extraction level. The predominance of injection after relaxation is attributed to the shielding effect of the surface states which reduces the magnitude of the field effect.

SPIN RELAXATION OF OPTICALLY ALIGNED RUBIDIUM VAPOR. W. Franzen, Arthur D. Little, Incorporated, Cambridge, Massachusetts (Received March 23, 1959).

A new optical method for studying the spin relaxation of optically aligned rubidium vapor is described. In this method, the pumping radiation, consisting of circularly polarized D_1 resonance radiation, is suddenly shut off and then turned on again after a known time interval. The relaxation which takes place during the interval of darkness causes the vapor to become more opaque to the pumping radiation at a rate which is determined by the relaxation time. A large degree of alignment, as well as a relaxation time of about 80 milliseconds, were observed in a closed-off evacuated cylindrical glass cell completely lined, except for 1/200 of the wall area, with a thin film of tetracontane ($C_{40}H_{82}$). The variation of relaxation time with buffer gas pressure was studied in this cell and in an unlined glass cell. From the observations with the unlined cell, diffusion coefficients for rubidium in neon and argon of 0.31 cm^2/sec and 0.24 cm^2/sec, respectively, can be deduced. Observed cross sections for disorientation collisions between aligned ground-state rubidium atoms and neon, argon, krypton, and xenon atoms are 5.2×10^{-23} cm^2, 3.7×10^{-22} cm^2, 5.9×10^{-21} cm^2 and 1.3×10^{-20} cm^2, respectively. In the evacuated tetracontane-lined cell, the relaxation time decreased by 30% for a tenfold increase in rubidium vapor pressure. An explanation for this relatively weak dependence is suggested.

The longest observed relaxation time was approximately 0.4 second in a tetracontane-lined cell filled with neon to a pressure of 3 cm Hg.

LOW-TEMPERATURE SPECIFIC HEAT OF LIQUID He^3 NEAR THE SATURATED VAPOR PRESSURE AND AT HIGHER PRESSURES.

D. F. Brewer,* J. G. Daunt, and A. K. Sreedhar, The Ohio State University, Columbus, Ohio (Received March 16, 1959).

The specific heat of liquid He^3 has been measured near the saturation vapor pressure in the range 0.085°K to 0.75°K, and at pressures up to the melting pressure between 0.12°K and 0.6°K. There is no evidence of a specific heat transition in the range of measurements. Near 0.1°K the specific heat near the saturated vapor pressure appears to tend linearly to zero at 0°K with a slope of 4.0 ± 0.1 cal/mole-deg^2, providing evidence for regarding He^3 as a Fermi liquid near this temperature with an effective excitation mass of $(2.00 \pm 0.05) \times$ the mass of a He^3 atom. Entropies calculated with this linear extrapolation and with the assumption that no transition occurs below 0.085°K agree well with previous evaluations. Measurements at higher pressures show a negative dependence of specific heat on pressure above 0.16°K, but a positive dependence below this temperature, in contradistinction to the case of an ideal Fermi gas.

*On leave of absence from a Nuffield Foundation Research Fellowship held at the Clarendon Laboratory, Oxford University, Oxford, England.

EXPANSION COEFFICIENT AND ENTROPY OF LIQUID He^3 UNDER PRESSURE BELOW 1°K.

D. F. Brewer* and J. G. Daunt, The Ohio State University, Columbus, Ohio (Received March 16, 1959).

Measurements have been made of the change of temperature on adiabatic expansion of liquid He^3 in the temperature range 0.15°K to 1.15°K, at average pressures up to 22 atmospheres. From these measurements, evaluations have been made of the expansion coefficient, α_p, at constant pressure, and of the change in entropy on compression from the saturated vapor pressure to higher pressures. The latter calculations, combined with the previously determined entropy at the saturated vapor pressure, give values of S_p, the absolute entropy under pressure. It is found that at all pressures α_p is negative up to a temperature T_0 which is a monotonically increasing function of pressure. Correspondingly, at sufficiently low temperatures $(\partial S_p/\partial p)_T$ is positive for all pressures, in agreement with theory. The S_p isobars allow plausible extrapolations to the absolute zero, from which the limiting slope at 0°K has been estimated. Comparison of these slopes with the very low-temperature nuclear magnetic susceptibility yield some information concerning the variation with pressure of the spin-dependent interactions in liquid He^3.

*On leave of absence from a Nuffield Foundation Research Fellowship held at the Clarendon Laboratory, Oxford University, Oxford, England.

NONRESONANT NUCLEAR SPIN ABSORPTION IN LITHIUM, SODIUM, AND ALUMINUM.

A. G. Anderson, International Business Machines Research Laboratory, San Jose, California (Received March 30, 1959).

Audio-frequency spin absorption has been observed in the nuclear spin systems of the metals lithium, sodium, and aluminum. In lithium and sodium, the observed second moment of the absorption line at zero dc magnetic field is in agreement with calculations assuming only magnetic dipole-dipole interactions; in aluminum the zero-field absorption extends to frequencies as high as 50 kc/sec and the second moment of the absorption line appears to be about 50% larger than expected. Spin absorption has also been observed at small applied dc magnetic fields, H_0, for audio-frequency magnetic excitation both parallel to and perpendicular to H_0. In both of these cases, absorption occurs at γH_0 and $2\gamma H_0$ in agreement with theory.

ELECTRIC AND MAGNETIC PROPERTIES OF THE HYDROGEN MOLECULE.

T. P. Das* and R. Bersohn, Department of Chemistry, Cornell University, Ithaca, New York (Received January 9, 1959).

The hydrogen molecule ground state has been studied for a long time by valence theorists. Comparison with experiment has been limited to the energy, bond distance, vibration frequency, and

the electric and magnetic polarizabilities. Recent radio-frequency experiments on hydrogen have yielded new quantities, the nuclear magnetic shielding constant, the spin-spin coupling constant, and the electric field gradient at the nucleus. In this paper, variational methods are described for the calculation of the new types of polarizability. These methods can be applied to more complex molecules and appear to open new possibilities for the semiquantitative interpretation of the results of high-resolution nuclear magnetic resonance. An extensive comparison is made between the experimental quantities and theoretical values using various wave functions. The most important factor affecting the accuracy of the charge density is the use of an effective nuclear charge.

*On leave of absence from Saha Institute of Nuclear Physics, Calcutta, India.

MESON CORRECTIONS TO THE HYPERFINE STRUCTURE IN HYDROGEN. C. K. Iddings and P. M. Platzman, California Institute of Technology, Pasadena, California (Received March 30, 1959).

The authors have previously shown that the form factor of the proton, measured by Hofstadter, implies an energy shift in the hyperfine structure of atomic hydrogen. Uncertainties in this method of applying the Hofstadter data, due to the effects of virtual mesons, are investigated in an approximate way and found to be small, on the order of one to two percent of the total correction. Under certain assumptions about the form of the amplitudes for various photoproduction processes, we conclude that the value of the fine-structure constant implied by the hyperfine-structure measurement of Kusch disagrees with the value obtained from the Lamb shift by 34 ± 21 parts per million.

RESONANCE ELECTRON EXCHANGE IN LARGE-ANGLE SCATTERING OF He^+ ON He AT kev ENERGIES. F. P. Ziemba and A. Russek, Department of Physics, University of Connecticut, Storrs, Connecticut (Received March 17, 1959).

Recent differential scattering measurements at 5° scattering angle of He^+ on He at energies of 2 to 250 kev have shown several pronounced resonance peaks when the fraction of the scattered particles which were neutral (electron exchange) was plotted as a function of incident energy. A detailed comparison of those experimental data is made with the theoretical predictions of the impact parameter method for resonance electron capture. The agreement between the theory and experiment is found to be quite good at high energies despite experimental indications of a large amount of excitation. The contribution of electron exchange with excitation is then considered in the light of this fact.

COLLISION-INDUCED SPIN FLIP OF HYDROGEN ATOMS. Oldwig von Roos, Jet Propulsion Laboratory, California Institute of Technology, Pasadena, California (Received March 30, 1959).

The cross section of a radiationless electronic spin state transition (triplet-singlet transition) of two colliding, unexcited, hydrogen atoms has been calculated for low relative velocities. The low-velocity limit of this cross section exhibits a logarithmic divergence and decreases rapidly to a value of the order of πr_0^2 (r_0 = classical electron radius $e^2/4\pi mc^2$) with increasing energy of relative motion.

CIRCULAR POLARIZATION OF GAMMA RADIATION FOLLOWING ALLOWED BETA TRANSITIONS. R. M. Steffen, Department of Physics, Purdue University, Lafayette, Indiana (Received March 23, 1959).

The degree of circular polarization of gamma rays following allowed beta transitions has been investigated as a function of the angle $\Theta_{\beta\gamma}$ between beta-particle momentum and gamma direction and as a function of the energy of the beta particle. The anisotropy of the beta-gamma circular polarization correlation observed for pure Gamow-Teller transitions ($\Delta I = 1$) is used to determine the validity of $C_A' = C_A$. The experimental results for Co^{60} and Na^{22} are $W(\Theta_{\beta\gamma}) = 1 - (0.345 \pm 0.019)(v/c)\cos\Theta_{\beta\gamma}$ and $W(\Theta_{\beta\gamma}) = 1 + (0.35 \pm 0.02)(v/c)\cos\Theta_{\beta\gamma}$, respectively. These values yield $C_A' = (1 \pm 0.2)C_A$.

The degree of circular polarization of the gamma rays following mixed beta transitions ($\Delta I = 0$) confirms the existence of V-A interference terms. For Sc^{46} and Na^{24} the beta-gamma circular polarization correlations, $W(\Theta_{\beta\gamma}) = 1 + (0.24 \pm 0.02)(v/c)\cos\Theta_{\beta\gamma}$, and $W(\Theta_{\beta\gamma}) = 1 + (0.07 \pm 0.03)(v/c)\cos\Theta_{\beta\gamma}$, were observed. From these

measurements the ratio of Fermi to Gamow-Teller components for the Sc^{46} beta transition, $(M_F/M_{GT})^2 = 0.13 \pm 0.04$, and for the Na^{24} beta transition, $(M_F/M_{GT})^2 = 0.002 \pm 0.010$, was determined.

INELASTIC DIFFRACTION SCATTERING. John S. Blair, Department of Physics, University of Washington, Seattle, Washington (Received March 30, 1959).

The mechanism of inelastic diffraction scattering, introduced by Drozdov and Inopin to discuss scattering from nuclei with quadrupole surface deformation, has been extended for scattering amplitude linear in the deformation to arbitrary multipolarity. The resulting angular distributions and gamma-ray angular correlations correspond closely to Born-approximation predictions. The model provides a natural explanation for why the inelastic angular distributions of strongly absorbed projectiles are characterized by sharp and persistent oscillations. Comparsion is made to observed inelastic scattering of alpha particles and deuterons by light nuclei. Large quadrupole deformations are indicated in many nuclei. The systematic appearance in $4n$ nuclei of states corresponding to octupole excitation is noted.

EXCITATION FUNCTIONS FOR ALPHA-INDUCED REACTIONS ON ZINC-64. Norbert T. Porile, Chemistry Department, Brookhaven National Laboratory, Upton, New York (Received March 23, 1959).

Eleven excitation functions for alpha-induced reactions on Zn^{64} have been measured up to incident energies of 41 Mev. The values of $\sigma(\alpha,p)/\sigma(\alpha,n)$ and $\sigma(\alpha,pn)/\sigma(\alpha,2n)$ in the region of maximum yield were found to be 1.7 and 9, respectively. Reactions involving alpha-particle emission account for about 20% of the total inelastic cross section at 40 Mev. The total inelastic cross section was found to agree with calculated values for $r_0 = 1.6$ fermis. The competition between different reactions was analyzed in terms of the statistical theory by use of a level density expression of the form $W(E) = C\exp\{2[a(E-\delta)]^{1/2}\}$. Values of a ranging from 0.8 to 2.8 were required to fit the experimental results, indicating that the statistical theory is not completely applicable.

SHELL-MODEL THEORY OF INELASTIC SCATTERING ON Be^9. William T. Pinkston, Palmer Physical Laboratory, Princeton University, Princeton, New Jersey (Received March 27, 1959).

A study is made of the energy levels of Be^9 with particular emphasis on comparing the inelastic-scattering data with the shell-model predictions. The differential cross sections for inelastic scattering by alpha particles are calculated in distorted-wave Born approximation using a central spin-independent potential to represent the interaction between the incident alpha and each target nucleon. The target wave functions are taken to be intermediate-coupling shell-model wave functions. The agreement between theory and experiment is excellent for values of the intermediate coupling parameter, a/K, which best reproduce the level spectra. The results favor a value $a/K = 2.86$ over the other popular value, $a/K = 1.4$. It is suggested that the 1.7- and 11.3-Mev levels do not arise from the $(1p)^5$ configuration.

ABSOLUTE ACTIVATION CROSS SECTIONS FOR REACTIONS OF BISMUTH, COPPER, TITANIUM, AND ALUMINUM WITH 14.8-Mev NEUTRONS. A. Poularikas and R. W. Fink,* Department of Chemistry, University of Arkansas, Fayetteville, Arkansas (Received November 18, 1958; revised manuscript received May 4, 1959).

Absolute neutron activation cross sections at 14.8 Mev have been measured for bismuth, copper, titanium, and aluminum based on comparison with the $Cu^{63}(n,2n)Cu^{62}$ reaction (556 millibarns) which served as a standard for monitoring the flux. The reactions studied, measured half-lives, and cross sections are as follows: $Bi^{209}(n,\alpha)Tl^{206}$, 4.29 ± 0.05 min, 1.1 ± 0.3 mb; $Bi^{209}(n,p)Pb^{209}$, 3.31 ± 0.03 hours, 0.83 ± 0.40 mb; $Bi^{209}(n,\gamma)Bi^{210}$, ≤ 1.7 mb; $Cu^{65}(n,2n)Cu^{64}$, 12.85 ± 0.05 hours, 954 ± 130 mb; $Cu^{65}(n,p)Ni^{65}$, 2.56 ± 0.20 hours, 27 ± 11 mb; $Ti^{50}(n,p)Sc^{50}$, 1.8 ± 0.2 min, 27 ± 6 mb; $Ti^{50}(n,p)Sc^{50}$, 22 ± 3 min, 48 ± 15 mb; $Ti^{50}(n,\gamma)Ti^{51}$, ≤ 9 mb; $Ti^{49}(n,p)Sc^{49}$, 58 ± 2 min, 29 ± 5 mb; $Ti^{48}(n,p)Sc^{48}$, 44.0 ± 0.9 hours, 58 ± 8 mb; $Ti^{47}(n,p)Sc^{47}$, 3.45 ± 0.06 days, 230 ± 40 mb; $Ti^{46}(n,2n)Ti^{45}$, 3.06 ± 0.08 hours, 50.4 ± 8.0 mb; $Ti^{46}(n,p)Sc^{46}$, 85 ± 2 days, ~ 520 mb; $Al^{27}(n,\alpha)Na^{24}$, 15.00 ± 0.06 hours, 114 ± 7 mb; $Al^{27}(n,p)Mg^{27}$, 9.46 ± 0.02 min, 53 ± 5 mb.

Comparisons of the experimental cross sections with values estimated according to the continuum theory of the compound nucleus outlined by Blatt

and Weisskopf show deviations within one order of magnitude, except in the case of the bismuth results which exhibit large discrepancies.

From irradiations of natural titanium and highly enriched Ti^{50}, a new activity was observed having a half-life of 22 ± 3 minutes. This activity is not produced from enriched Ti^{47} or Ti^{49} samples, and it is therefore assigned tentatively to an isomer of Sc^{50}. Further work on this activity is in progress.

*On leave from the University of Arkansas. Temporary address: Department of Physics, University of Birmingham, England.

ELASTIC SCATTERING OF 14-Mev NEUTRONS BY Al, S, Ti, AND Co. Claude St. Pierre,* M. K. Machwe,† and Paul Lorrain, Département de Physique, Université de Montréal, Montréal, Canada (Received March 23, 1959).

Differential cross sections have been measured for the elastic scattering of 14-Mev neutrons by Al, S, Ti, and Co over the angular range from 10 to 138 degrees using a ring geometry and a plastic scintillator as detector. The experimental results are essentially in agreement with the optical model calculations of Bjorklund and Fernbach.

*Present address: Canadian Armaments Research and Development Establishment, Valcartier, P. Q., Canada.

†On leave from the University of Delhi, Delhi, India. Present address: University of Delhi, Delhi, India.

ANGULAR DISTRIBUTIONS OF PROTON GROUPS FROM THE $Al^{27}(n,p)Mg^{27}$ REACTION AT 14 Mev. O. E. Overseth, Jr.,* and R. A. Peck, Jr., Brown University, Providence, Rhode Island (Received March 18, 1959).

A study has been made of the high-energy proton groups from the $Al^{27}(n,p)Mg^{27}$ reaction at 14 Mev with emulsion detectors making a continuous survey in the interval 10°-70°. Proton groups corresponding to the residual Mg^{27} nucleus left in the ground state and at excitations of 1.0, 1.6, 2.1, 2.8, and 3.5 Mev are identified. Several of these groups are characterized by a pronounced peaking in forward directions characteristic of direct-interaction processes. The protons leading to the ground state peak in the vicinity of 30°, those to the 1.0-Mev level at 36°, and those to the 1.6-Mev level at about 50°. The 3.5-Mev group is not resolved from known close-lying levels, and the cluster exhibits an isotropic distribution. The 2.1- and 2.8-Mev groups, corresponding to no previously reported levels in Mg^{27}, also display an isotropic distribution and probably represent several unresolved levels. The three lowest lying levels shown give approximate fits to theoretical curves consistent with reactions proceeding either by direct collision or by excitation of collective modes.

*Present address: Palmer Physical Laboratory, Princeton University, Princeton, New Jersey.

RESONANCE DETECTION OF NEUTRON ENERGY GROUPS FROM THE $Mn^{55}(p,n)Fe^{55}$ REACTION. L. L. Lee, Jr., and F. P. Mooring, Argonne National Laboratory, Lemont, Illinois (Received March 16, 1959).

The excitation energies of low-lying levels in Fe^{55} and the Q-value of the $Mn^{55}(p,n)Fe^{55}$ reaction have been measured by determining the proton energies at which 257-kev neutrons are produced in this reaction. The ratio of the number of neutrons scattered by a $\frac{1}{2}$-inch thick lithium slab to the number of neutrons transmitted was measured as the energy of a proton beam striking a thin manganese target was varied monotonically. Peaks in the ratio curve, indicating the presence of 257-kev (the energy for resonant neutron scattering from lithium) neutron groups from the reaction, occur at particular proton energies and Q-values can readily be computed. A ground-state Q-value of -1.011 ± 0.005 Mev has been measured for the $Mn^{55}(p,n)Fe^{55}$ reaction and states in Fe^{55} were located at excitations of 437, 936, 1315, 1414, and 2156 kev. Advantages and limitations of the method are discussed.

RESULTS OF STRIPPING ANALYSIS OF THE REACTION $K^{39}(d,p)K^{40}$. H. A. Enge, E. J. Irwin, Jr., and D. H. Weaner,† Laboratory for Nuclear Science and Department of Physics, Massachusetts Institute of Technology, Cambridge, Massachusetts (Received March 19, 1959).

The MIT-ONR electrostatic generator and the broad-range spectrograph have been used to study the energies and angular distributions of protons

emitted from a KI target bombarded with 6-Mev deuterons. Excitation energies are given for fifty-two levels in K^{40}. Orbital angular momenta of captured neutrons in the stripping process are given for thirty-eight of these excited levels and for the ground state. The reaction energy for the ground-state transition has been measured as $Q = 5.569 \pm 0.010$ Mev.

*Now at Cornell University, Ithaca, New York.
†Now at Gettysburg College, Gettysburg, Pennsylvania.

RESONANT ABSORPTION BY THE 9.17-Mev LEVEL IN N^{14}. S. S. Hanna and Luise Meyer-Schützmeister, Argonne National Laboratory, Lemont, Illinois (Received March 16, 1959).

The 9.17-Mev radiation from the reaction $C^{13}(p,\gamma)N^{14}$, $E_p = 1.75$ Mev, was used to obtain resonant absorption in the inverse process $N^{14}+\gamma \rightarrow N^{14*}(E_{ex} = 9.17$ Mev). The strength of the absorption was measured as a function of absorber thickness. Analysis of the measurements gives $\Gamma = (77 \pm 12)$ ev and $\omega\Gamma_\gamma = (14.5 \pm 2)$ ev. The latter value indicates dipole radiation.

MAGNETIC MOMENT OF THE TRITON IN UNITS OF THE MAGNETIC MOMENT OF THE PROTON. William Duffy, Jr.,* Department of Physics, Stanford University, Stanford, California (Received March 27, 1959).

High-resolution nuclear magnetic resonance techniques were used to perform a precise measurement of the ratio of the Larmor frequencies of tritons and protons in a sample of 20% tritiated water. The measured ratio ω_T/ω_H is 1.06663975(2). From this frequency ratio and an estimate of the magnetic shielding correction, a value of 1.06663986(11) is obtained for the moment of the triton in units of the proton moment. From this value and the hfs measurements of Kusch, and of Prodell and Kusch, one obtains a hfs anomaly of $(-5.62 \pm 0.13) \times 10^{-6}$ for tritium. This observed anomaly may be compared with the theoretical predictions of Adams. The longitudinal relaxation time T_1 of the protons and tritons in the sample was measured and found to be 1.02 ± 0.10 sec and 0.83 ± 0.10 sec, respectively.

*Present address: Department of Physics, University of Santa Clara, Santa Clara, California.

SCATTERING OF 2- TO 4-Mev POLARIZED NEUTRONS BY CARBON. W. P. Bucher, W. B. Beverly, G. C. Cobb, and F. L. Hereford, Department of Physics, University of Virginia, Charlottesville, Virginia (Received March 30, 1959).

The right-left asymmetry in elastic scattering of partially polarized neutrons by carbon has been observed for a 45° (c.m.) scattering angle and for neutrons in the 2- to 4-Mev energy range. The $C^{12}(n,n)$ polarization, inferred from the measured asymmetries, has a direction and energy dependence in agreement with phase shift analyses obtained previously by others. The magnitude of the polarization is generally larger than predicted.

BACK-ANGLE ELASTIC SCATTERING OF 14.6-Mev NEUTRONS FROM ALUMINUM, COPPER, AND ZIRCONIUM. John D. Anderson, Calvin C. Gardner, John W. McClure, M. P. Nakada, and Calvin Wong, Lawrence Radiation Laboratory, University of California, Livermore, California (Received March 26, 1959).

Differential elastic scattering cross sections have been measured for 14.6-Mev neutrons on aluminum, copper, and zirconium in 5° steps from 85° to 155°. The copper and zirconium angular distributions are in good agreement with optical-model calculations by Bjorklund and Fernbach, who employ a spin-orbit coupling term in their potential. The aluminum differential cross sections are systematically higher than the predictions at the back angles, indicating that the Bjorklund-Fernbach optical-model parameters which fit the medium and heavy elements are not as successfully applied to an element as light as aluminum.

ELECTRON-DEUTERON INELASTIC SCATTERING CROSS SECTIONS AT HIGH ENERGIES. Loyal Durand III, Institute for Advanced Study, Princeton, New Jersey (Received March 31, 1959).

The effects on the cross sections for the electron-deuteron inelastic scattering process $e+d \rightarrow e+n+p$ of interactions between the outgoing nucleons are examined in detail. The cross sections are calculated in the first Born approximation with respect to the electromagnetic interac-

tion using nucleon wave functions modified by the final-state interactions. Crude estimates indicate that the peak value of the cross section $d^2\sigma/(d\Omega_e dE_e')$ may be decreased by ~5-10% in the presence of such interactions. It is shown in an Appendix that additional decreases of ~5% will result when proper account is taken of the D-state component of the deuteron wave function. These changes in the cross section affect appreciably the determination of the neutron magnetic form factor from the experimental scattering cross sections. A new method of measuring the magnetic form factor based on the angular distribution of the outgoing nucleons is therefore proposed which eliminates almost all the uncertainties relating to the deuteron wave function and the effects of final-state interactions. This method may also be used in conjunction with the dependence of the cross sections on the electron scattering angle to study the behavior of the neutron charge form factor in the region of large momentum transfers. The polarization of the outgoing nucleons is also calculated. While significant information may in principle be obtained from polarization measurements, the required experiments do not appear to be feasible at the present time. In an Appendix, the modifications of the cross sections resulting from relativistic effects are considered, and some uncertainties inherent in previous work are clarified.

PHOTOPRODUCTION OF K^+ MESONS. B. D. McDaniel, A. Silverman, R. R. Wilson, and G. Cortellessa,* Cornell University, Ithaca, New York (Received March 26, 1959).

The photoproduction in hydrogen of K^+ mesons in association with hyperons has been studied by using an 1160-Mev bremsstrahlung beam from the Cornell synchrotron. The K mesons were selected with a magnetic analyzer and counter telescope system. They were further identified by bringing them to rest in a stopping block and by the detection, in coincidence, of the particles arising from their decay. The angular distribution for the associated production of K^+ mesons with Λ^0 hyperons at the photon energies of 980 and 1010 Mev has been studied. Measurements were also made of the cross section as a function of photon energy for the center-of-mass angle of 85 degrees. The results of these measurements are compatible with S-wave production. The photoproduction of Σ^0 hyperons in association with K mesons has also been measured for one set of kinematical conditions. The measured $(K^+ - \Sigma^0)$ cross section is comparable to that of the $(K^+ - \Lambda^0)$ process.

*Now at Istituto Superiore di Sanità, Rome, Italy.

SEARCH FOR $550m_e$ PARTICLES IN THE SEA LEVEL COSMIC RADIATION. I. B. McDiarmid, Division of Pure Physics, National Research Council, Ottawa, Canada (Received March 30, 1959).

An attempt has been made to observe a $550m_e$ particle in the sea level cosmic radiation. A counter arrangement biased against the detection of μ mesons was used to select particles stopping in a multiplate cloud chamber. From the mass spectrum of these particles, determined from ionization and range measurements, an upper limit of 0.02% was obtained for the intensity of $550m_e$ particles relative to μ mesons stopping in the same range interval. A similar upper limit was also obtained by a method independent of mass measurements for the particular case in which one of the decay products of a $550m_e$ particle is a π^0 meson.

NUCLEAR INTERACTION OF θ_2 MESONS IN EMULSION. U. Camerini* and W. F. Fry, Department of Physics, University of Wisconsin, Madison, Wisconsin, and M. Baldo-Ceolin, H. Huzita,†‡ and S. Natali, Instituto di Fisica dell' Università, Istituto Nazionale di Fisica Nucleare, Sezione di Padova, Padova, Italia (Received March 27, 1959).

Additional observations in emulsion on the nuclear interaction of neutral K mesons are reported. A total of 1 τ^+, 7 K^-, 7 Σ^+, 10 Σ^-, and 18 hyperfragments have been observed. The relative frequencies of different types of strange particles produced in the emulsion are consistent with the assumption that the neutral K meson is a particle admixture and that interactions in the θ and $\overline{\theta}$ modes are similar to interactions of K^+ and K^-, respectively.

*On leave of absence from Centro Brasileiro de Pesquisas Fisicas, Rio de Janeiro, Brazil.

†On leave of absence from St. Paul's University,

Tokyo, Japan.
†Present address: Department of Physics, University of Wisconsin, Madison, Wisconsin.

RELATIVISTIC THEORY OF UNSTABLE PARTICLES II. P. T. Matthews and Abdus Salam, Imperial College, London, England (Received March 16, 1959).

This paper is a direct continuation of an earlier paper (I) where an attempt was made to set up a field-theoretic foundation for the theory of mean mass and lifetime of an unstable particle. It was argued in I that the decay-time plot of a beam of unstable particles is a concept peculiar to a single-particle theory; that from a field-theoretic point of view mass (the variable conjugate to proper time) rather than time has the primary significance. Here we show that the spectral function, $\rho(m^2)$, appearing in the (field-theoretic) one-particle propagator has a direct significance as the probability of finding, in production, an unstable particle of mass m. This allows us to define a "one-particle" state for the unstable particle as a superposition of its outgoing decay states suitably weighted in mass space [with a factor which is the square root of $\rho(m^2)$]. The proper-time propagation of this state gives directly the decay amplitude, and its modulus is the experimentally observed decay-time plot.

The time plot is explicitly evaluated for π decay. Insofar as the distribution of mass values for the π meson starts with μ mass (assumed stable), the time plot is not merely the conventional decay exponential $e^{-\tau/\tau_0}$. There are additional terms of the form $(1/Q\tau_0)^2(\tau_0/\tau)\sin Q\tau$ where Q is the Q-value for decay. These become important about a hundred lifetimes after the decay starts.

Finally we compare the time plots for particle and antiparticle decays on the basis of CTP invariance.

GREEN'S FUNCTION APPROXIMATION METHOD. I. THE NUCLEON. David S. Falk, Harvard University, Cambridge, Massachusetts (Received March 16, 1959).

A method for the approximate construction of the nucleon Green's function is presented. The development is such that the approximate Green's function automatically has the same analytical properties as the exact one. This method involves the symmetrical treatment of the Green's function and, ultimately, the assumption that certain particles behave in an uncorrelated manner. The approximation results in a linear integral equation for the Green's function which is completely renormalized. This equation is solved exactly through the use of the spectral representation which, by construction, is consistent with the approximation.

GREEN'S FUNCTION APPROXIMATION METHOD. II. THE POLARON. David S. Falk, Harvard University, Cambridge, Massachusetts (Received March 16, 1959).

A method previously derived for the approximate construction of the nucleon Green's function is here applied to that of the polaron. After making an arbitrary translation of the phonon variables, a linear integral equation for the Green's function is derived by means of a symmetrical treatment and a noncorrelation assumption, in complete analogy to the nucleon problem. This equation is solved through the introduction of a spectral representation in the special case of zero total momentum. The lowest energy state of the system is calculated in terms of the arbitrary translations and then minimized with respect to them. Using the simplest nontrivial cutoff procedure to obtain the variational equation and its solution, results are obtained for values of the coupling parameter $\alpha \leq 3$, and are compared with those of Feynman.

INELASTIC FINAL-STATE INTERACTIONS: K^- ABSORPTION IN DEUTERIUM. Robert Karplus and Leonard S. Rodberg, Physics Department, University of California, Berkeley, California (Received March 19, 1959).

In a reaction from which several strongly interacting particles emerge, it is often possible to isolate the effects of forces between two of the outgoing particles. There are many cases in which this final-state interaction can produce inelastic reactions. The formalism that describes this situation is developed here, and the reaction $K^- + d \rightarrow \pi + \Sigma + N \rightarrow \pi + \Lambda + N'$ is studied in detail as an example. It is found that large Λ/Σ branching

ratios can result and can be used to restrict the Σ-N and K-N interaction parameters. The gross features of the spectrum can be understood using a simple model. It does not seem possible to determine the parities of the strange particles from the momentum spectra. When the inelastic reaction in the final state is exothermic, as in the example, high partial waves may contribute.